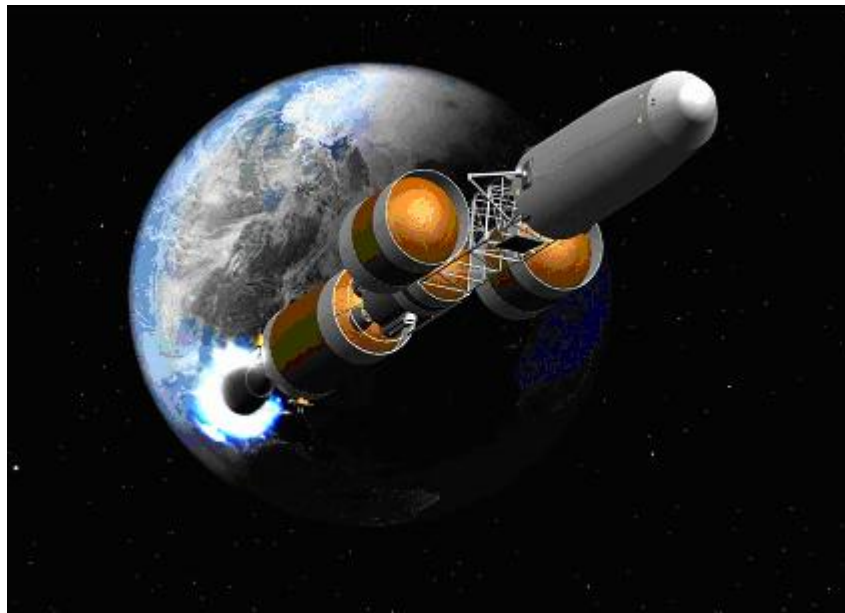


Mission and System Analysis and Requirements Support

Task #6: Mission Systems Analysis and Trade Studies

Phase 2 (January - April, 2006)

Nuclear Thermal Propulsion Requirements Analysis of the ESAS Reference Human Mars Mission Architecture



Final Report

Marshall Space Flight Center Advanced Concepts Office

July 20, 2006

Table of Contents

1	Study Plan	3
1.1	Goals	3
1.2	Objectives and Study Tasks	3
1.3	Study Team	6
2	Analysis of ESAS Reference mission.....	7
2.1	Mission Analysis.....	7
2.2	Vehicle Design Concept Ground Rules and Assumptions	10
2.3	NTP Vehicle Concepts.....	11
2.3.1	ESAS Architectcture Earth-to-orbit Launch Vehicle Requirements	12
3	NTP VEHICLE AND ENGINE SENSITIVITY ANALYSIS	15
3.1	Integrated Vehicle and Engine Shielding Analysis	15
3.1.1	Radiation Shielding Requirements Assessment.....	16
3.1.2	Hydrogen Tank Shielding Assessment	20
3.1.3	External Shield Trade Study	22
3.2	NTP Engine Sensitivities	25
3.2.1	Single vs. Multiple Engine Trade	25
3.2.2	Mars Transfer Time Sensitivity Trade.....	31
3.2.3	Graphite Prismatic Fuel Elements vs. New Technologies.....	31
4	NTP ENGINE Development cost analysis	33
5	NTP Requirements for the ESAS Reference Mars Mission	34
5.1	NTP MSA Phase 2 Study Conclusions.....	34
	Apendix A Shadow shield vs. 2-Pi shield Mass Cmparison Graphs as a function of shadow shield half-angle	35
	Apendix B Shadow shield vs. 2-Pi shield Mass Cmparison Graphs as a funtion of dose plane distance	51
	Apendix C Shadow shield vs. 2-Pi shield Mass Cmparison Graphs Carpet plots....	55

1 STUDY PLAN

1.1 Goals

The Nuclear Thermal Propulsion Mission and System Analysis (NTP MSA) Phase 2 Study was initiated by Marshall Space Flight Center's (MSFC) Advanced Concepts Office (VP11) in December, 2005 in support of MSFC's Nuclear Systems Office (VP31) NTP for Exploration Study. The Mission and Systems Analysis Study was task # 6 of a set of 14 tasks within the NTP for Exploration Study. The primary goal of the NTP MSA Phase 2 Study was to identify the range of potential NTP engine and vehicle requirements for NASA Exploration Systems Mission Directorate (ESMD) Mars human exploration reference mission

1.2 Objectives and Study Tasks

This task includes the analyses, trade studies and conceptual design activities outlined in Table 1.1, necessary to develop nuclear thermal propulsion (NTP) stage and engine point-of-departure concepts and associated system requirements to perform the ESMD Reference Mars mission. The Study work breakdown structure is shown on Table 1.3 and the study schedule is shown in Figure 1.1

Table 1.1 NTP Mission and System Analysis Study Products

• Product	• Date
• NTP System Analysis of the ESMD reference mission <ul style="list-style-type: none">- Mission Analysis- NTP point-of-departure design concept	March 31, 2006
• NTP Vehicle and Engine Sensitivity Analysis <ul style="list-style-type: none">- Integrated vehicle/engine shielding analysis- Single vs. multiple engines- NTP Engine Parameter Sensitivities	April 17, 2006
• NTP Engine Requirements for the ESMD Reference Mission <ul style="list-style-type: none">- Solid core NTP- Advanced NTP	April 30, 2006
• Phase 2 Final Report	May 15, 2006

Table 1.2 Work Breakdown Structure

1. NTP Analysis of ESMD Reference Mission
1.1. Mars Mission Analysis
1.1.1. Mission analysis ground rules and assumptions
1.1.2. Cargo mission trajectories
1.1.3. Piloted mission trajectories
1.1.4. Sensitivity to transit times and Mars stay time
1.2. Define NTP Vehicle Design Concept for ESMD Reference Mission
1.2.1. Vehicle design concept ground rules and assumptions
1.2.2. Cargo vehicle concept
1.2.3. Piloted vehicle concept
1.2.4. Vehicle scaling equations
2. NTP Vehicle and Engine Sensitivity Analysis
2.1. Integrated Vehicle/engine Shielding Analysis
2.1.1. Internal shielding
2.1.2. External shielding
2.1.3. Hydrogen tank shielding design
2.1.4. Hydrogen tank shielding verification
2.1.5. Crew habitat radiation shielding
2.2. Single vs. Multiple Engine Trade
2.3. NTP Engine Parameter Sensitivities
2.4 NTP Cost Analysis
3. NTP Engine Requirements Analysis
3.1. Solid Core NTP (Advanced NERVA)
3.2. Advanced NTP (PBR, CERMET)
4. Phase 2 Study Documentation
4.1. Documentation Template
4.2. Phase 2 Final Report Preparation

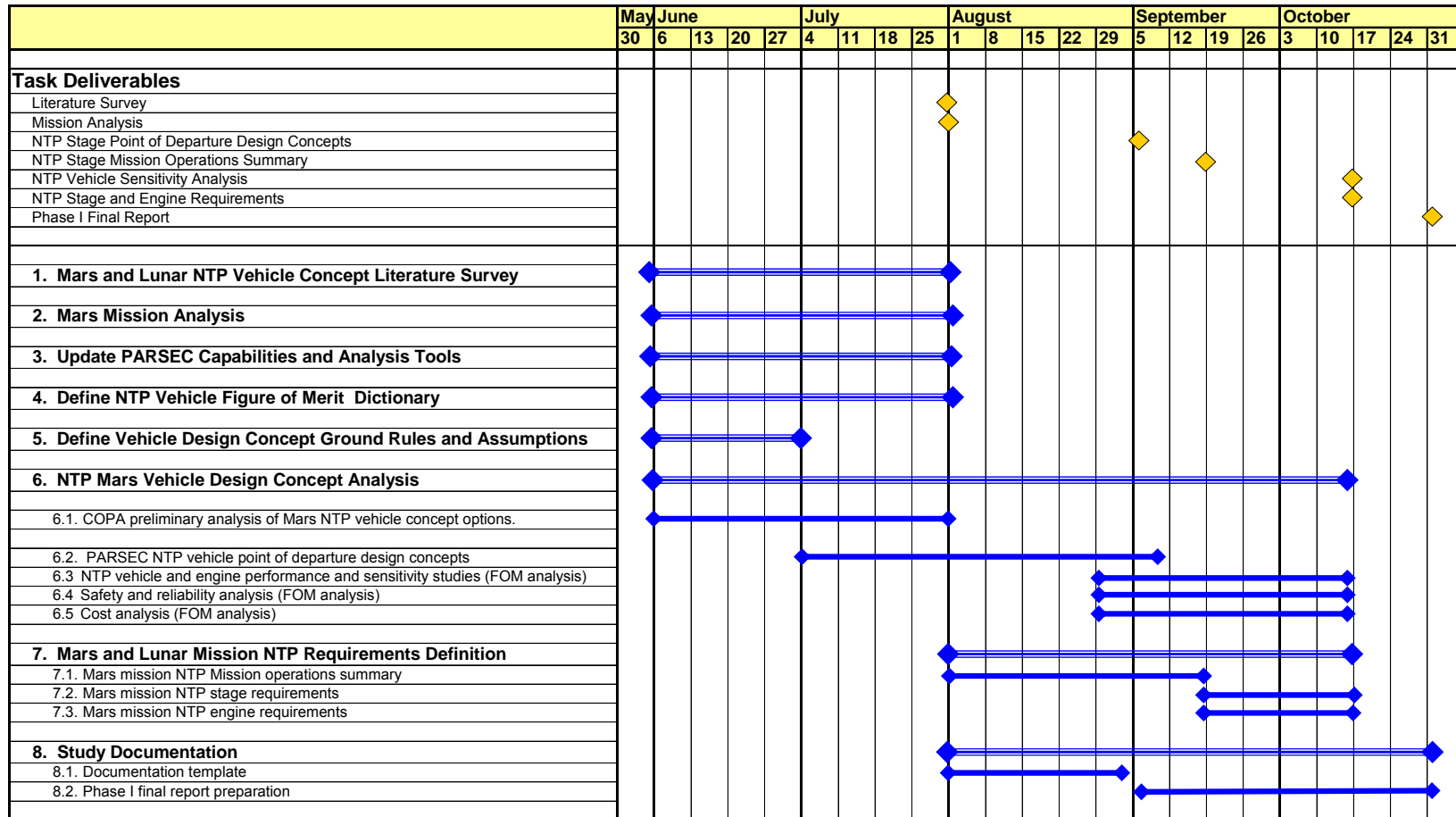


Figure 1.1 Nuclear Thermal Propulsion Mission and System Analysis Study – Task Schedule

1.3 Study Team

The NTP MSA study participants included members of Advanced Concepts Office design team, and contracted support from SAIC, as well as participation of the MSFC Nuclear Systems Office. Due to funding constraints, the Advanced Concepts design team was unable to support the NTP MSA Phase 2 effort. The vehicle concepts were scaled from the Phase 1 results. The Phase 2 study team is listed in Table 1.3

Table 1.3 NTP Mission and System Analysis Study Participants

NTP MSA Phase 2 Analysis Team

Discipline	Company	Name
NTP MSA Task Lead	NASA	Mulqueen, Jack
NTP	SAIC	Chiroux, Robert
NTP Radiation Shielding Analysis	SAIC	Moton, Tryshanda

NTP Engine System Analysis (NTP for Exploration, Task 7)

Discipline	Company	Name
ER11 NTP Engine Studies Lead	NASA	Nelson, Karl
ER11 NTP Propulsion	NASA	Simpson, Steve

2 ANALYSIS OF ESAS REFERENCE MISSION

2.1 Mission Analysis

The objective of the Phase 2 Mission Analysis task was to determine Mars mission trajectories for the ESAS Reference Mission Architecture, which is based on the Design Reference Mission 3 and 4 developed in the late 1990's. The mission architecture is based on split mission-long stay time, Mars mission profiles. Two Mars transfer opportunities space about two years apart, would be used. Two cargo delivery missions during the first opportunity would be used to deliver a Mars surface habitat and descent stage to Mars. These missions would use aerocapture for Mars orbit insertion. The crew would travel to Mars during the following Mars mission opportunity using a long Mars stay-time (conjunction-class) mission trajectory.

Trajectories were defined for the Mars mission opportunities between 2024 and 2037. Representative trajectories are illustrated in Figures 2.1 and 2.2.

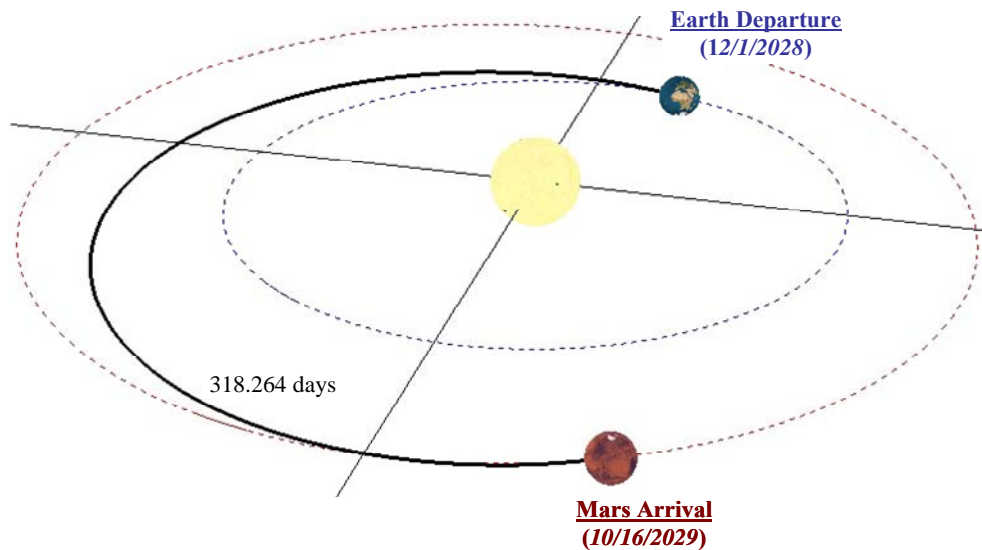


Figure 2.1 Cargo Mission Trajectory Profile

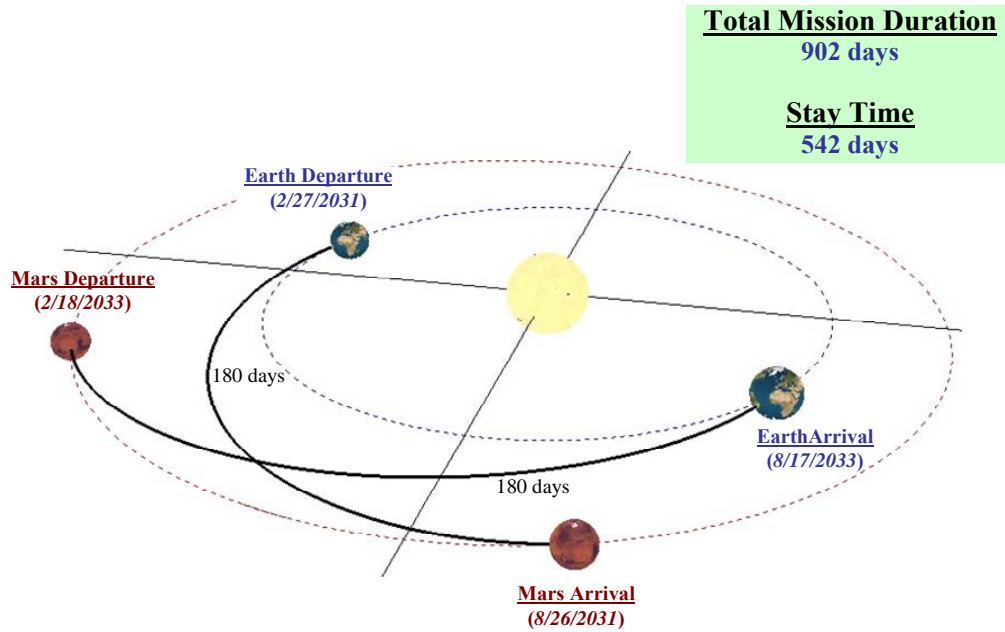


Figure 2.2 Piloted Mission Trajectory Profile

The trajectory data is presented in tables 2.1 and 2.2 The Mars transportation vehicles were sized using the worst case delta velocities for each maneuver. The values used in the sizing are shown in bold color in the tables below.

Table 2.1 Cargo Opportunities with Aerocapture at Mars

Earth Departure Date (GMT)	TOF (days)	TMI ΔV (km/s)	Mars Arrival V_{∞} (km/s)
10/5/2024 05:23	344.91	3.7538	2.5411
10/30/2026 03:51	294.72	3.6573	2.6993
12/1/2028 20:49	318.26	3.6473	3.2636
02/20/2031 08:14	318.91	3.6149	5.4500
04/28/2033 13:37	273.89	3.5930	4.3788
06/23/2035 01:09	195.49	3.7068	2.6959
09/6/2037 14:41	395.42	3.9249	3.3457

Table 2.2 All-propulsive, Piloted Opportunities

Earth Departure Date (GMT)	Mars Stay Time (days)	ΔV (km/s)			
		TMI	MOI	TEI	Earth Return
<i>12/12/2026 13:09</i>	<i>533.95</i>	<i>4.6170</i>	<i>2.7038</i>	<i>1.9633</i>	<i>0.0000</i>
<i>01/17/2029 10:46</i>	<i>531.18</i>	<i>4.4396</i>	<i>2.4934</i>	<i>1.3103</i>	<i>0.0000</i>
<i>02/27/2031 17:37</i>	<i>542.26</i>	<i>4.0651</i>	1.9497	<i>0.9087</i>	<i>0.0000</i>
<i>05/2/2033 15:00</i>	565.00	4.2641	<i>1.3039</i>	<i>1.0919</i>	<i>0.0000</i>
<i>07/3/2035 11:05</i>	<i>563.21</i>	<i>3.7482</i>	<i>0.9707</i>	1.5883	<i>0.0000</i>
<i>09/5/2037 21:10</i>	<i>535.26</i>	<i>4.1885</i>	<i>1.3606</i>	1.8120	<i>0.0000</i>
<i>10/22/2039 02:36</i>	<i>533.39</i>	<i>4.5108</i>	<i>2.1400</i>	<i>2.0583</i>	<i>0.1894</i>

2.2 Vehicle Design Concept Ground Rules and Assumptions

Table 2.3 NTP MSA Phase 2 Ground Rules and Assumptions

NTP MSA Phase II Ground Rule and Assumptions		Baseline	Reference	Trades
1.0	General			
1.1	Mission Type	Split Mission		
1.2	Trajectory type / surface stay time option	Low energy / long stay time		
1.3	Number of crew	6		
1.4	Propulsion technologies	Nuclear Thermal Propulsion (NTP)		
1.5	Cargo pre-deployment (split /sprint)	Cargo lander w/ascent vehicle to surface (surface payload) & surface habitat to Mars orbit.		
1.6	Pilot Vehicle Mars Orbit Insertion	Propulsive Capture		
1.7	Cargo Vehicle Mars Orbit Insertion	Aerocapture		Propulsive Capture
1.8	In-situ Resource Utilization	ISRU for Mars ascent propellant only		
1.9	Sub-system design	2-fault tolerance		
1.10	Mass Margin	~		
1.10.1	NTR system and non-heritage components	25%		
1.10.2	Chemical system and heritage components	20%		
1.10.3	Payload	0%		
2.0	Structures			
2.1	Factor of Safety for Composite Materials	~		
2.1.1	Yield Factor of Safety	1.5	NASA STD-5001	
2.1.2	Ultimate Factor of Safety	1.5	NASA STD-5001	
2.2	Factor of Safety for Metallic Materials	~		
2.2.1	Yield Factor of Safety	1.25	NASA STD-5001	
2.2.2	Ultimate Factor of Safety	1.4	NASA STD-5001	
2.3	Minimum Allowable Frequency	15 Hz		
3.0	Main Propulsion System			
3.1	MPS performs all major propulsive maneuvers	TMI, MOI, TEI, NTR disposal, Plane Changes at Mars		
3.3	Propellant tank ullage	3% of propellant volume		
3.4	Nuclear Thermal Propulsion	~		
3.4.1	NTP thrust	25,000 to 250,000 lbf thrust		
3.4.2	Nominal Isp	875 sec		
3.4.3	Start-up and Shut-down Losses	3%		
3.5	Chemical Propulsion System	~		
3.5.1	LOX/LH2 Engine Isp	473.4 sec		
3.5.2	Performance Reserve	1% Isp reduction		
4.0	Reaction Control System			
4.1	RCS maneuvers	Midcourse, directional control, ullage burn, planetary orbital maneuvers		
4.2	RCS Transit Allocation	50 m/s for each interplanetary leg		
4.3	Ullage Burn	1 m/s before each MPS burn		
4.4	Directional Control	5 m/s during each MPS burn		
4.5	On-Orbit (Mars) ΔV	30 m/s		
5.0	Environments			
5.1	Transit Habitat (DRM4 & JCS) Shielding Assumptions	Shielded for radiation by central storm shelter		
5.2	Closest approach to the Sun	No Limit		
5.3	All electronics	Radiation-hardened		
6.0	Power Systems			
6.1	Power for Payload	Provided by main vehicle		
6.2	Propulsion reactor	Propulsion Only (no electrical power generated)		
6.3	Initial Solar Panel power density	363 W/m ² (Values are at start of mission at 1 AU)		
6.4	Solar panel areal density	2.42 kg/m ² (Values are at start of mission at 1 AU)		
7.0	Thermal Control			
7.1	Heat rejection for payload	Provided by Main Vehicle		
7.2	Propellant Storage	Cryogenic		
7.3	Deployed radiator areal density, one-sided/two-sided	8.0/4.5 kg/m ²		
7.4	Fixed radiator areal density, one-sided/two-sided	5.0/2.8 kg/m ²		
7.5	Radiator area contingency	20%		
7.6	Optical Properties	End-of-mission Values		

Table 2.3 NTP MSA Phase 2 Ground Rules and Assumptions (con't)

NTP MSA Phase II Ground Rule and Assumptions		Baseline	Reference	Trades
8.0 Payload				
8.1	Total Crew Mass	0.6 mT	JSC DRM v4.0, 1999	
8.2	Crew Consumables	2.45 kg/day/person		
8.3	Cargo 1	51.8 mT		
8.3.1	Surface Habitat	22.8 mT	JSC DRM v4.0, 1999	
8.3.2	Surface Payload	9.9 mT	JSC DRM v4.0, 1999	
8.3.3	Descent Stage (with propellant mass)	19.1 mT	JSC DRM v4.0, 1999	
8.4	Cargo 2	55.8 mT		
8.4.1	Crew Return Vehicle	9.5 mT	Block II ESAS	
8.4.2	Ascent Stage (without propellant mass)	4.8 mT	JSC DRM v4.0, 1999	
8.4.3	Surface Payload	24.4 mT	JSC DRM v4.0, 1999	
8.4.4	Descent Stage (with propellant mass)	17.1 mT	JSC DRM v4.0, 1999	
8.5	Crew Vehicle	36.1 mT		
8.5.1	Transit Habitat	27.5 mT	JSC Trans Hab, 1999	
8.5.2	Crew Exploration Vehicle (CEV)	9.5 mT	Block II ESAS	
9.0				
9.1	Aerobrake	$M_{AB} = \text{SQRT}(M_{PLYD}) \cdot (a + b \cdot V_e) + M_{STR}(\text{mt})$ Where: M_{PLYD} = Mass of captured payload, mt (not incl. shell) V_e = Entry Speed at 125 km Mars altitude, km/s M_{STR} = Aeroshell structure support mass, mt Scaling Coefficients: A = -0.55, b = 0.19	Ames Research Center	
10.0 Main Propellant				
10.1	Residuals on Propellant Mass	3%		
11.0 RCS Propellant				
11.1	Residuals on Propellant Mass	3%		
12.0 Operational Elements				
12.1	X Launch Vehicle	~		
12.1.1	Configuration	Inline shuttle derived		
12.1.2	Earth to Orbit (ETO) Lift Capability	125 mT	ESAS	
12.1.3	Payload Volume	7.5 x 30 m		
12.1.4	Max size of un-shrouded payload	8.4 x 30 m plus nose cone		
12.1.5	Delivery Orbit	55 x 296 km		
12.1.6	Delivery Orbit Inclination	28.5 degree		
12.1.7	Axial Launch Loads	4.0 g		
12.1.8	Lateral Launch Loads	2.5 g		
12.2	Assembly Orbit	407 x 407 km		
12.3	Method of On-Orbit Assembly	Autonomous		
12.4	Post NTP reactor start-up	Proximity operations must be performed within the area protected by the reactor shadow shield		
12.5	Reactor/Crew Operations	Vehicle proximity operations must be within shadow shield for 4 hours after last reactor criticality	Lenard Report	
12.6	Reactor disposal burn	Disposal burn and closest crew occupied vehicle pass must be separated by 1 km		
13.0 Trajectory				
13.1	Mission duration	< 2.5 years		
13.2	Stay at Mars	Long Stay (~ 500-600 days)		
13.3	Earth departure date range	2030-2035		
13.4	Outbound/Inbound Transit Times	<180 days		
13.5	Parking Orbit at Mars	250 x 33793 km		
13.6	V_∞ at Earth	< 8.568 km/sec (< 6.813 km/sec used in previous studies)	ESAS (8.568 km/sec based on 125 km a Altitude entry)	
13.7	V_∞ at Mars	< 5.45 km/sec	JSC DRM v4.0, 1999	
13.8	Mission ΔV	Include gravity losses		
13.9	Design ΔV Mission Coverage	Worst case ΔV 's between 2030-2035 chosen for each major burn.		
13.10	Midcourse correction ΔV	30 m/s prior to each planetary encounter		
13.11	Plane Change at Mars	500 m/s pre TEI		
13.12	All Stage Disposal	non-Earth/Mars crossing heliocentric orbit		

2.3 NTP Vehicle Concepts

The vehicle concepts used for this study were adapted from the NTP MSA Phase 1, Case 4 vehicle concepts. Vehicle sizing was performed using the scaling equations developed in Phase 1 with updated NTP engine masses. The cargo vehicles utilized bi-conic aerobrakes for Mars Aerocapture. The piloted vehicle used NTP propulsion for Mars orbit insertion. Representative vehicle configurations are shown in Figure 2.3

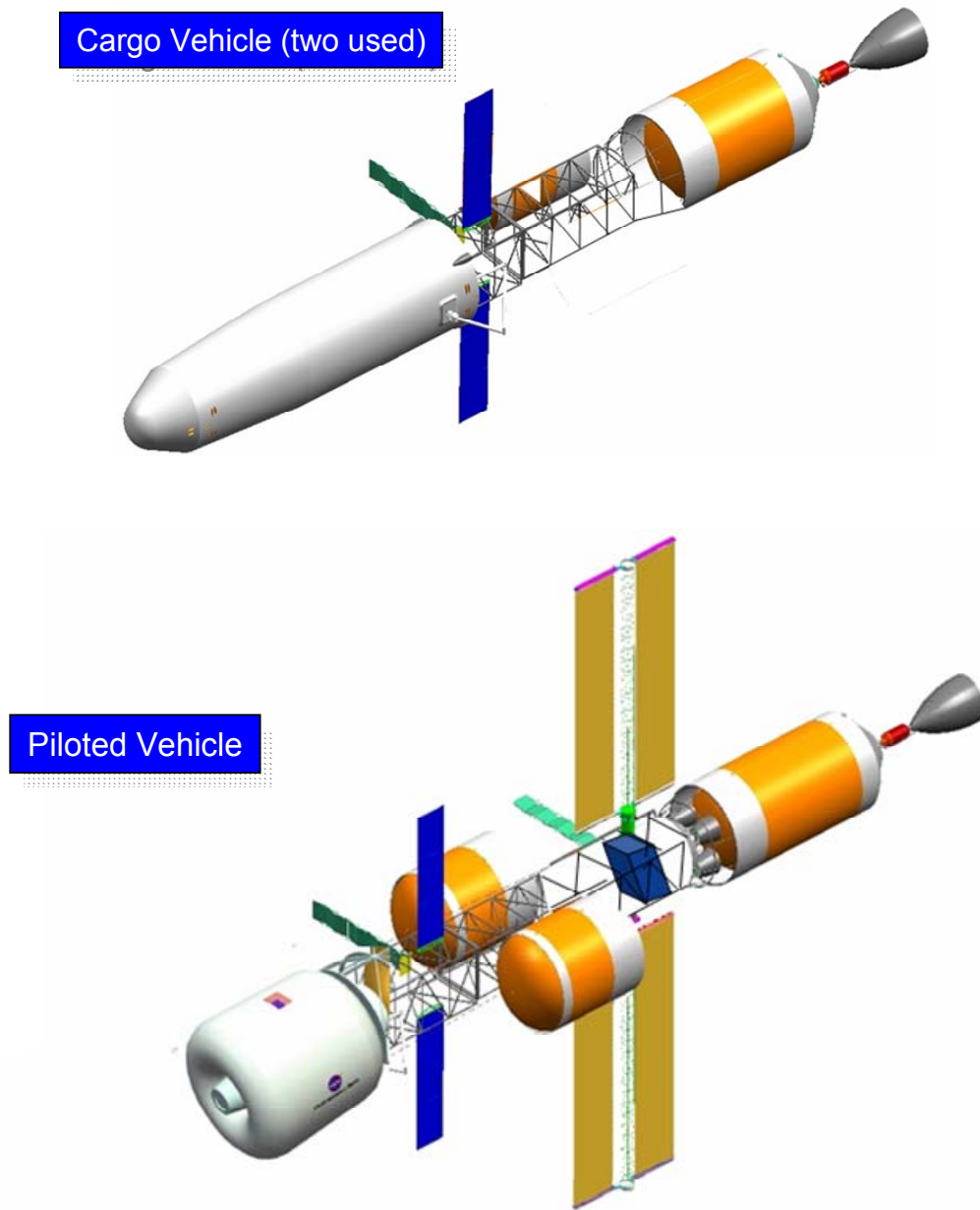


Figure 2.3 NTP MSA Phase 2 NTP Vehicle Concepts.

2.3.1 ESAS Architecture Earth-to-orbit Launch Vehicle Requirements

Each mission to Mars requires a total of eight earth-to-orbit launches. The elements of the Mars transportation systems are assembled in low Earth orbit. The two cargo missions each require two launches. And the piloted mission requires four launches. The required launch vehicle lift capability ranges from 70 to 90 mt. The launch manifest and ETO requirements for the Cargo and Piloted missions are shown in Figure 2.4 and 2.5.

First Mission Opportunity (~2028)

Two separate NTP Vehicles are used

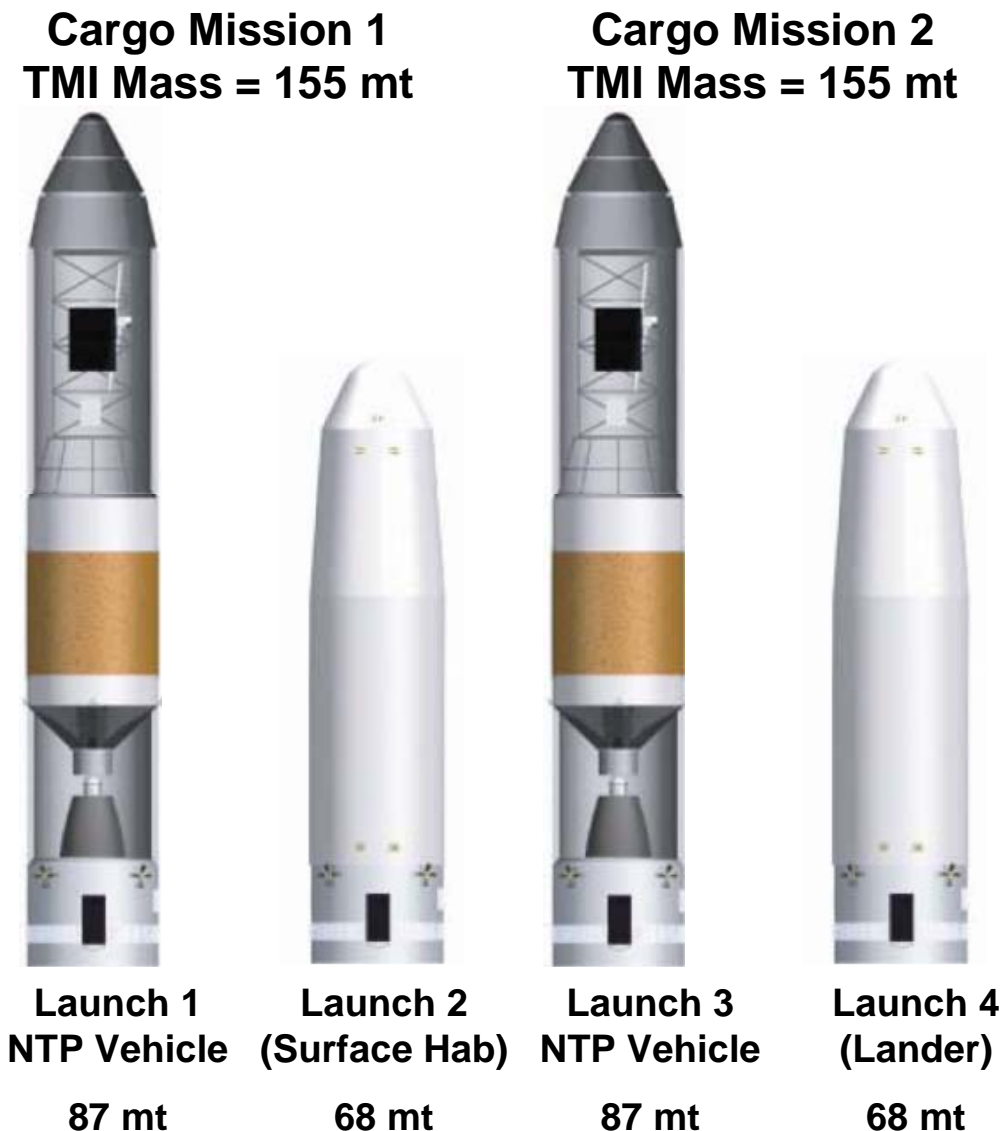


Figure 2.4 Cargo Mission ETO Launch Requirements

Second Mission Opportunity (~2031)

Piloted Mission
TMI Mass = 293 mt

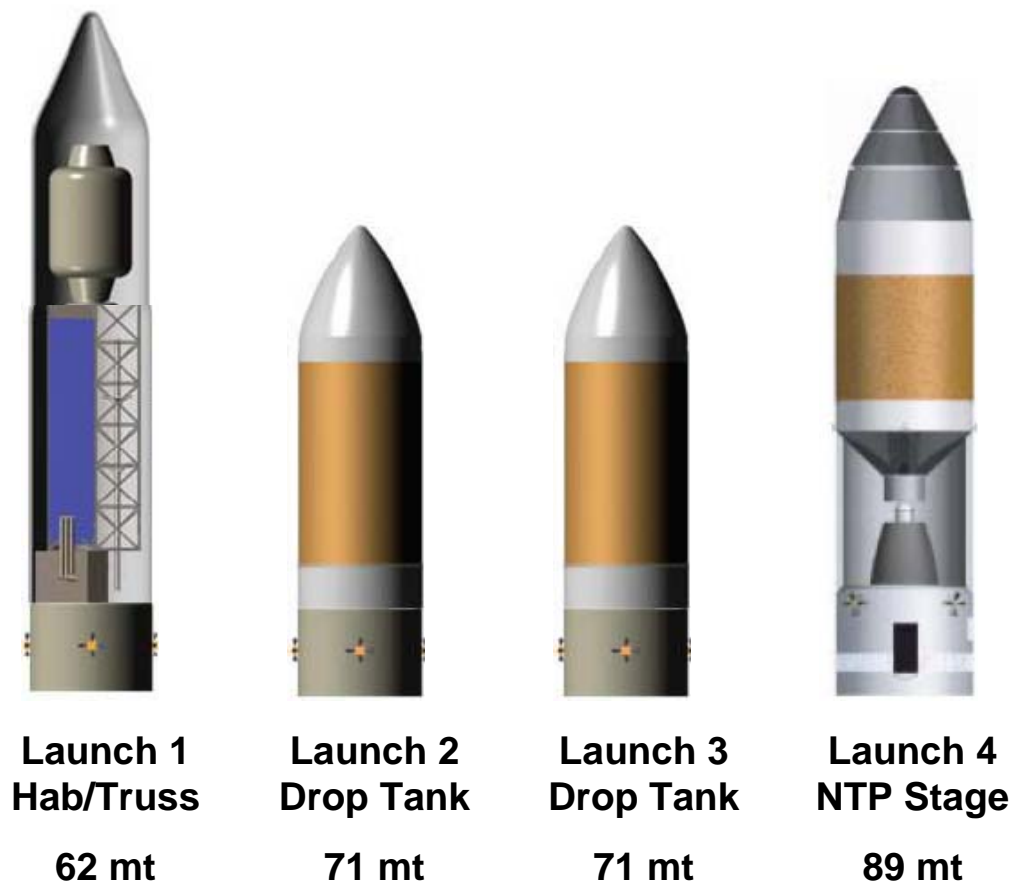


Figure 2.5 Piloted Mission ETO Launch Requirements

3 NTP VEHICLE AND ENGINE SENSITIVITY ANALYSIS

3.1 Integrated Vehicle and Engine Shielding Analysis

The following is a summary of the baseline engine designs for which various parameters were changed to perform the sensitivity trades. The 2 mission vehicle configurations analyzed for this study led to 2 different thrust level requirements: 50 klbf and 75 klbf. In addition several other engines sizes were analyzed, both for possible use in the final vehicle configuration, and to provide sufficient options for the multiple engine vs. single engine trade analysis. Each engine was optimized for minimum mass at an Isp of 875 seconds and a nozzle ratio of 115:1. The engine system extends from the nozzle to the inlet piping system and turbo pumps but did not include the fuel tanks. Although the 2 engines are of different sizes, their configuration is essentially identical with few exceptions. The main differences are physical size and the number of supporting turbo pumps. Each engine limits the turbo pumps to 25,000 rpm and assumes a nominal LH₂ tank pressure of 35 psi. Both designs assume a rechargeable cold gas spin method for the start up. Each design utilizes a nozzle ratio of 115:1 with a short regeneratively cooled section followed by a radiatively cooled extension. Each engine includes an internal radiation shield consisting of BATH for gamma radiation and lead for neutrons. The engine design for each utilizes a solid core, NERVA derivative reactor. Each Reactor core utilizes a number of hexagonal, graphite, fuel elements, 93.15 percent enriched U 235, for every support element loaded with lithium hydride for neutron moderation. The 25 klbf reactor utilizes two fuel elements for each support element; the 50 klbf and 75 klbf reactors utilize three fuel elements for each support element; the 100 klbf, 125 klbf and 150 klbf engines utilize six fuel elements for each support element. The varying fuel element to support element ratio allows additional moderation, provided by the support elements, for the smaller reactors, to further boost their reactivity in order to reach criticality. Reactivity control is primarily achieved by beryllium reflector drums around the core perimeter. All maintain chamber pressures were 500 psi and chamber temperatures were between 2,570 K and 2,606 K.

The sensitivity trades performed as part of this study are the following: external shield configuration (shadow vs. 2 Pi) and design, liquid hydrogen fuel tank shielding feasibility, single vs. multi engine configurations, and current graphite fuel technology vs. potential new fuel technologies. In addition, as part of the trade study, the potential shielding requirements for JSC's crew habitation module were reviewed. Trades were conducted using the 2 baseline architectures. The multi-engine sensitivity analyzed the mass impact on the vehicle. The mass impact is primarily from shielding and secondarily due to small thrust NTR engines are less mass efficient. The shielding impact dominates due to the need to either shield each engine individually or size one, large shadow shield for the entire configuration, closing the interior between the engines to minimize forward scattering. Next a thrust level trade was carried out to see the affects on the vehicle's mass. The engine thrust to weight trades involved comparison of graphite, prismatic fuel elements (NERVA-like) vs. XNR-CERMET and SLHC Foam fuel elements. The potential impact of the GCR (Galactic Cosmic Radiation) on the unshielded crew habitat

is discussed as is the potential for use of the hydrogen propellant tanks for reactor shielding.

3.1.1 Radiation Shielding Requirements Assessment

3.1.1.1 ESMD Reference Mission Shielding Concerns

In planning missions to Mars, it is essential to study potential space radiation damage, especially where humans will be involved in the missions. Radiation in the space environment remains one of the greatest risks to human health. The radiation environment fluctuates considerably over time and location, meaning that the crew will likely require different protection or countermeasure approaches over the course of a long-duration mission. In assessing the transit habitat module of the Exploration Systems Mission Directorate (ESMD), it was determined that the module masses included therein do not appear to adequately accommodate shielding for protection during deep space, piloted missions. This section provides an assessment of radiation shielding requirements for crew protection during a prescribed Mars mission.

It has been determined that the crew habitat module, supplied by NASA-JSC does not include any external shielding at this time. Shielding around the crew habitat will be essential to sufficiently reduce the background GCR (global Cosmic Radiation) that will be present during deep space, manned missions beyond the immediate protection of the Earth's magnetic field. In all likelihood the extent of that shielding will be more than sufficient to handle any additional attenuation from the NTR during scheduled major thrust maneuvers.

Piloted and cargo space vehicles represent different shielding requirements, which largely drive the shield design. Although there are known sensitivities to payload equipment, such as electronics and some structural devices, cargo missions will usually have less restrictive radiation dose criteria than missions involving human crews. Radiation exposure is critical and the reactor and local crew shielding should be optimized for the total dose from natural radiation and the radiation from the reactor. For space missions, most of the radiation exposure is due to galactic cosmic radiation (GCR) and solar particle events (SPEs).

3.1.1.2 Radiation Effects

The use of nuclear reactor power systems in space is frequently accompanied by the presence of nuclear radiations resulting from the large quantities of gamma rays and neutrons that accompany the fission process. Gamma rays and neutrons, because they are so penetrating, can have severe effects on the cells of humans and other animals. Attenuating gamma rays and neutrons, as well as shielding against SPEs and GCR (both of which contain X-rays and other harmful particles), is of most concern in shield design for crewed missions. Conventional shielding involves significant thicknesses of matter used to absorb, attenuate or deflect radiation. From best to worst, typical radiation shielding materials are LH₂, LiH, H₂O, Al, Fe, Pb, etc. The intensity of gamma rays or X-rays decreases exponentially in any absorbing material as a function of mass density.

The absorption of neutrons is more linear, especially if the medium has hydrogen as whole or part of its composition.

The astronaut crew and electronics are most sensitive to radiation damage and dominate the requirements for radiation shielding. Thus, the need for a radiation shield to protect the crew and radiation-sensitive spacecraft equipment and payload from the damaging effects of radiation is paramount. Attenuating gamma rays and neutrons, as well as shielding against galactic radiation, is of most concern in reactor shield design for piloted and cargo missions. The establishment of permissible radiation levels to protect the crew and/or sensitive equipment is one of the major steps in shielding design.

3.1.1.3 Radiation Dose Limits and Sensitivities

Radiation dose limits for spaceflight crewmembers have been established by the ICRP and the NCRP for use by NASA in planning and developing radiation protection strategies for future piloted space missions, including those missions using nuclear power supplies (See Table 3.1).^{1,2} Regulatory requirements have been established for LEO operations to control radiation effects. Currently accepted sex-and age-dependent cancer risks limits are expressed in terms of dose equivalent. Deterministic effect limits pertain to three particularly sensitive tissue (ocular lens, skin, and blood-forming organs (BFOs) over 30-day, annual and lifetime periods.

Table 3.1. Human radiation exposure limits.¹ (1 Sv (Sievert) = 100 rem)

Time Period	Dose Equivalent (Sv)*		
	Blood Forming Organs	Lens of the Eye	Skin
30-day	0.25	1.0	1.5
Annual	0.50	2.0	3.0
Career (10-year)	1.0 – 4.0	4.0	6.0

It is important to note that the above limits are estimates for whole body exposure in the LEO environment (assumed to be mainly proton exposure), and no exposure limits have been established by the NCRP for GCR exposure (although 85% of the radiation is due to proton particles (hydrogen nuclei)). This is because the biological risk to the ions of high charge and energy (HZE) are not known.

Because exposure from cosmic background sources is usually much higher than from the reactor, careful consideration must be given to the radiation shielding requirements of both natural space environments and the on-board reactors in designing spacecraft for both piloted and cargo missions.³ However, in all likelihood the extent of the crew habitat shielding will adequately protect astronauts from any radiation resulting during any major NTR engine thrust maneuvers. In designing for human and equipment protection, the dose rate to equipment has to be considered.

Table 3.2 presents a composite description of typical radiation damage thresholds for certain materials, components, and systems that might be used in a nuclear-powered spacecraft.² The establishment of permissible radiation levels to protect the astronaut

crew and/or sensitive equipment is one of the major steps in the design of a radiation shield.² The natural radiation environment in outer space provides an additional source of exposure concern for the crew and equipment. While not all radiations are of equal importance for shielding, all forms of radiation are potentially harmful to the crew, delicate electronic components on the spacecraft, and other payloads. Therefore, space system planners must include radiation protection as a fundamental design consideration.

Table 3.2. Typical sensitivities to radiation doses. ([†]1 Gy (gray) =100 rad)

Material	Damage Threshold (Gy) [†]
Humans and animals	$10^{-1} - 10^0$
Electronics	$10^0 - 10^4$
Lubricants, hydraulic fluid	$10^3 - 10^5$
Ceramics, glasses	$10^4 - 10^6$
Polymetric material	$10^5 - 10^7$
Structural metals	$10^7 - 10^9$

3.1.1.4 Radiation Shielding Design Requirements and Limitations

The required radiation protection is provided by placing shielding material around the radiation source (in the present case, the reactor) and also around the crew habitat in order to absorb enough particles and energy to reduce the level to one which human beings can tolerate. The local shielding of the crew compartment and shadow shield at the reactor should be distributed in an optimum way to meet the guideline limits of both the annual exposure and short-term exposure. The optimal shield is one which resolves all radiation shielding issues, including those associated with GCR and SPEs, while minimizing the mass of the entire nuclear reactor vehicle system. Because solar flare activity can be monitored, it is assumed that a warning system can be provided so that the crew can take shelter in a “storm cellar” in the event of anomalously large solar particle events (ALSPEs).

Unlike LEO, which is often dominated by trapped radiation, deep space exposure is dominated by GCR. Currently, insufficient data exists on the biological effects of GCR, meaning that specific exposure requirements for deep space operations have not been established. The quantities and limits defined from LEO operations are normally used for all mission studies, but the scientific and regulatory communities can hardly be expected to retain these standards when concrete planning for beyond LEO commences in earnest.

Detailed analysis has shown that the main limitation of shielding design for deep space results from uncertainty in applying the known risk coefficient—with their own associated uncertainty—to the space exposures and not the related evaluation of exposure conditions. The greatest uncertainty arises from the uncertainty in the relative biological effectiveness of different radiation types (or quality factor) while the remaining uncertainty in risk coefficients from other sources is comparable to uncertainty arising from the estimation of LET-related dose contributions in specific tissues for the specific space shielding.

3.1.1.5 Radiation from GCRs & SPEs

Crew shielding provides some protection from cosmic rays. Unfortunately much of the cosmic ray flux is at high energies and the massive amount of shielding required to stop it is impractical. The cosmic ray intensity does vary with the 11-yr solar activity cycle, which is a recording of solar flare activity, so missions to Mars could be restricted to the phase of cycle when the galactic cosmic ray intensity is low. Unfortunately, the phase of lowest cosmic ray intensity during the cycle coincides with the period when solar flares are most likely. One would have to rely on a massive onboard storm shelter to avoid additional radiation exposures from solar flares. Also such launch window restrictions would have an adverse programmatic impact.

Galactic cosmic rays (GCRs) are relatively constant in terms of distribution of particle types and energies over time, but they do decrease in intensity by roughly a factor of 10 during solar events because the increased energy emitted from the sun produces an increased interplanetary magnetic field that deflects a large fraction of the galactic cosmic rays. This change in intensity is a variation with time and does not reflect uncertainty in our knowledge of the spectrum. The uncertainty lies in our ability to predict the intensity over appropriate periods of time. The variability of the instantaneous galactic cosmic ray intensity is approximately a factor of 10, but the probability of solar events occurring varies cyclically with the periodicity of the 11-year solar cycle, and thus planetary missions would be less exposed to galactic cosmic rays during solar maximum. Therefore, depending on when missions are flown, variation in cosmic ray intensity may not be a major factor in the uncertainty of risk estimates for radiation exposure. Nevertheless, the uncertainty in the absolute amount of particles and their energies is significant to factors of 2 to 4 at the modal energies, but with larger uncertainties at the lower particle energies.

Solar particle events (SPEs) produce substantial intensifications of the most energetic particles (including protons, heavier ions and electrons) emanating from the sun. The risk of harmful effects to space crews is generally assumed to be primarily from the protons and to a lesser extent, the heavier particles, which are relatively less abundant than in the case of cosmic rays.

The galactic cosmic radiation provides a steady radiation dose to the crew and is a long-term hazard to the health of the crew. In contrast the solar particle events present a short-term hazard and jeopardize the success of the flight. In addition, radiation plays a significant role in the performance of electronic devices, particular concern being single event upsets and latch-ups. Although no radiation safety levels for long-term stay in space have been established most recent research on space radiation protection cites the space workers' radiation limit of 50 rem per year, which was set by the National Council on Radiation Protection (NCRP) for LEO. Based on this limit, Simonson and Nealy (1991) have shown that small uncertainties in calculated dose-equivalent lead to a very large penalty in the shielding mass, and hence the total mission mass. Their calculations show that under 1991 radiation environment models, the ICRP-26 definition of linear energy transfer dependent quality factor, and current model of fragmentation cross-sections, the dose-equivalent received by the crew under 2 g cm⁻² of aluminum shielding,

will lead to a dose-equivalent at the allowable limit, and a 30% uncertainty in rem dose leads to a 200% increase in the shielding mass. It is thus important to develop an accurate model of the galactic cosmic radiation in free space.

Exposures can be reduced for specific missions through planning, technology choices, and shielding. A number of approaches are available to limit radiation exposure to space-faring crews. For example, limiting the launch windows to coincide with solar cycle variation reduces GCR exposure but introduces a rising risk of SPE exposure. Shielding against the radiation environment involves the entire spacecraft, meaning that apparently simple design choices (e.g., aluminum structures as opposed to polymer composites) can have adverse effects on radiation exposures^{7,8}. Shielding during every aspect of the mission is necessary to assure crew safety, health, and performance. For example, the minimal protection afforded by spacesuits and rovers (due to mobility requirements) requires that careful attention is devoted to developing a shelter for SPE storms.

3.1.2 Hydrogen Tank Shielding Assessment

Liquid hydrogen has been shown to be effective in absorbing neutron and, to some degree, gamma radiation. For the point of departure design of our study, it has been determined that the amount of hydrogen propellant required to absorb neutrons from the reactor for crew protection is about 1m. (Lenard, et al, ref. 2006) However, regarding the current point of departure study, there are several issues surrounding the use of the propellant tank that limit its effectiveness for shielding.

Another recurring issue concerning external shielding of sensitive equipment and personnel forward of an NTR engine has been the use of the liquid hydrogen fuel tanks for radiation shielding. The presence of hydrogen, in any form, will always provide attenuation of high energy particles, such as neutrons emitted from fission. The presence of hydrogen, although far less effective than heavy metals, will also provide absorption of gamma radiation, which is the other penetrating radiation concern resulting from fission. In sufficient quantities liquid hydrogen can be argued to be of sufficient shielding value to eliminate the need for external shielding of an NTR engine.

For this reason, during this study, consideration was given to removing the neutron portion of the shadow shield between the reactor and the spacecraft, in lieu of a centerline hydrogen tank. A hydrogen tank would provide neutron shielding and, as mentioned above, some degree of gamma shielding. The use of a shadow shield versus a centerline LH2 tank produces a matrix of Mars architecture design configurations that are fundamentally different from the previous Mars vehicle study architecture and would require fundamental redesign.

An important factor involved in this configuration trade is the quantity of liquid hydrogen that will be needed to provide adequate decay heat removal after the reactor is shutdown, subsequent to each and every burn. A 3% reduction to the ISP of all burns has been applied to account for the small degree of performance loss during reactor start up, shut

down, initial core cool down and subsequent decay heat build up removal. The 3% reduction is drawn from “AIAA 93-2506, *Decay Heat Removal Option in Nuclear Thermal Rocket Engines*, L. Felton, C. Dunn, Rockwell International, Canoga Park, CA, AIAA 29th Joint Propulsion Conference, July 1993”.

Early in this study 13,000 kg of LH2 was estimated to be needed for the final mission NTR burn, the TEI (Trans Earth Injection) burn along with another 200 to 300 kg for the disposal burn. This estimate also assumed a 50 klbf engine would be sufficient. Assuming the TEI burn is the final burn combined with the original assumption of 3% (for 13,000 kg that would be 390 kg) the fuel remaining for decay heat removal and disposal burn would be only 690 kg optimally. Adding additional fuel for no other reason than to provide adequate neutron shielding at the end of the TEI burn and into the post shut down power decay represents potential dead weight carried throughout the mission. Utilizing the shield tool, noted in the previous section, the mass of the neutron and gamma shield of a shadow shield for a 50Klbf engine were determined. Assuming electronics are at least 10 meters forward of the shadow shield the neutron attenuation section of the shield (Lithium-Hydride) is 2931 kg. Sensitive electronics are likely farther away, but 10 meters is conservative. The logical conclusion is the additional LH2 carried as dead weight, for shielding purposes must be less than this amount to be of consideration as an alternative to hard shielding.

An important issue to be considered is that subsequent to the TEI burn the vehicle experiences zero acceleration and a partially filled LH2 tank could not be relied upon to maintain consistent LH2 shielding thicknesses as the fuel disperses throughout a partially filled tank. An Estimate of the mass of fuel contained within a minimum tank of 3 meters length, 4.86 meters diameter, including the two dome heights was determined. A liquid hydrogen run tank any shorter would become dome to dome, not providing the minimum of 1 meter of LH2, best case, to ensure adequate neutron attenuation (*Report on Shielding Effects of Hydrogen Contained in Propellant Tanks*, Lt. Col. Roger X. Lenard, GPS Solutions, Inc.). An analysis of the minimum diameter needed for the tank with the bottom of the tank immediately forward of the NTR support/feed system structure determined a minimum tank diameter of no less than 4.86 meters in order to provide a 26.6 degree shadow shield half angle. The mass of fuel in a 3 meter long, 4.86 meter diameter tank was determined to be 5,473 kg. The tank being full ensures consistent LH2 thickness in a zero-g environment and therefore represents the absolute minimum fuel tank size and fuel mass that must be present after the final TEI burn.

The LH2 dead weight for the 3% reduction logic is 4,783 kg (5,473 kg for the minimum possible tank size to ensure shielding – 690 kg needed for decay heat removal and disposal burn) compared to the Lithium-Hydride shield section mass of 2,931 kg. Utilizing Lithium-Hydride for neutron shielding is 1,852 kg lighter than using LH2, under conditions most favorable for LH2.

One final consideration is the safety concerns of using LH2 for shielding. There are many scenarios that can be envisioned that would lead to the LH2 tank unexpectedly venting, leaving the crew and equipment exposed to harmful radiation levels. An event

that would be sufficient to remove a hard shadow shield, made of Tungsten and Lithium-Hydride, would likely be of such impact as to have completely destroyed the spacecraft.

3.1.3 External Shield Trade Study

The most basic design for an NTR engine system utilizes a single, large reactor with several flow paths. For this configuration an external shadow shield is the default design option except in extreme cases requiring large shadow angles combined with close proximity of sensitive equipment and/or personnel. When considering clustering NTR engines several issues must be considered. Radiation emitted from the engines both during operation and during shutdown has the potential to scatter forward toward the crew and equipment unless blocked by an extended shadow shield or individual 2 Pi shields. Also, during operation, neutrons escaping one reactor have the potential of affecting the reactivity of the other reactors in the cluster, unless shielded by individual 2 Pi shields. Between the two choices of shielding, the 2 Pi shield approach provides coverage for both scattering and reactivity interaction. An extended shadow shield, although not shielding against reactivity interaction, remains a viable option due to the sizable distance between the reactors. Considering nozzle ratios of at least 115:1 and the clearance needed between their exit planes, the resulting distance between the reactors likely reduces reactivity interaction to minimal. Setting this issue aside the choice between individual 2 Pi shields and one extended shadow shield is governed by minimum mass. Due to the interaction of many different parameters, such as the distance to the dose plane and the shadow shield's half angle, the choice of minimum mass shield configuration is not always readily apparent.

The first step in the engine comparisons was an extensive review of the shielding impact to engine system mass for dose plane distance and shadow shield half angle, for one, two and three engine configurations. This was accomplished with the development of a shielding simulation program capable of handling a 2 Pi shield design as well as a shadow shield design, for up to three engine cluster configurations. In the multiple engine configurations it was assumed the reactors were placed side by side, in the two engine configuration, and in a triangular formation for a three engine cluster. Spacing between the reactors was governed by maintaining a one meter clearance between the outer nozzle exit diameters of each engine. The overall shield geometry for the shadow shield is shown in Figure 3.1 and the 2Pi shield in Figure 3.2. The two engine configuration, without shielding, is shown in Figure 3.3 and the three engine configuration, without shielding, is shown in Figure 3.4.

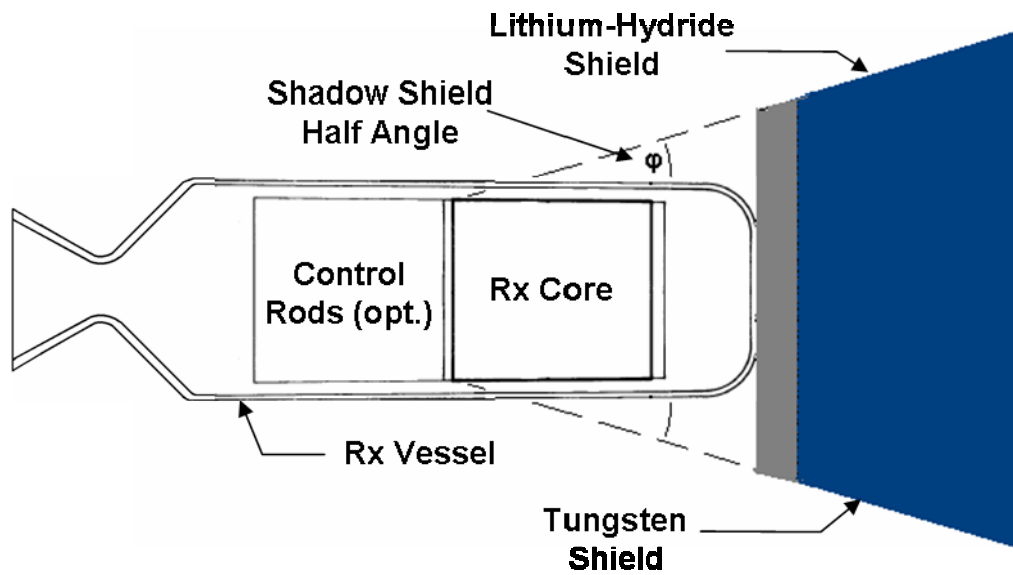


Figure 3.1: Shadow Shield Configuration

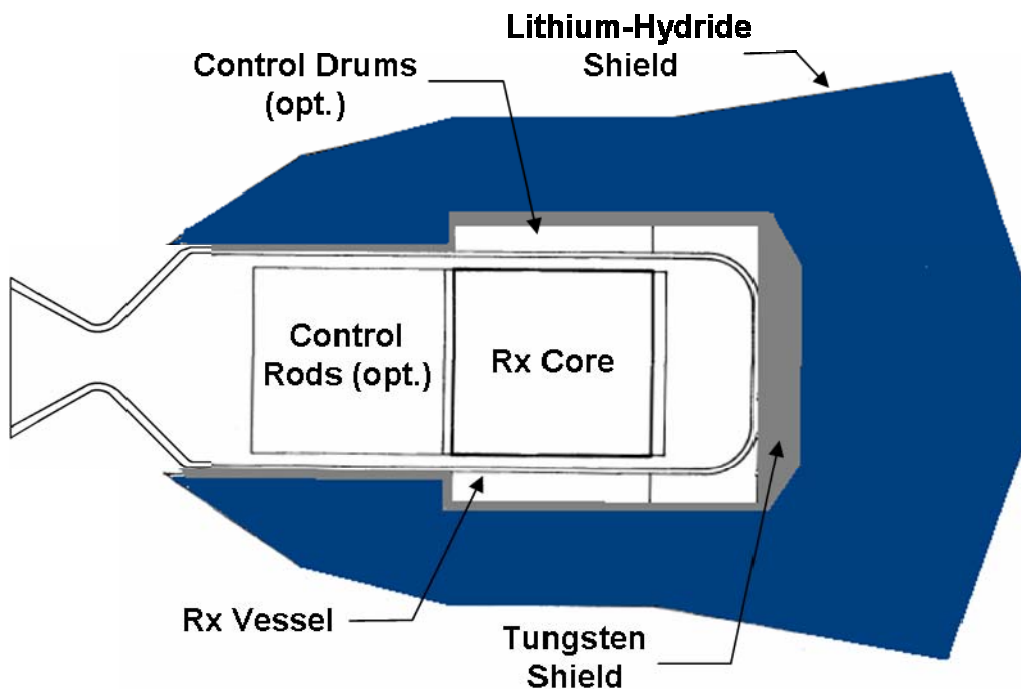


Figure 3.2: 2 Pi Shield Configuration



Figure 3.3: Two Engine Configuration with shadow shield cross-section



Figure 3.4: Three Engine Configuration with shadow shield cross-section

A series of trades were analyzed with the shield program XTSHIELD, written for MSFC/NASA, varying the number of engines, dose plane distance and shadow shield half angle.

The first series of graphs, shown in Appendix A, compare the mass of a 2 Pi shield vs. a shadow shield, for all six engine thrusts, over a range of shadow shield half angles, from 10 to 45°, for a given number of engines and dose plane distances. In all cases the mass of the 2 Pi shield is constant as it is not affected by shadow shield half angle. Each of the fifteen graphs includes curves for the 2 Pi and Shadow shields for each of the six engine thrust levels.

The second series of graphs, shown in Appendix B, compare the mass of a 2 Pi shield vs. a shadow shield, for all six engine thrusts, over a range of dose planes, from 10 to 100 meters, for a given number of engines and a shadow shield half angle of 26.6°. Each of the three graphs includes curves for the 2 Pi and Shadow shields for each of the six engine thrust levels.

The final series of graph, shown in Appendix C, combine the variation of dose plane, from 10 to 100 meters, to shadow shield half angle, from 10 to 45°, to produce a carpet plot of shield mass. The series of eighteen graphs cover the variation in engines, from one to three, and engine thrust levels. In order to generate one carpet plot the mass scale is actually a “difference”. At each data point the mass of the 2 Pi shield, at that congruence of dose plane and shadow shield half angle, is subtracted from the mass of the shadow shield, at that same combination of parameters. Any negative result (i.e.: the 2 Pi shield mass exceeded the shadow shield mass) is artificially set to zero. This leaves a single carpet plot that clearly shows where a shadow shield’s mass exceeds the 2 Pi shield mass, at that combination of parameters. In all cases this carpet plot rises (i.e.: heavier shadow shield) in the corner combination of high shadow shield half angles and relatively short dose planes. Where the carpet plot rises about zero is an indication that a 2 Pi shield, even in some cases for a single engine, is the better choice, from a minimum mass perspective.

The overall results of the shielding study, assuming a 26.6° shadow shield half angle are shown in Figure 3.5 defining the range of dose planes and thrust levels for the single, double and triple engine configurations for which a shadow shield or 2 Pi shield design would produce the lightest weight.

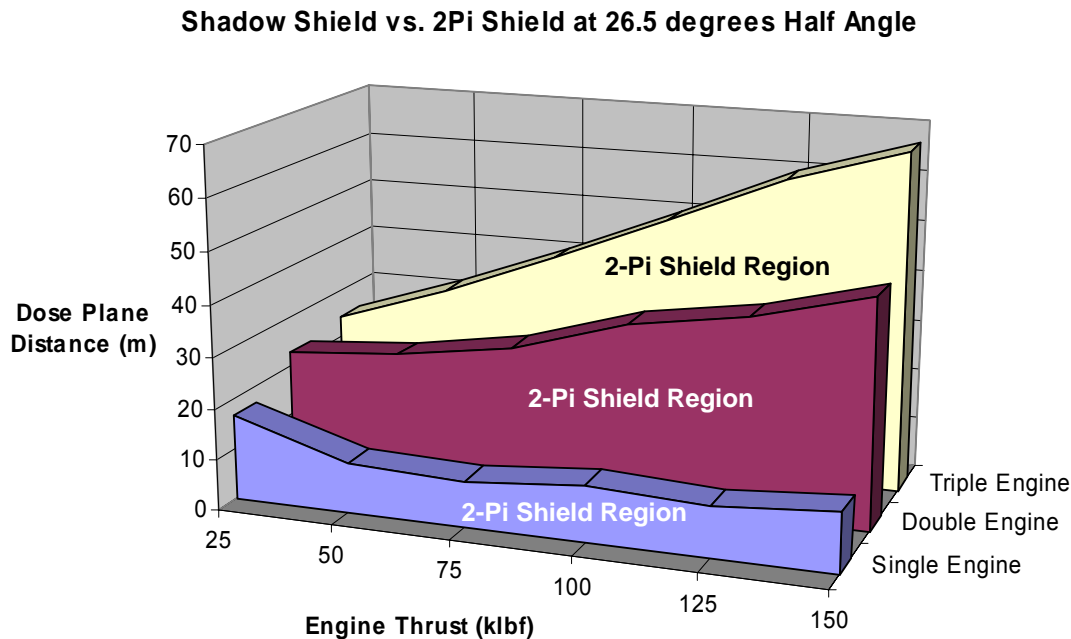


Figure 3.5: Range of 2 Pi Shield Preference for Minimum Mass (26.6° Half Angle)

3.2 NTP Engine Sensitivities

3.2.1 Single vs. Multiple Engine Trade

In addition to shielding issues the reactors themselves affect total mass. In order to maintain as balanced a power distribution as possible all reactors tend to be surrounded by fixed or adjustable neutron reflectors. This in turn leads to a consistent economy of scale for all reactors. As additional fuel elements are added, in concentric rings, total reactor power increases non-linearly with total reactor mass. As a result one large reactor will always deliver a given thrust, at a lower total mass, than two smaller reactors.

The NESS (Nuclear Engine System Simulation) Program, originally designed for and still in use by GRC/NASA, recovered from the COSMIC database and restored for use at MSFC/NASA, was used to size NTR systems for six different thrust levels, 25 klbf, 50 klbf, 75 klbf, 100 klbf, 125 klbf and 150 klbf. In each case the algorithm was iterated to produce the lowest mass for a given ISP of 875 sec. Each engine included two axial turbopumps, limited to 25,000 RPM, the lightest fuel option (graphite), a nozzle ratio of 115:1 and a chamber pressure of 500 psi. The chamber temperature was varied for each engine, which ranged from 2570 K to 2606 K, to produce the desired ISP. All engines were designed for 60 minutes total lifetime, with a single,

rechargeable, cold gas spin start up tank. The resulting engine masses, without external shielding, are given in Table 3.3.

Table 3.3 NTR Engine Masses

Thrust	25 klbf	50 klbf	75 klbf	100 klbf	125 klbf	150 klbf
Engine Mass	3917.7 kg	4725.8 kg	5651.4 kg	6887.2 kg	7497.6 kg	8997.3 kg

A mass comparison of potential unshielded engine clusters, based on the engine sizes above, is presented in Figure 3.6. The economy of scale, favoring a single reactor, over several smaller engines in a cluster, is readily apparent. This comparison does not include the effects of shielding, which will be reviewed in the next section.

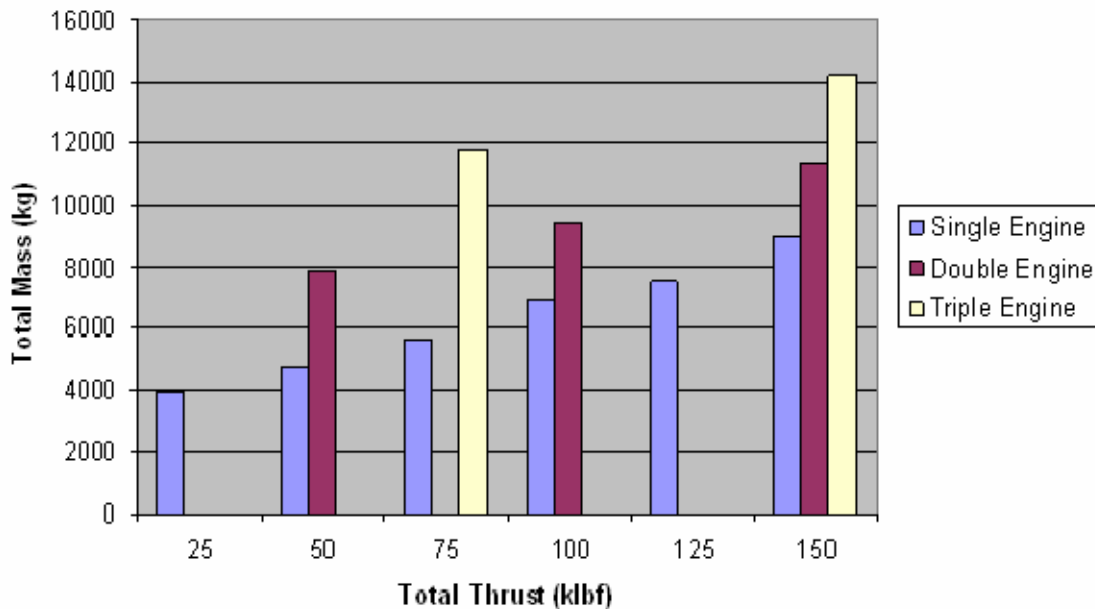


Figure 3.6: Unshielded Engine Cluster Mass Comparison

3.2.1.1 Detailed Shielded Engine Trade Space

Further vehicle definition determined a cargo vessel and piloted vessel would be developed separately. In both cases the shadow shield half angle was defined to be 26.6° while the dose plane was dependent on the vehicle. For the cargo vehicle the dose plane was defined to be 25 meters, while the piloted vehicle was defined to be 44 meters. These definitions allowed for a matrix of single, double and triple, shielded, graphite, prismatic fuel element engine configurations to be developed for each vehicle. The cargo vehicle matrices are displayed in Tables 3.4 through 3.6 while the piloted vehicle matrices are displayed in Tables 3.7 through 3.9.

Table 3.4: Cargo Vehicle, Single Engine Configuration

Total Thrust	25 klbf	50 klbf	75 klbf	100 klbf	125 klbf	150 klbf
Total Engine Mass (kg)	3917.7	4725.8	5651.4	6887.2	7497.6	8997.3
Shield Configuration	Shadow	Shadow	Shadow	Shadow	Shadow	Shadow
Shield Mass (kg)	2339.3	3137.4	3718.6	4550.0	4831.1	5764.7
T/W Ratios No Shld/Shld	2.89/1.81	4.79/2.88	6.01/3.63	6.58/3.96	7.55/4.59	7.55/4.60
Total Mass (kg)	6257.0	7862.8	9370.0	11437.2	12328.7	14762.0

Table 3.5: Cargo Vehicle, Double Engine Configuration

Total Thrust	50 klbf	100 klbf	150 klbf	200 klbf	250 klbf	300 klbf
Total Engine Mass (kg)	7835.4	9451.6	11302.8	13774.4	14995.2	17994.6
Shield Configuration	Shadow	Shadow	2 Pi	2 Pi	2 Pi	2 Pi
Shield Mass (kg)	5607.2	8836.4	10848.6	12299.7	13577.7	15180.4
T/W Ratios No Shld/Shld	2.89/1.68	4.79/2.48	6.01/3.07	6.58/3.47	7.55/3.96	7.55/4.10
Total Mass (kg)	13442.6	18288.0	22151.4	26074.1	28572.9	33175.0

Table 3.6: Cargo Vehicle, Triple Engine Configuration

Total Thrust	75 klbf	150 klbf	225 klbf	300 klbf	375 klbf	450 klbf
Total Engine Mass (kg)	11753.1	14177.4	16954.2	20661.6	22492.8	26991.9
Shield Configuration	Shadow	2 Pi	2 Pi	2 Pi	2 Pi	2 Pi
Shield Mass (kg)	8795.7	13287.8	16272.9	18449.5	20366.5	22770.6
T/W Ratios No Shld/Shld	2.89/1.65	4.79/2.47	6.01/3.07	6.58/3.47	7.55/3.96	7.55/4.10
Total Mass (kg)	20548.8	27465.2	33227.1	39111.1	42859.3	49762.5

Table 3.7: Piloted Vehicle, Single Engine Configuration

Total Thrust	25 klbf	50 klbf	75 klbf	100 klbf	125 klbf	150 klbf
Total Engine Mass (kg)	3917.7	4725.8	5651.4	6887.2	7497.6	8997.3
Shield Configuration	Shadow	Shadow	Shadow	Shadow	Shadow	Shadow
Shield Mass (kg)	1149.4	2009.8	2569.7	3218.1	3526.4	4243.1
T/W Ratios No Shld/Shld	2.89/2.23	4.79/3.36	6.01/4.13	6.58/4.48	7.55/5.14	7.55/5.13
Total Mass (kg)	5067.1	6735.6	8221.1	10105.3	11024.0	13240.4

Table 3.8: Piloted Vehicle, Double Engine Configuration

Total Thrust	50 klbf	100 klbf	150 klbf	200 klbf	250 klbf	300 klbf
Total Engine Mass (kg)	7835.4	9451.6	11302.8	13774.4	14995.2	17994.6
Shield Configuration	Shadow	Shadow	Shadow	Shadow	Shadow	2 Pi
Shield Mass (kg)	2743.3	5662.3	7942.8	10171.5	11941.3	14132.0
T/W Ratios No Shld/Shld	2.89/2.14	4.79/3.00	6.01/3.53	6.58/3.78	7.55/4.20	7.55/4.23
Total Mass (kg)	10578.7	15113.9	19245.6	23945.9	26936.5	32126.6

Table 3.9 : Piloted Vehicle, Triple Engine Configuration

Total Thrust	75 klbf	150 klbf	225 klbf	300 klbf	375 klbf	450 klbf
Total Engine Mass (kg)	11753.1	14177.4	16954.2	20661.6	22492.8	26991.9
Shield Configuration	Shadow	Shadow	Shadow	2 Pi	2 Pi	2 Pi
Shield Mass (kg)	4292.7	9749.3	14456.1	17204.1	19008.2	21198.0
T/W Ratios No Shld/Shld	2.89/2.12	4.79/2.84	6.01/3.24	6.58/3.59	7.55/4.09	7.55/4.23
Total Mass (kg)	16045.8	23926.7	31410.3	37865.7	41501.0	48189.9

The mass comparison of potential shielded engine clusters for the cargo vehicle is presented in figure 3.7. A similar mass comparison for potential shielded engine clusters for the piloted vehicle is presented in figure 3.8. The economy of scale, favoring a single reactor, over several smaller engines in a cluster, is readily apparent. This impact is slightly more pronounced between a single engine and two engines as the external shield configuration is shifting to an extended shadow shield or several 2 Pi shields, both intrinsically heavier than a single, simple shadow shield for one larger engine.

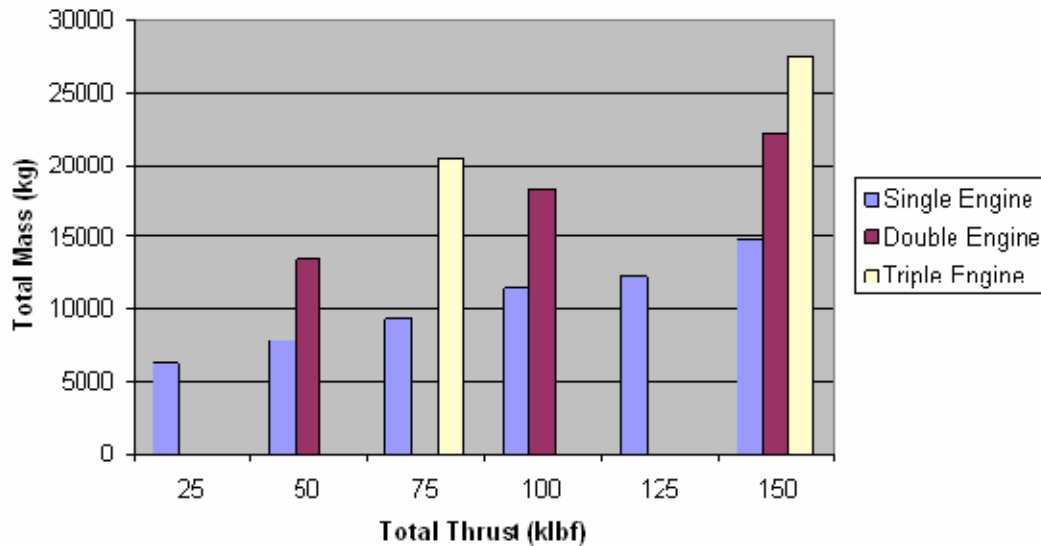


Figure 3.7: Cargo Vehicle Shielded Engine Cluster Mass Comparison

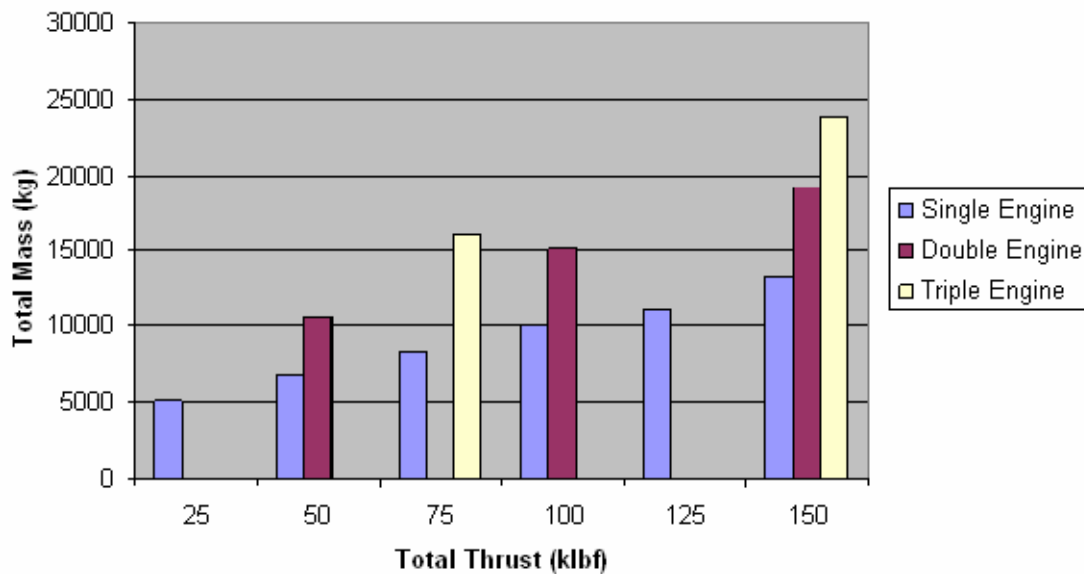


Figure 3.8: Piloted Vehicle Shielded Engine Cluster Mass Comparison

Figures 3.9 and 3.10 show the effect of multiple engines on the total vehicle mass at Earth departure for various thrust levels. The charts also show the effect of total thrust level on NTP engine burn time. In this study it was assumed that we would not want to significantly exceed 60 minutes of engine burn time.. A single 75 klbf thrust engine was selected as the recommended engine for the ESAS reference architecture.

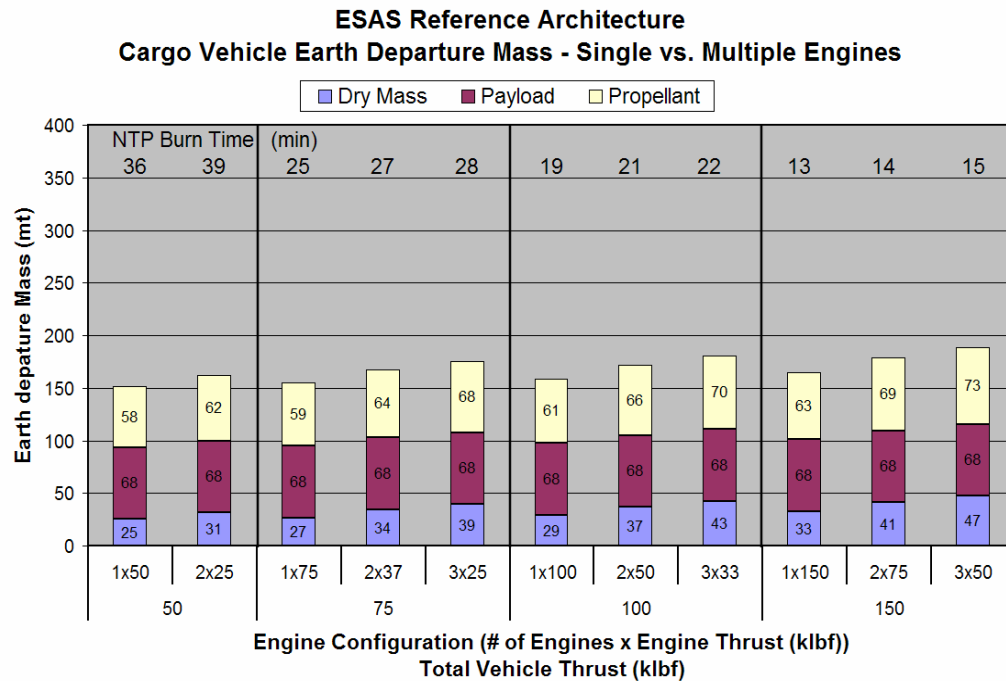


Figure 3.9 Single vs Multiple NTP Engine Trade - Cargo Vehicle Mass

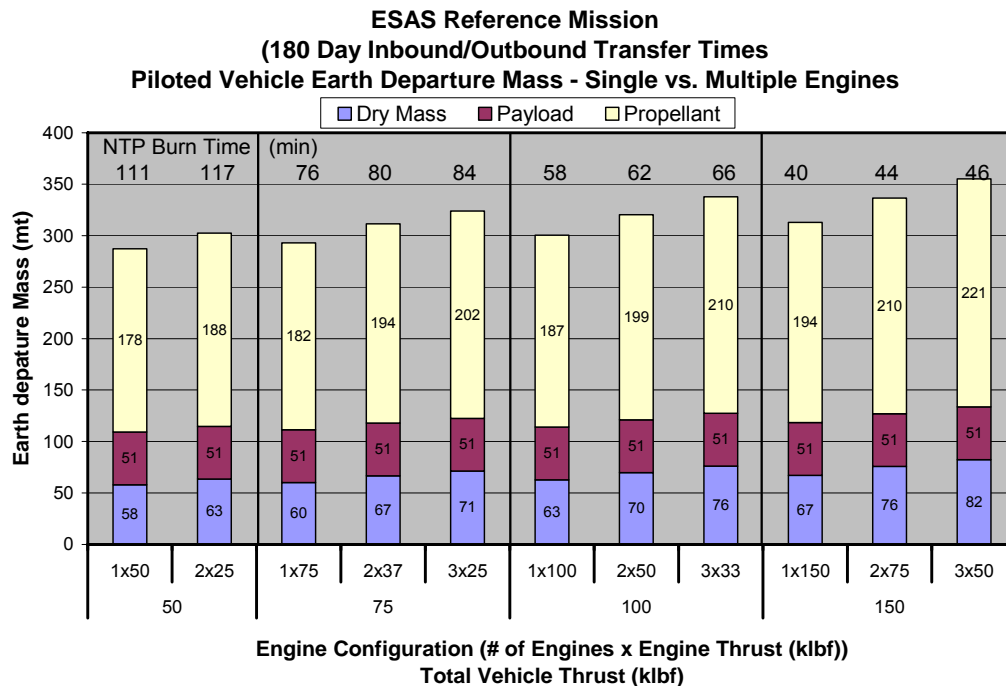


Figure 3.10 Single vs Multiple NTP Engine Trade - Piloted Vehicle Mass

3.2.2 Mars Transfer Time Sensitivity Trade

Figure 3.11 show the effect of interplanetary trajectory transfer time on the total Earth departure mass for two NTP engine options, a single 75 klb thrust engine or two 50 klb thrust engines. The mass of the vehicle increases dramatically for trip times under 140 days.

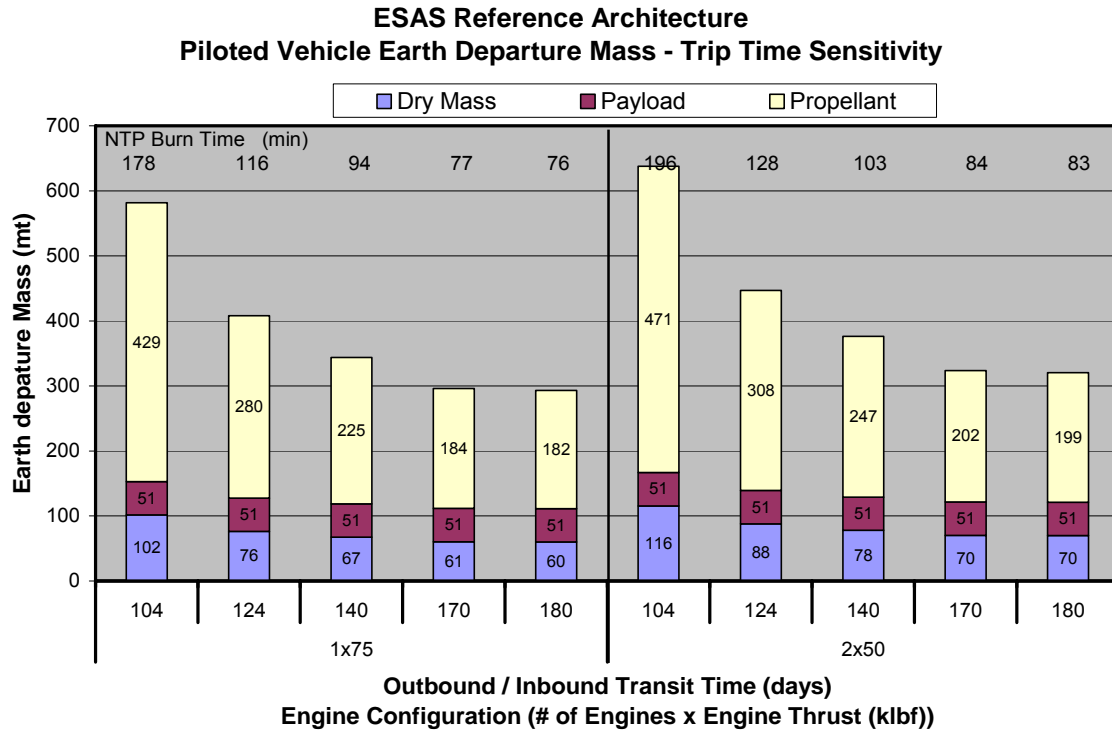


Figure 3.11 Piloted Vehicle Mass Sensitivity to Transfer Trip Time

3.2.3 Graphite Prismatic Fuel Elements vs. New Technologies

Another area of comparison was between present, close to state of the art technology vs. newer fuel element technology. Although graphite fuel element technology has not been proven it is very likely at the reasonable cutting edge that can be developed when a true commitment is made to build the next NTR engine. More advanced fuel technologies, like XNR-CERMET and SLHC/FOAM will likely require significant research and development to both develop and make applicable to the NTR operational environment. As with Particle Bed technology proposed during the TIMBERWIND program, new fuel technologies often appear attractive, in theory, but thorough vetting under operational conditions demonstrates engineering challenges that are fundamentally intrinsic to the extreme performance demands of an NTR engine. Based on Thrust to Weight comparisons provided by the Nuclear Systems Office at Marshall Space Flight Center a comparison of present graphite technology to these two theoretical improvements is presented in Table 3.10 and Figure 3.12.

Table 3.10: Graphite Fuel Element Engine Mass vs. Improved Fuel Theories (unshielded)

Total Thrust	25 klbf	50 klbf	75 klbf	100 klbf	125 klbf	150 klbf
Graphite Element Engine Mass (Isp = 875 s)	3917.7	4725.8	5651.4	6887.2	7497.6	8997.3
XNR-CERMET Engine Mass (Isp=925 s)	2178.0	2430.0	4299.0	5092.0	5836.0	6469.0
SLHC-FOAM Engine Mass (Isp=975 s)	1665.0	2177.0	2784.0	3021.0	3473.0	3882.0
Graphite Element T/W	2.89	4.79	6.01	6.58	7.55	7.55
XNR-CERMET T/W	5.20	6.60	7.90	8.90	9.70	10.50
SLHC-FOAM T/W	6.80	10.40	12.20	15.00	16.30	17.50

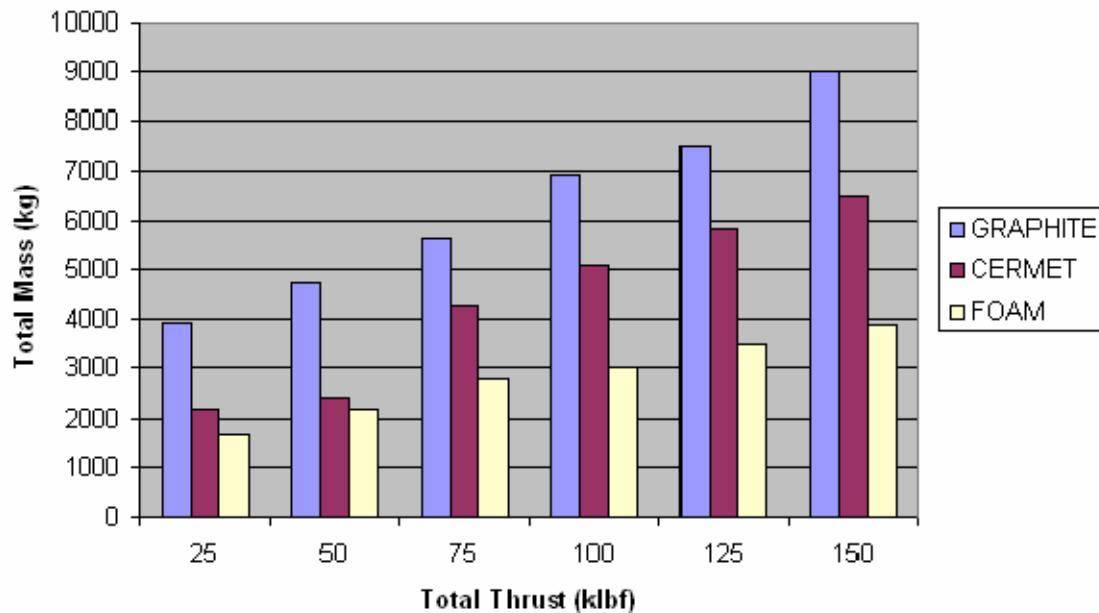


Figure 3.12: Graphite Fuel Element Engine Mass vs. Improved Fuel Theories (unshielded)

4 NTP ENGINE DEVELOPMENT COST ANALYSIS

This report describes the cost analysis activities conducted as a follow-on to the Nuclear Thermal Propulsion (NTP) Mission and Systems Analysis (MSA) study that concluded in the summer of 2005. NTP MSA was an adjunct to the Mars Exploration Propulsion Technology (MEPT) study. This brief follow-on effort focused on the new engine size, a new cost estimating approach to the engine analysis, adjustments to several other cost elements, e.g., launch, structures, and a comparison of the follow-on to the NTP MSA results. Additionally, the results of this effort were compared to a bottoms-up cost analysis conducted by the Nuclear Systems Office (NP50).

Previous cost analysis (Design, Development, Test & Evaluation (DDT&E) and unit cost) for the NTP engine had focused upon analogies to the NERVA program. Several weaknesses were identified for the use of this analogy including, granularity of data, data provenance, and the technology gap of a program some four decades past.

The new approach of estimating the cost of the reactor engine was to use an analogy from a liquid rocket engine, or various engines, and cost the reactor segment separately. With the design of the reactor engine broken into subsystems, the performance characteristics and requirements were compared to the J-2, RL-10, and the SSME.

After careful assessment of the subsystems, Dr. Robert Chiroux determined that the SSME was the best analog for each of the elements and that the most likely one-to-one comparison was for the 250Klbt reactor engine. Dr. Chiroux developed a scaling factor to be applied for thrusts less than 250Klbt, all the way down to 50Klbt. Costs for the SSME subsystems were applied to the reactor engine at the appropriate thrust. A factor was also developed from NAFCOM for below-the-line costs, e.g., program management, system integration.

This approach was used for DDT&E and Unit cost for the non-nuclear elements of the reactor engine, e.g., turbopumps, nozzle. For the DDT&E nuclear component cost, the estimate used the Rough Order of Magnitude (ROM) cost derived by the MEPT propulsion panel and is considered expert opinion. For the unit cost, the estimate employed the unit cost from Rick Ballard and is considered expert opinion. The results of the NTP engine cost analysis are shown in Table 4.1

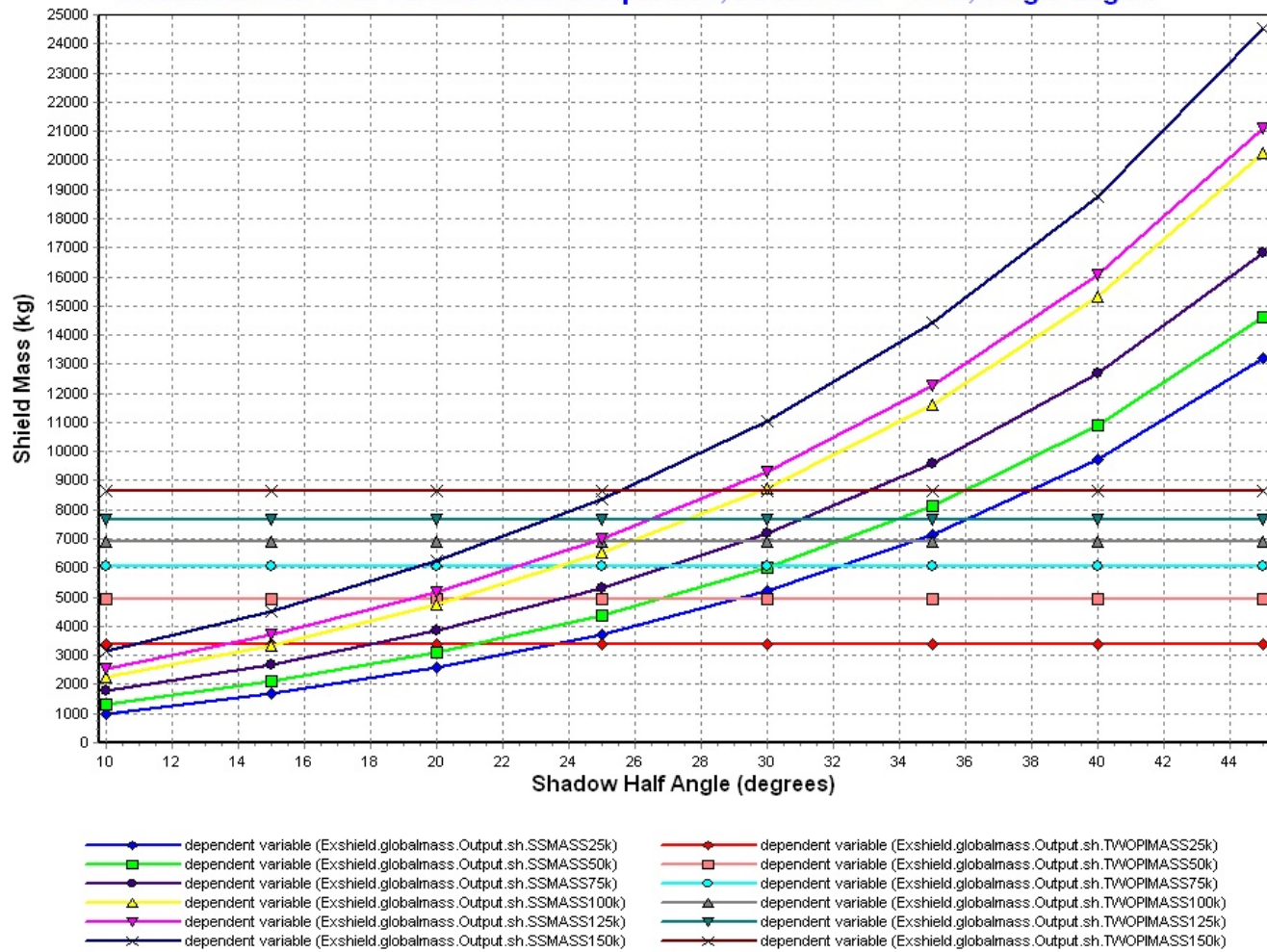
Table 4.1. NTP Engine Cost Analysis Results

75Klbt NTP Reactor Engine (FY05\$M)	
design, development, test & evaluation	2,460.0
theoretical first unit	172.2

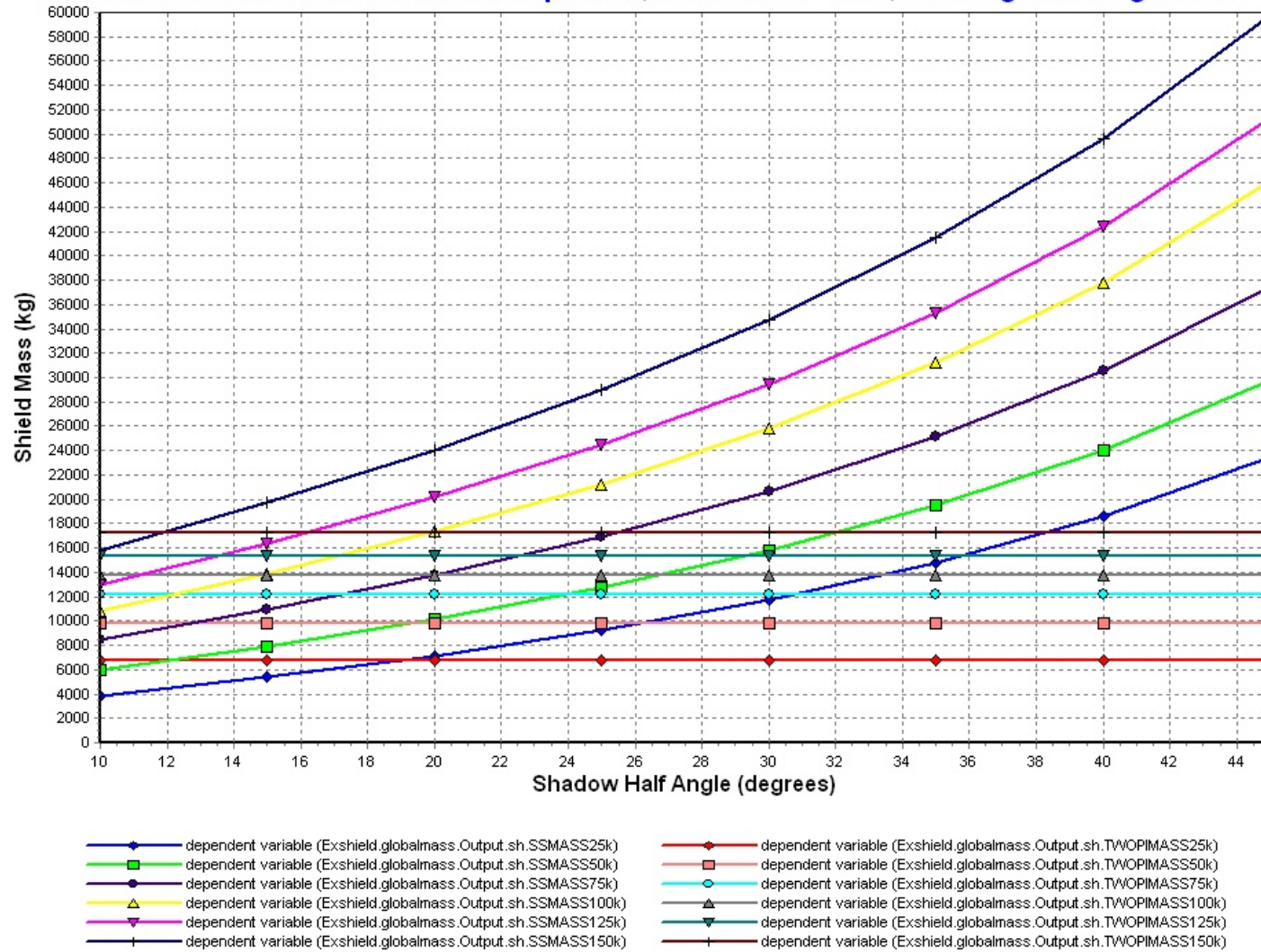
APENDIX A

SHADOW SHIELD VS. 2-PI SHIELD MASS CPMPARISON GRAPHS AS A FUNCTION OF SHADOW SHIELD HALF-ANGLE

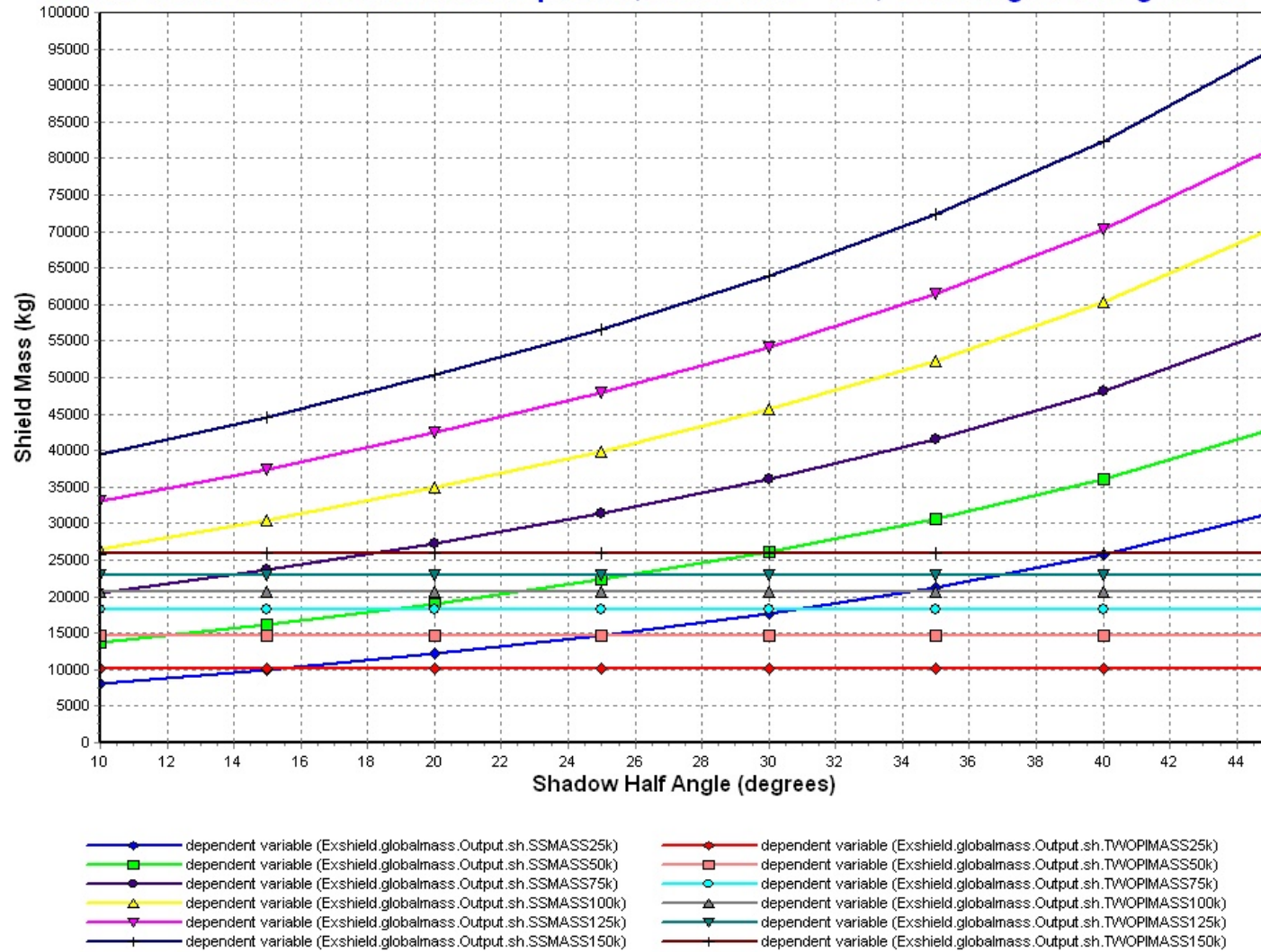
Shadow Shield vs 2Pi Shield Mass Comparison, Dose Plane = 10 m, Single Engine



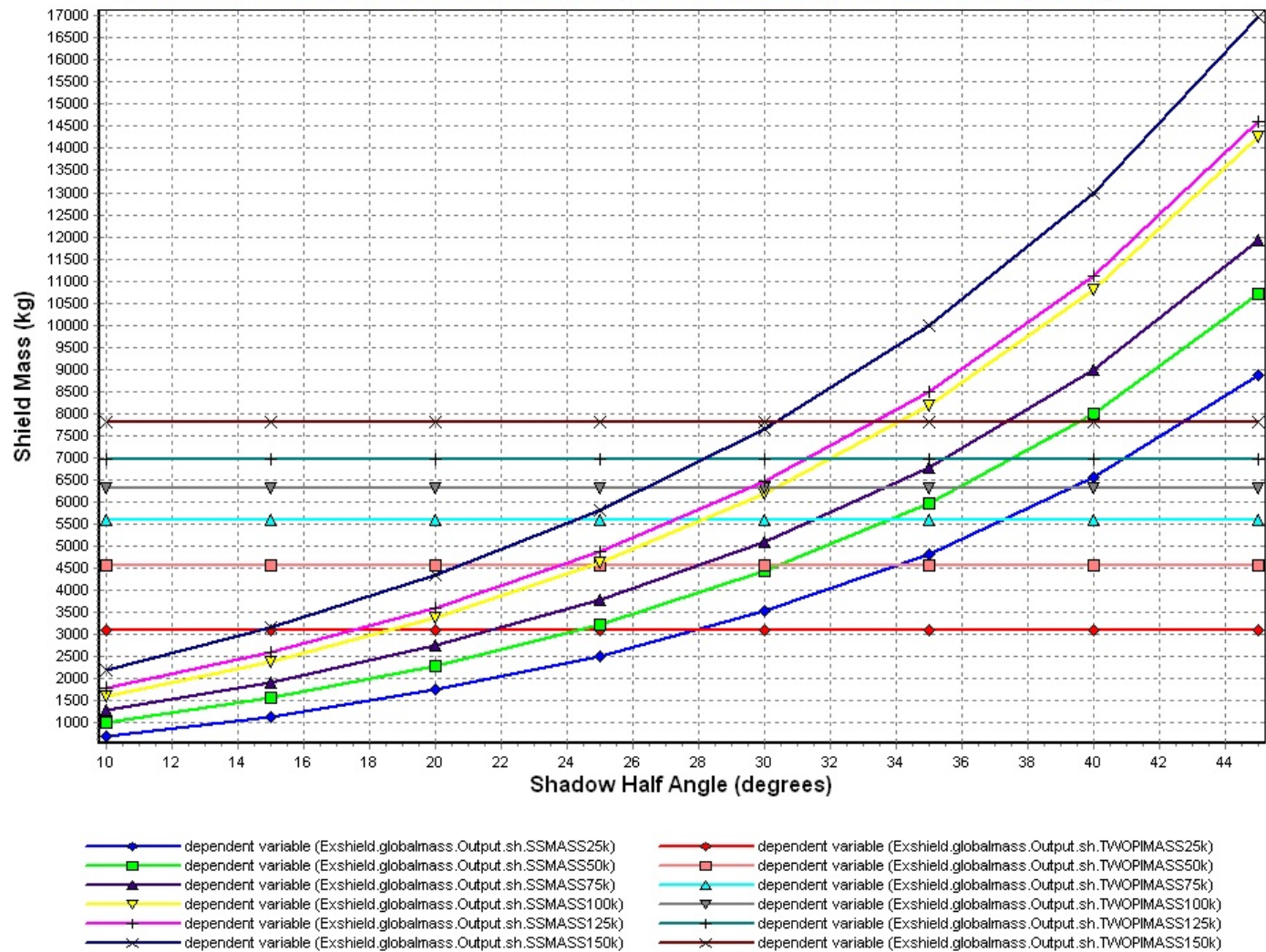
Shadow Shield vs 2Pi Shield Mass Comparison, Dose Plane = 10 m, Two Engine Configuration



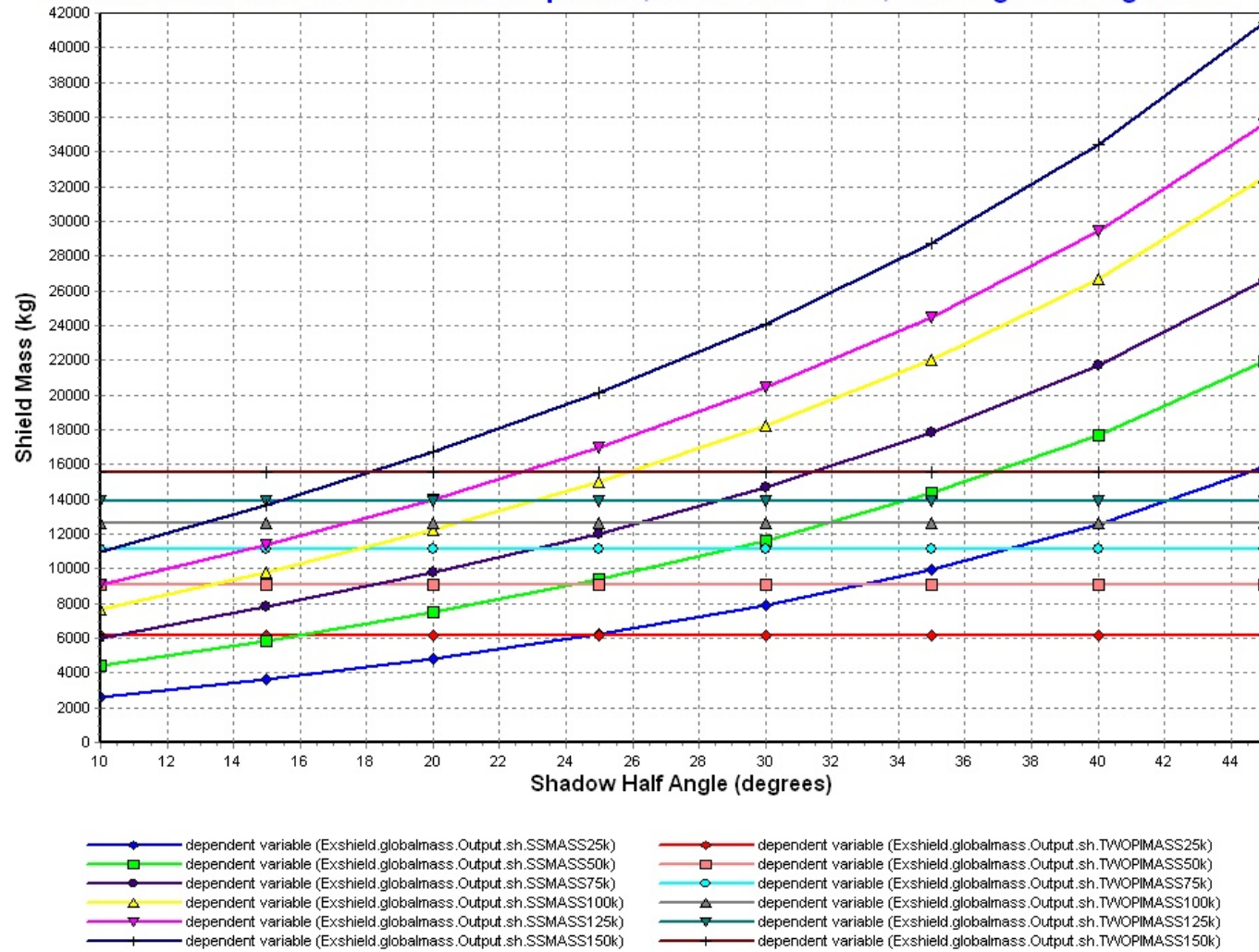
Shadow Shield vs 2Pi Shield Mass Comparison, Dose Plane = 10m, Three Engine Configuration



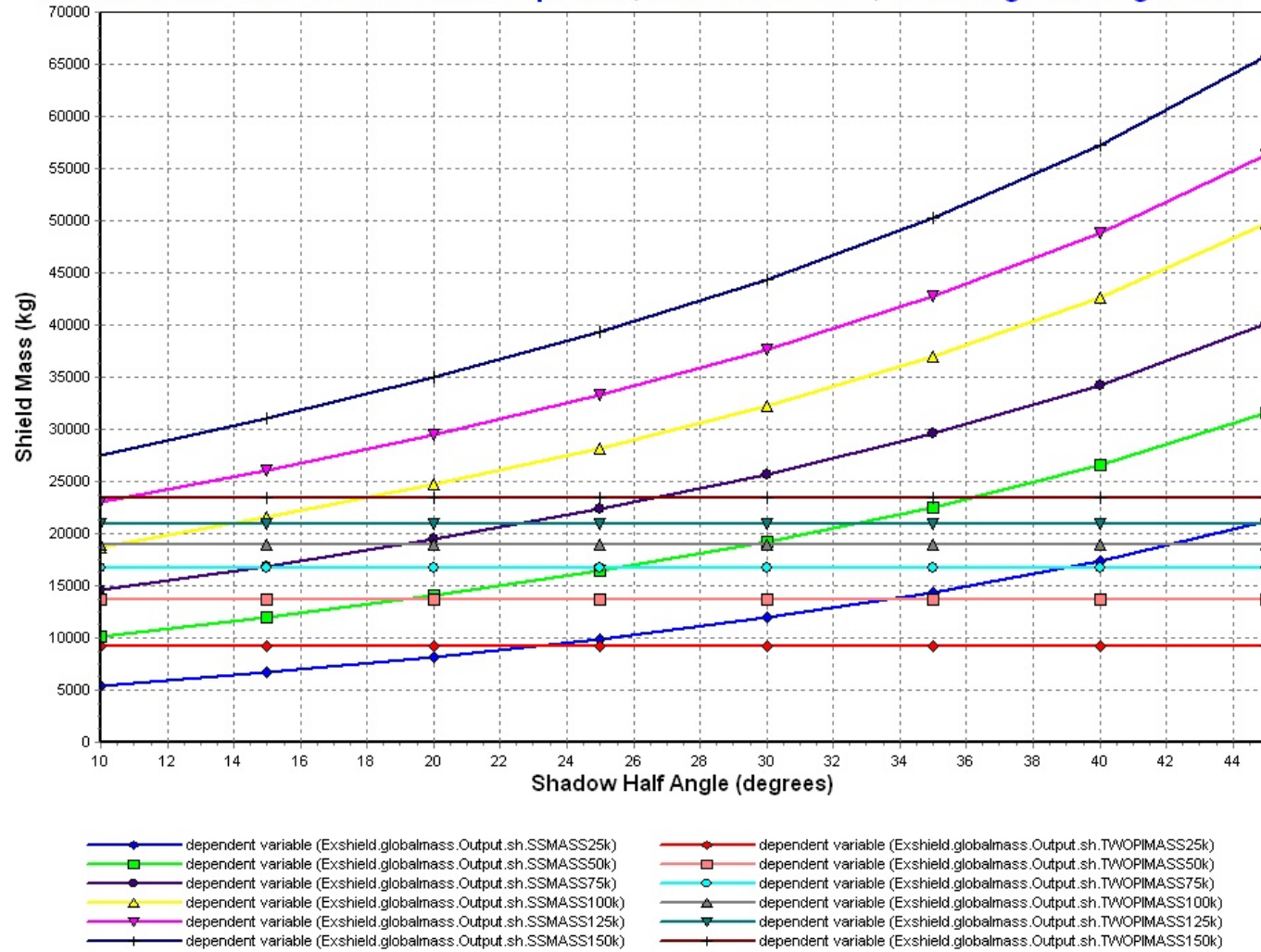
Shadow Shield vs 2Pi Shield Mass Comparison, Dose Plane = 20 m, Single Engine



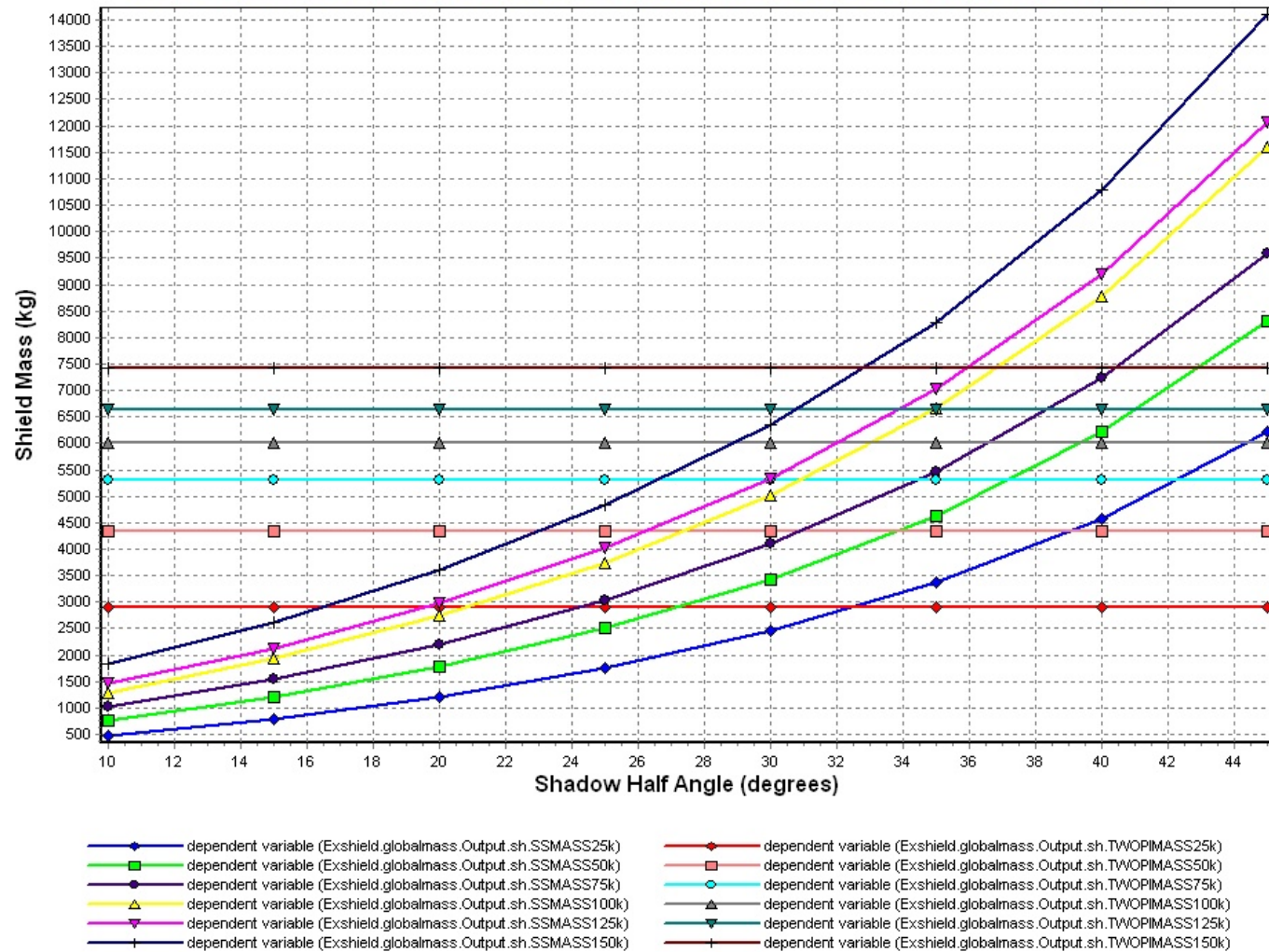
Shadow Shield vs 2Pi Shield Mass Comparison, Dose Plane = 20m, Two Engine Configuration



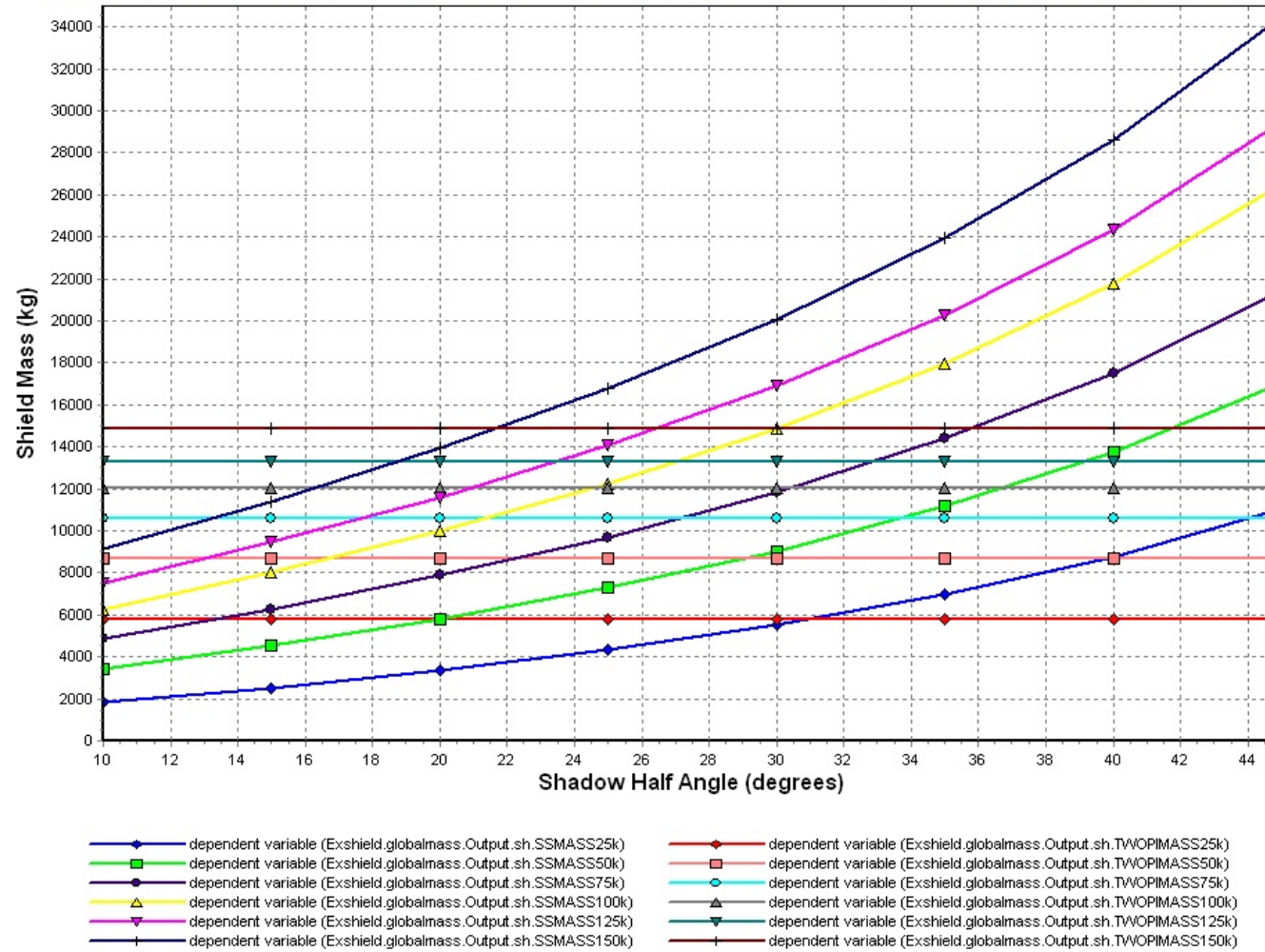
Shadow Shield vs 2Pi Shield Mass Comparison, Dose Plane = 20m, Three Engine Configuration



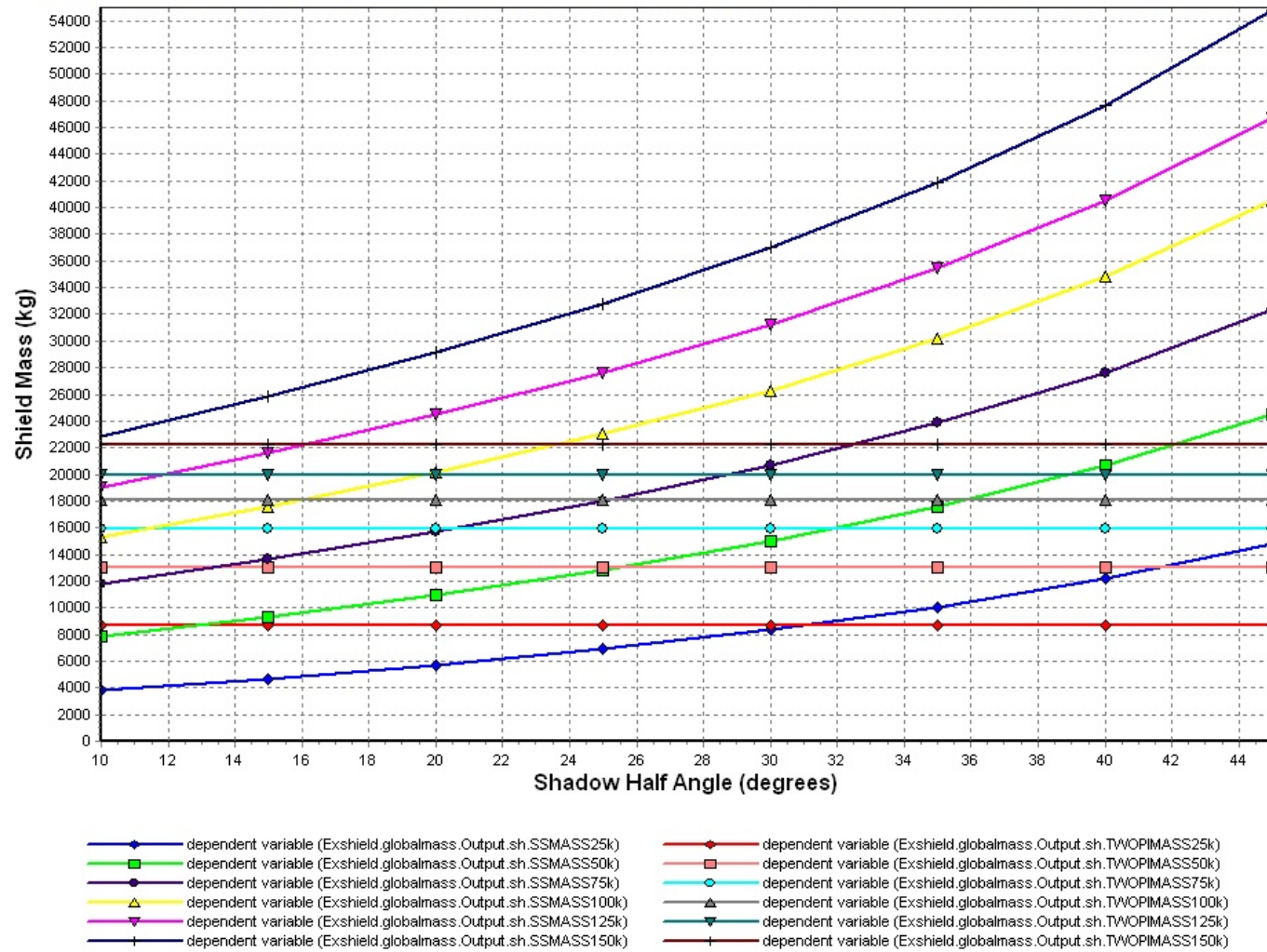
Shadow Shield vs 2Pi Shield Mass Comparison, Dose Plane = 30m, Single Engine



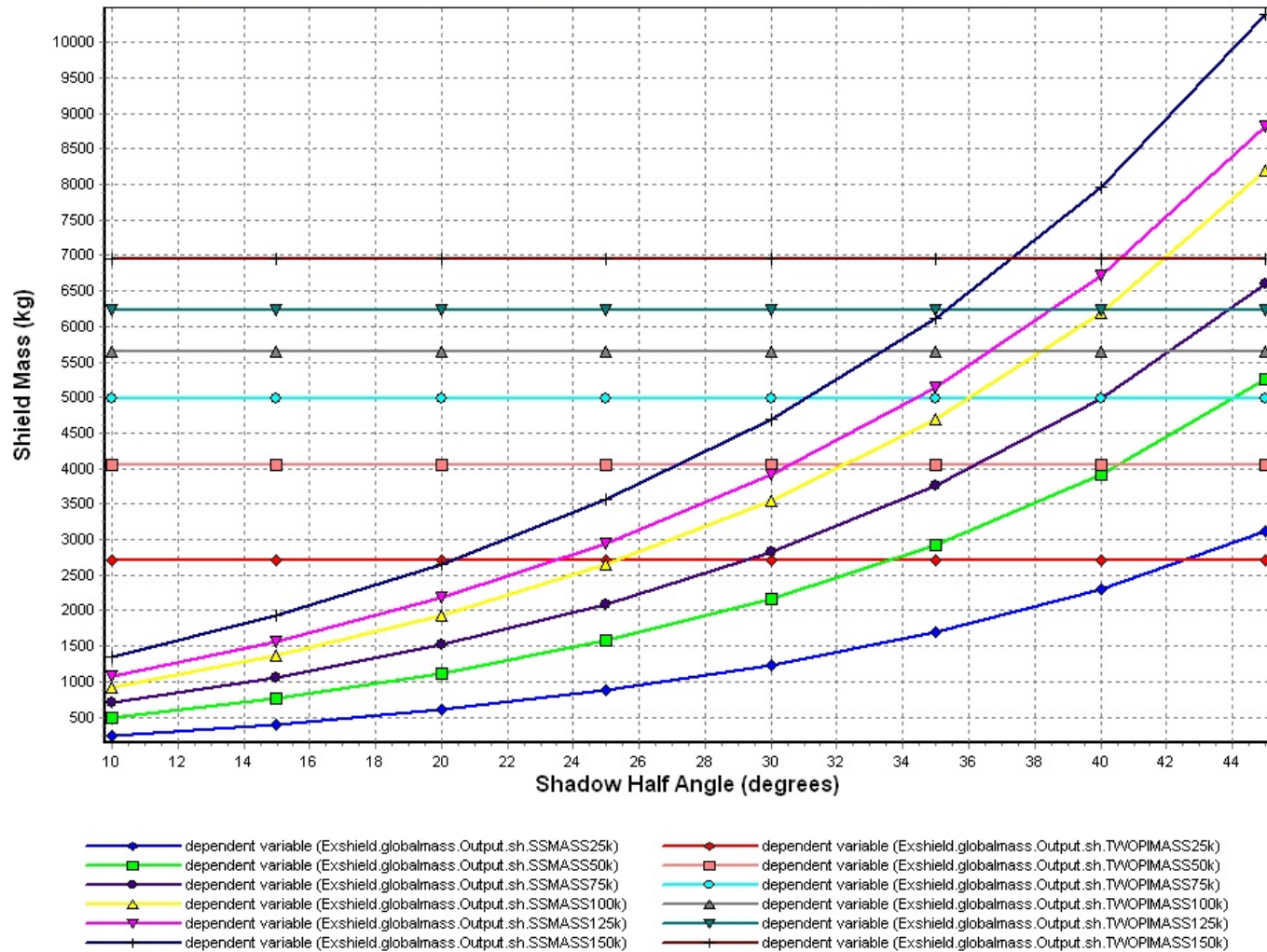
Shadow Shield vs 2Pi Shield Mass Comparison, Dose Plane = 30m, Two Engine Configuration



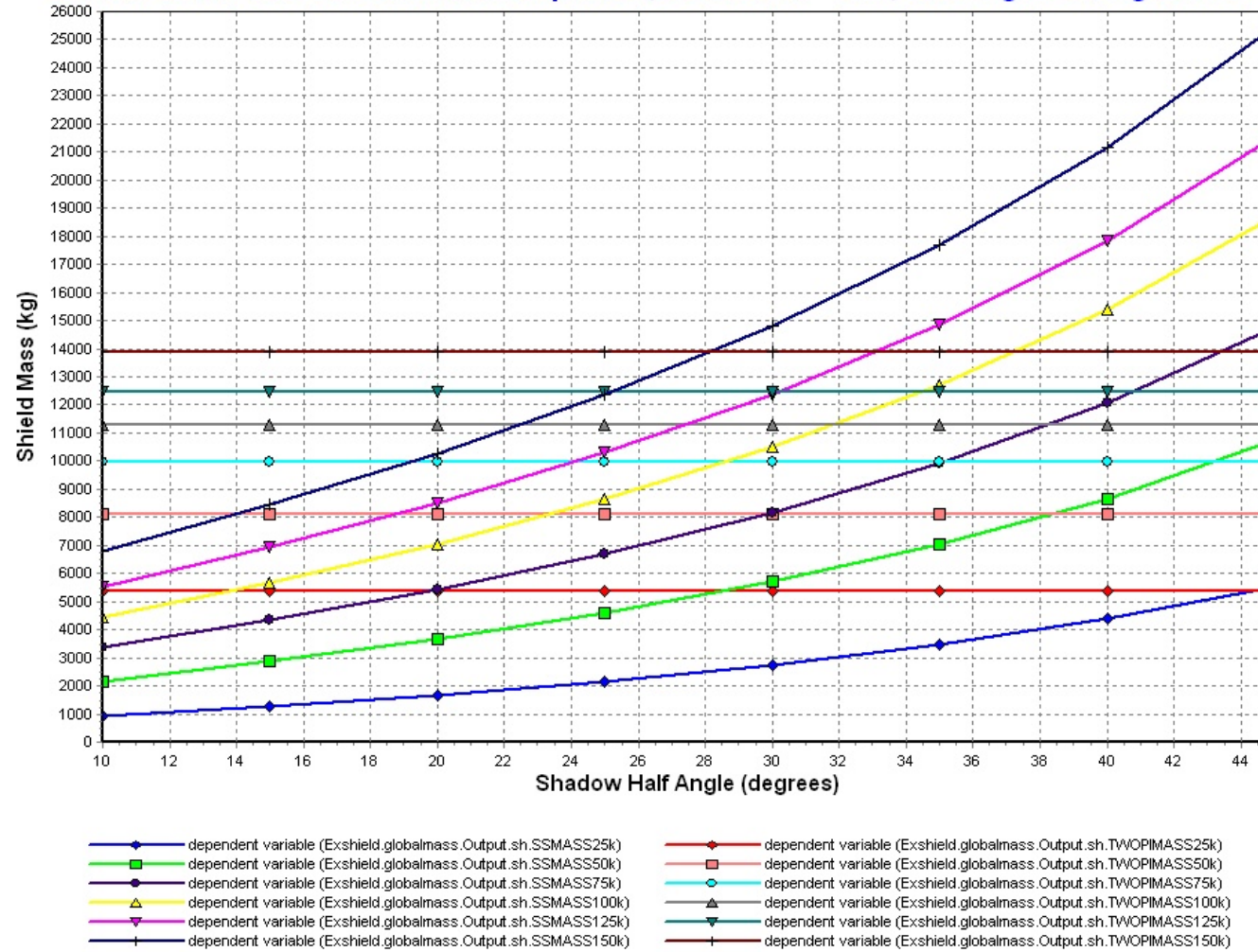
Shadow Shield vs 2Pi Shield Mass Comparison, Dose Plane = 30m, Three Engine Configuration



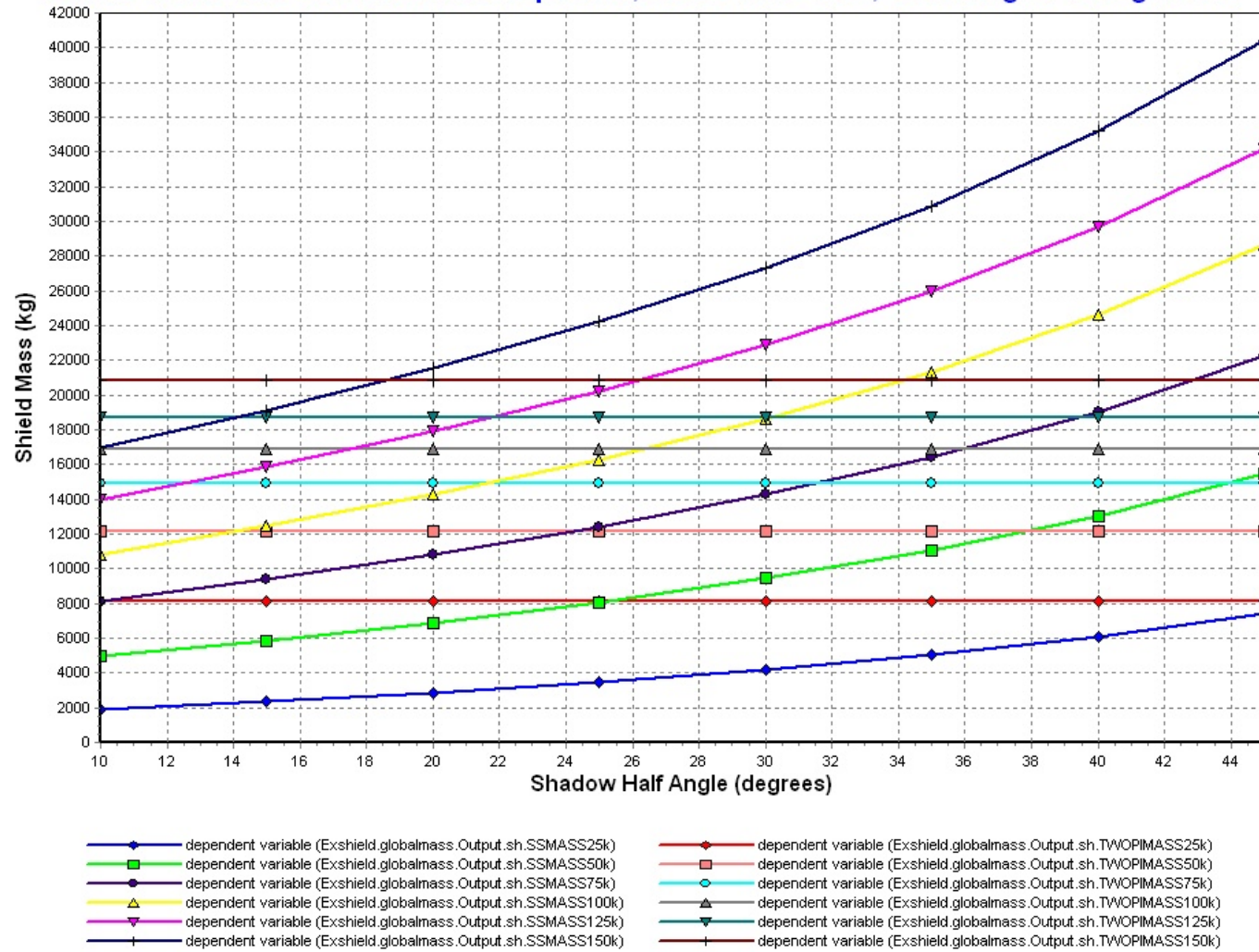
Shadow Shield vs 2Pi Shield Mass Comparison, Dose Plane = 50m, Single Engine



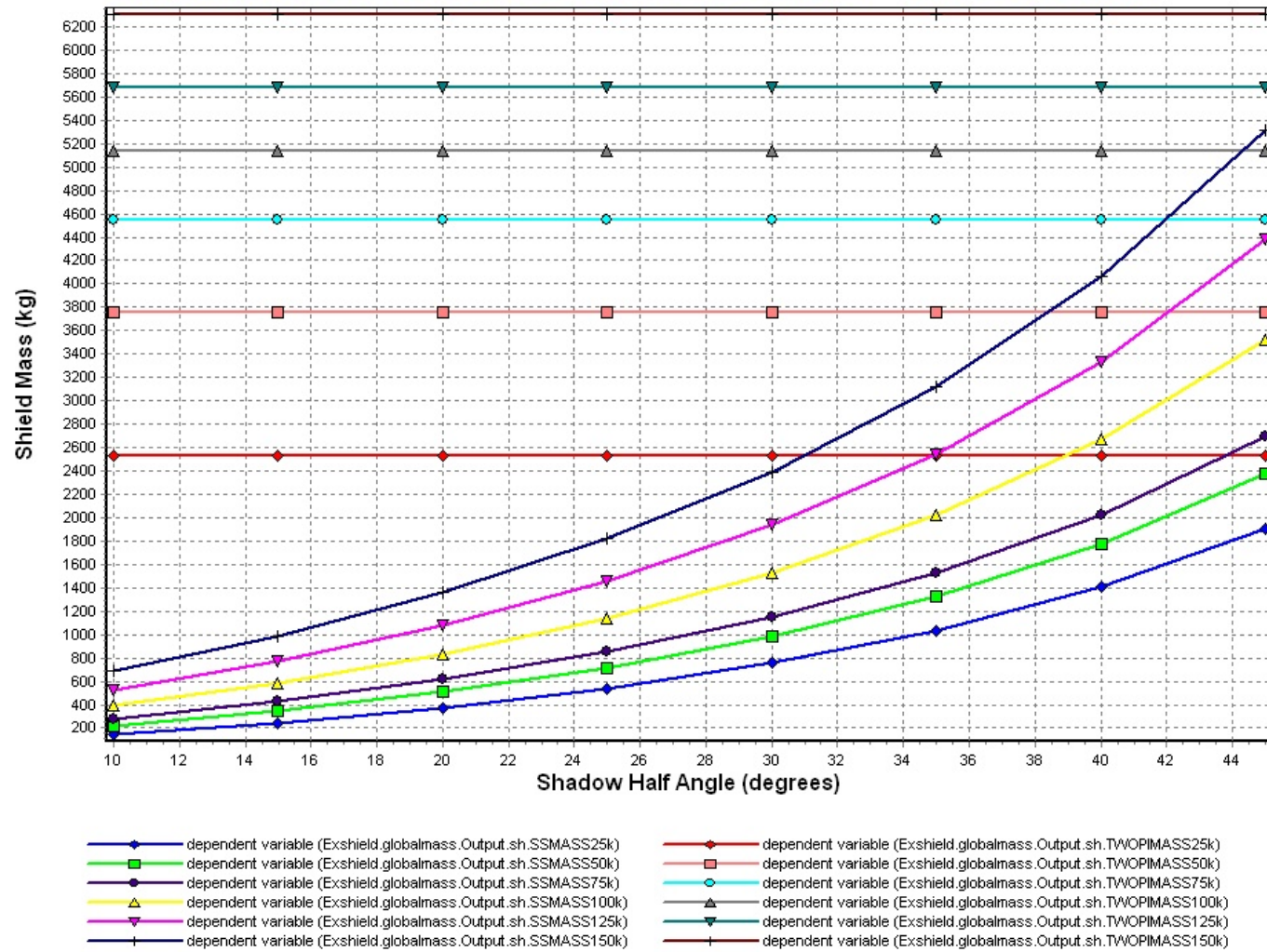
Shadow Shield vs 2Pi Shield Mass Comparison, Dose Plane = 50m, Two Engine Configuration



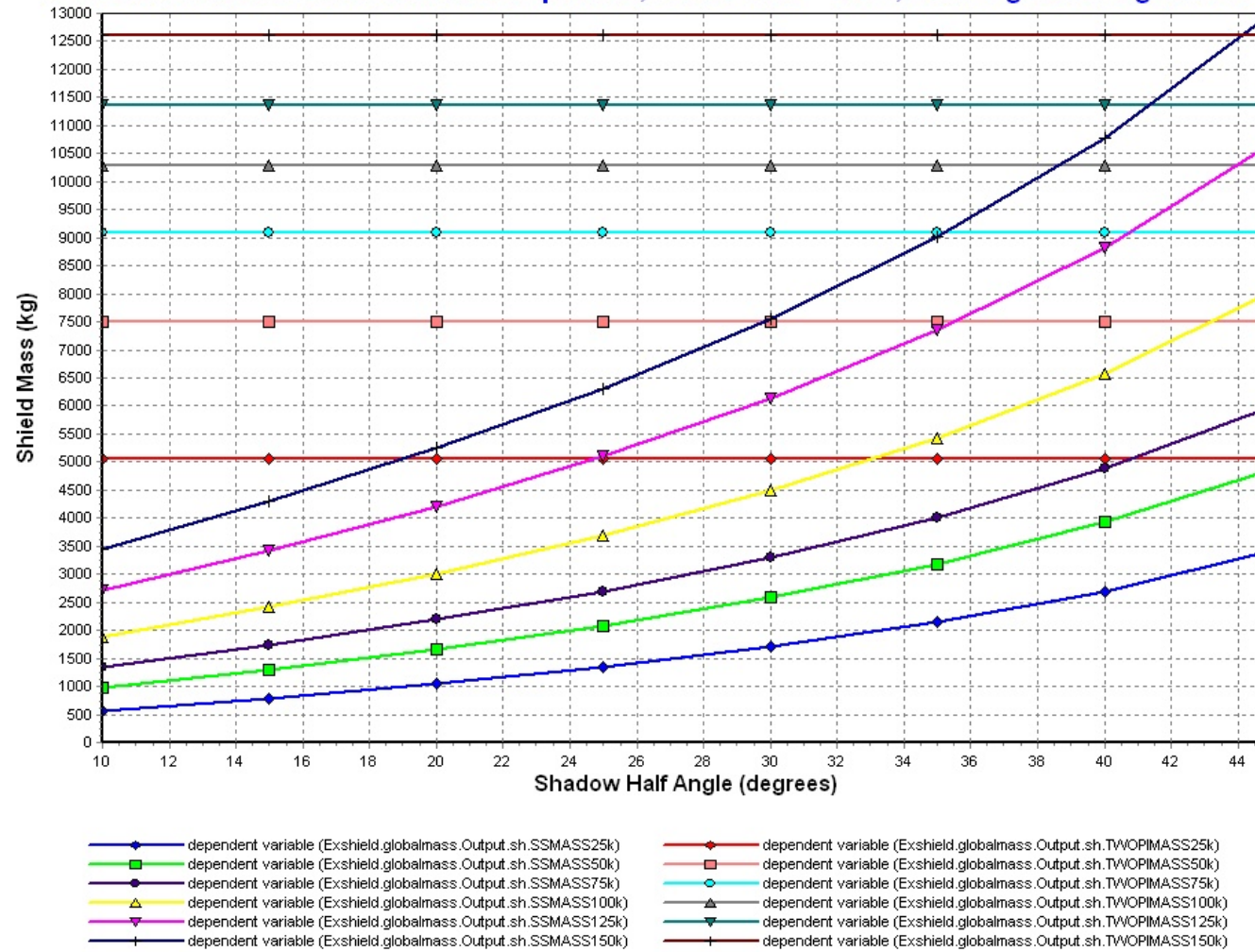
Shadow Shield vs 2Pi Shield Mass Comparison, Dose Plane = 50m, Three Engine Configuration



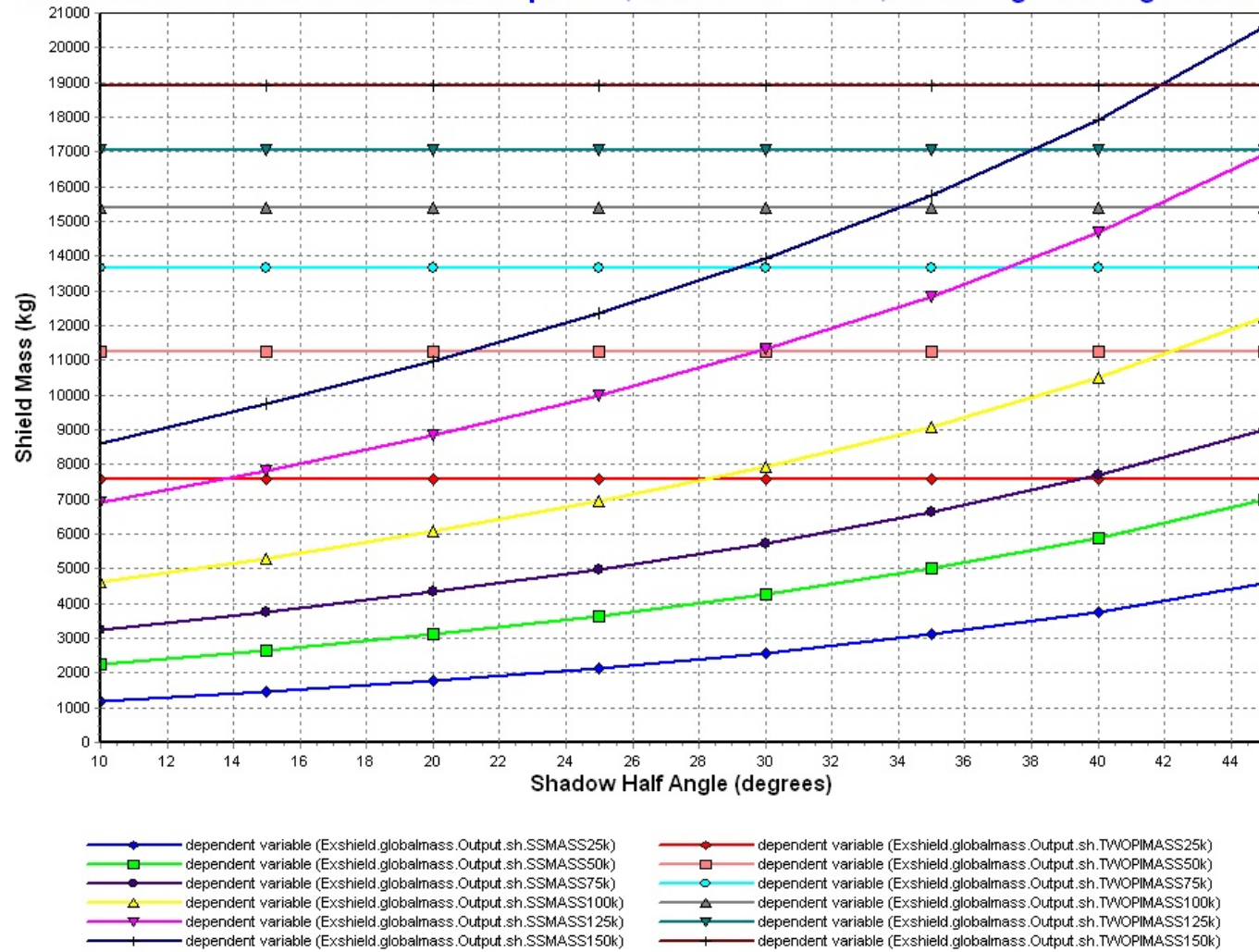
Shadow Shield vs 2Pi Shield Mass Comparison, Dose Plane = 100m, Single Engine



Shadow Shield vs 2Pi Shield Mass Comparison, Dose Plane = 100m, Two Engine Configuration



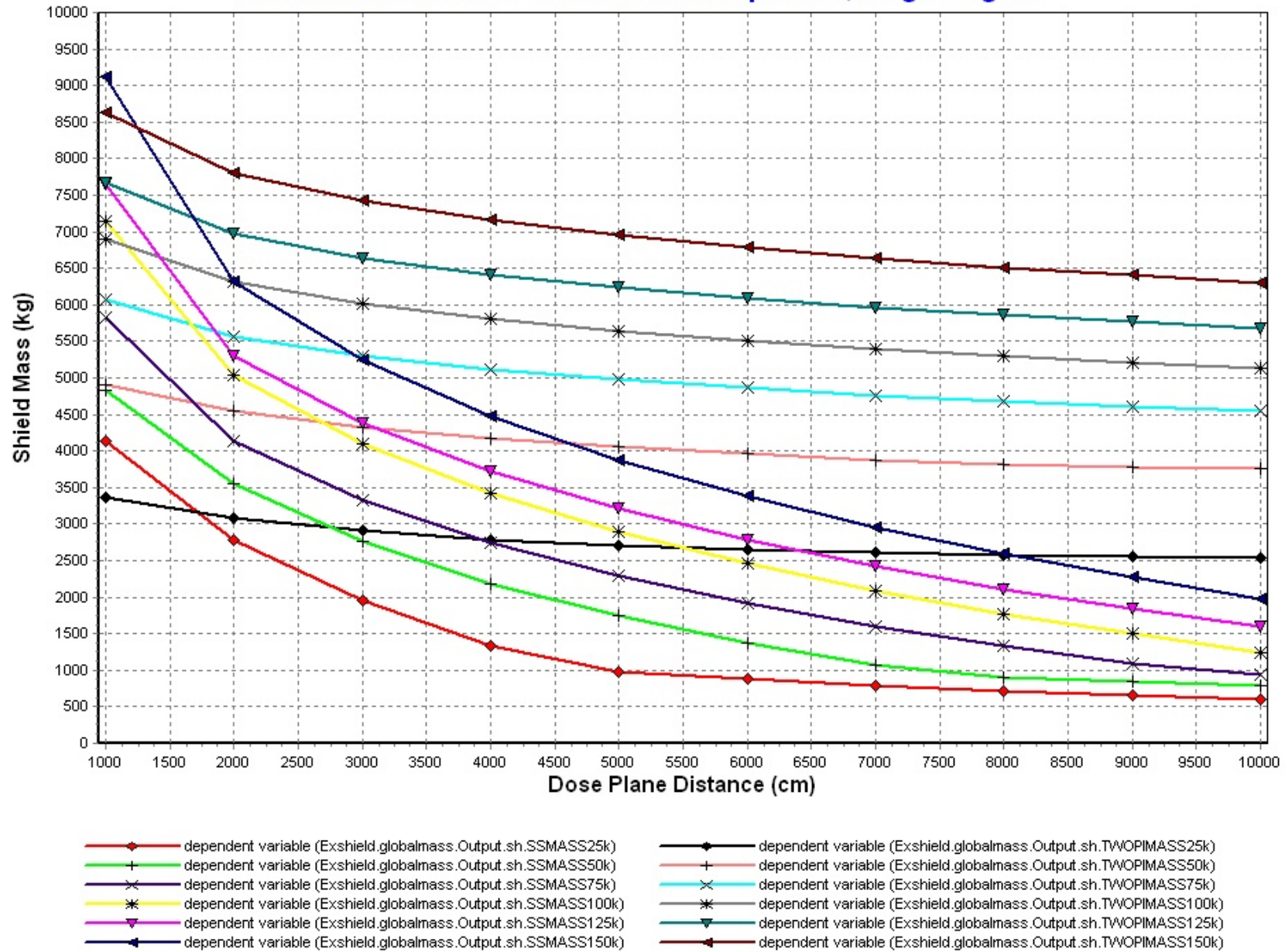
Shadow Shield vs 2Pi Shield Mass Comparison, Dose Plane = 100m, Three Engine Configuration



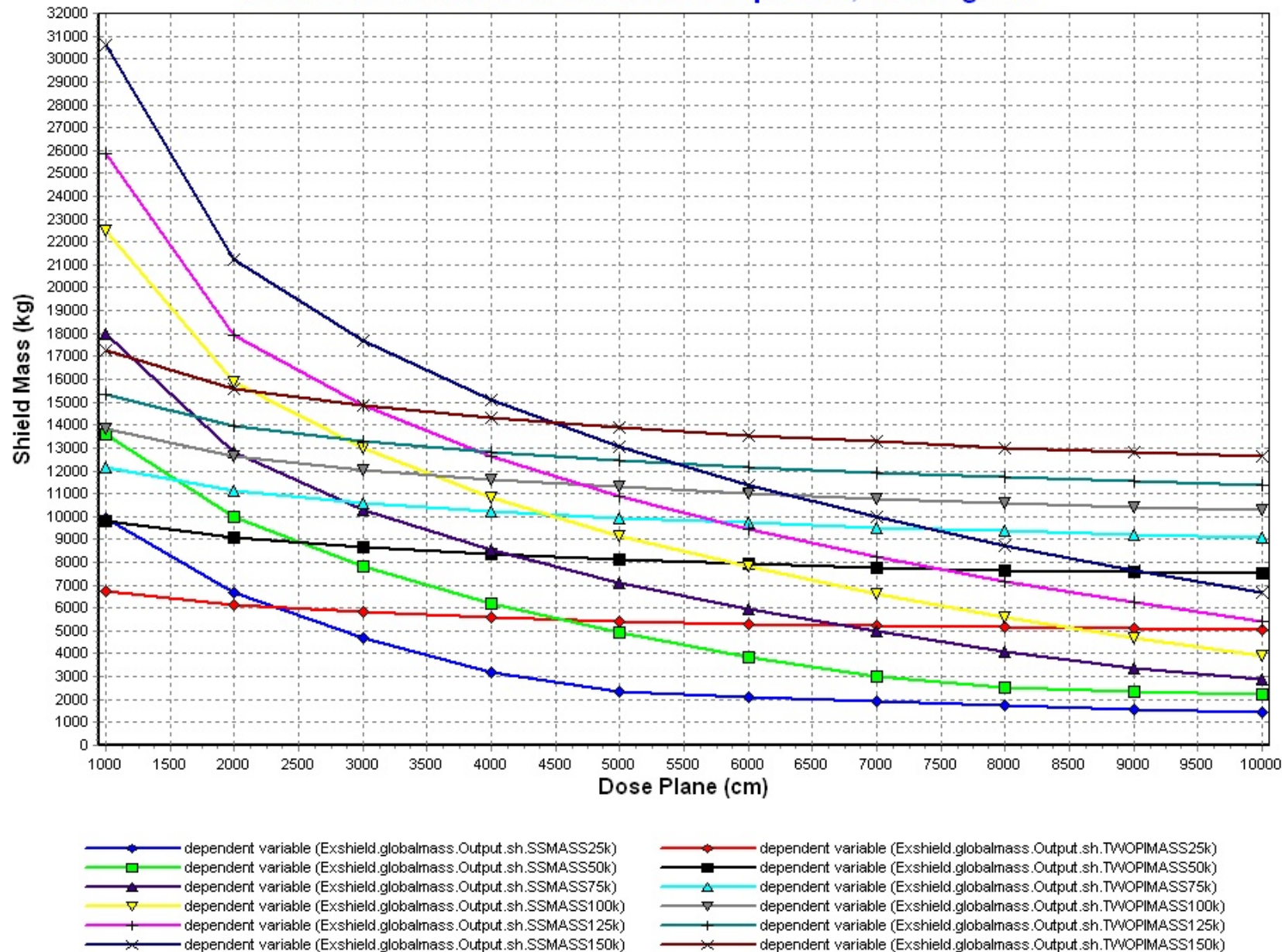
APENDIX B

SHADOW SHIELD VS. 2-PI SHIELD MASS CPMPARISON GRAPHS AS A FUNTION OF DOSE PLANE DISTANCE

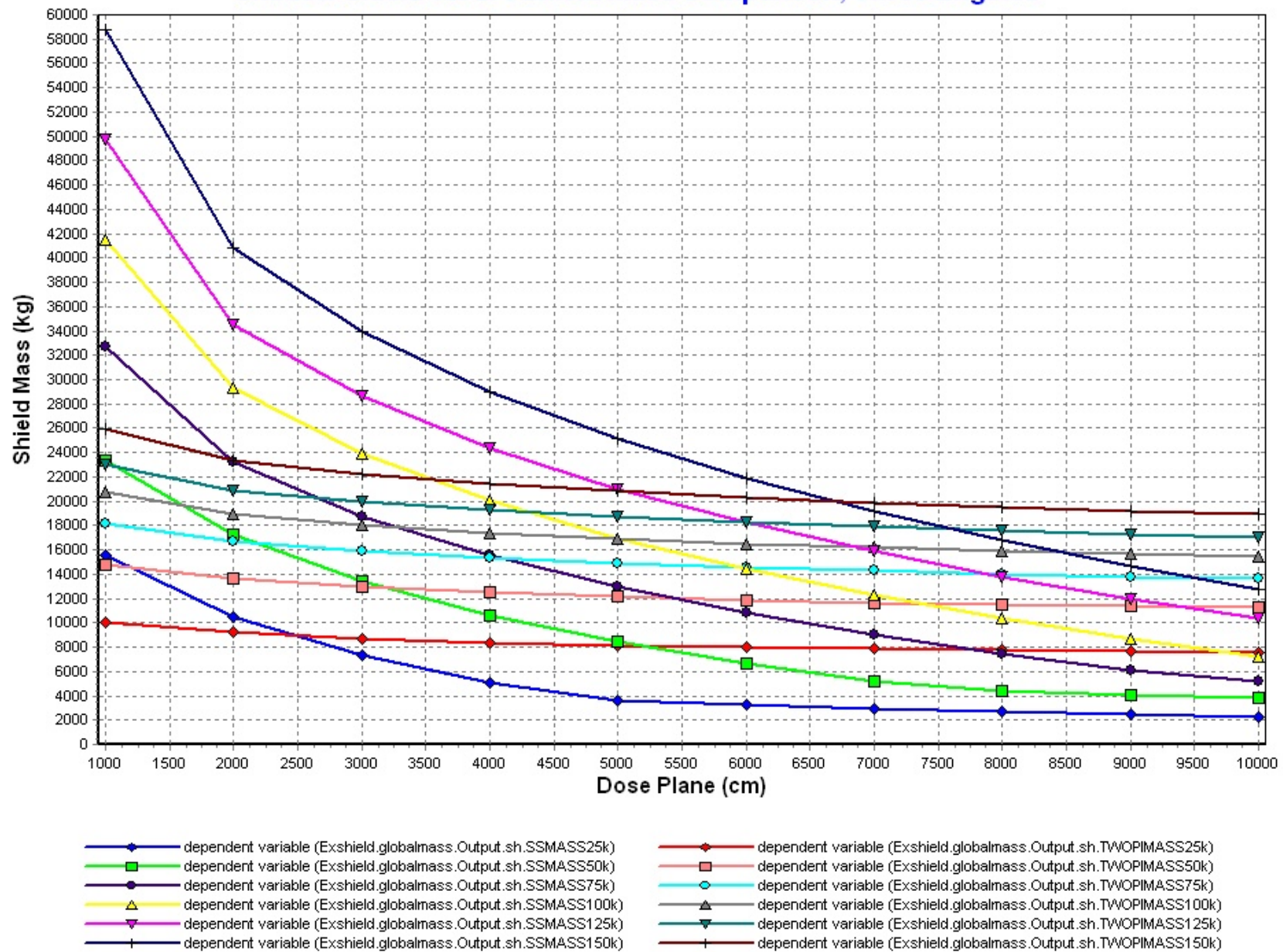
Shadow Shield vs. 2Pi Shield Mass Comparison, Single Engine



Shadow Shield vs. 2Pi Shield Mass Comparison, Two Engines



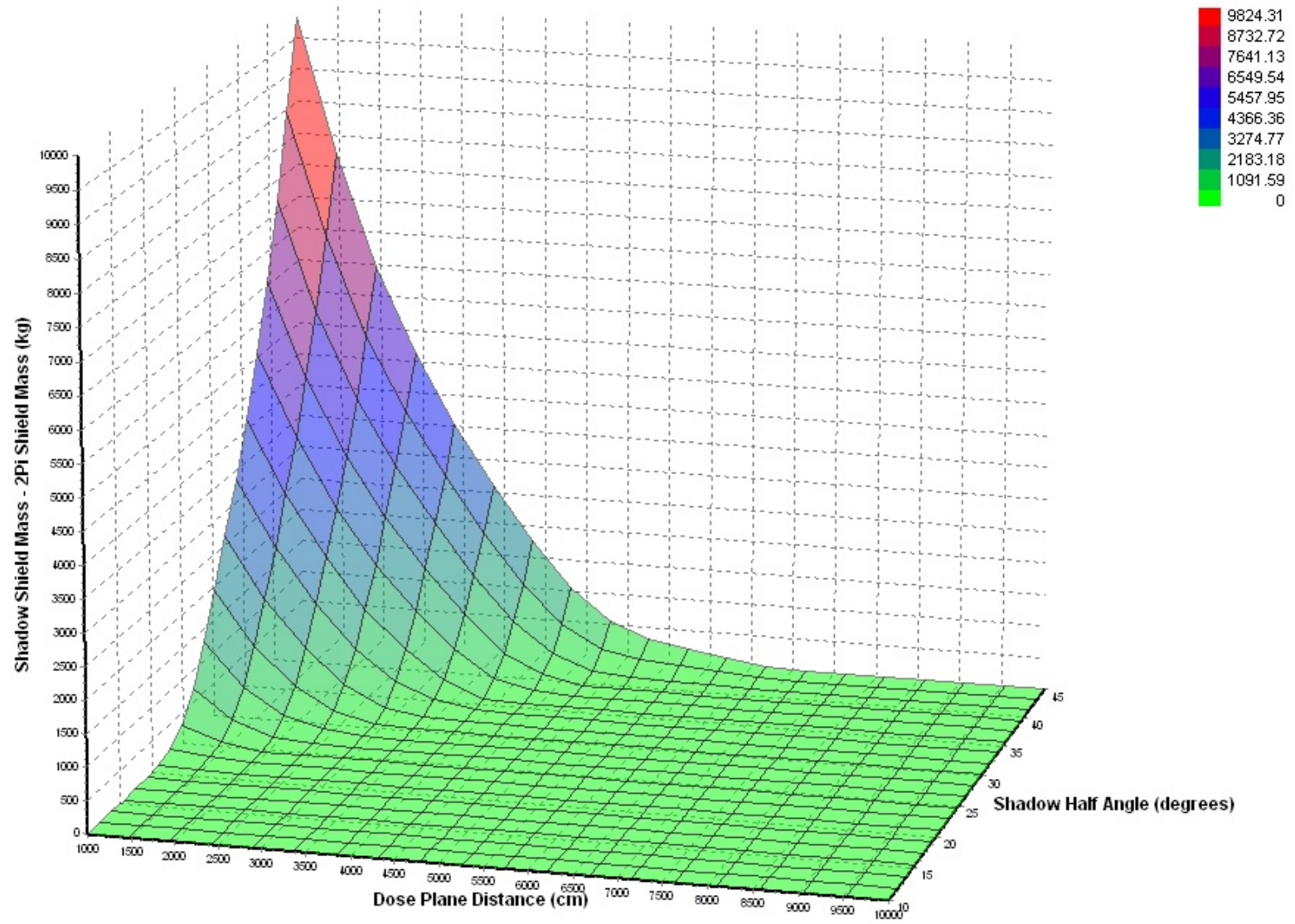
Shadow Shield vs. 2Pi Shield Mass Comparison, Three Engines



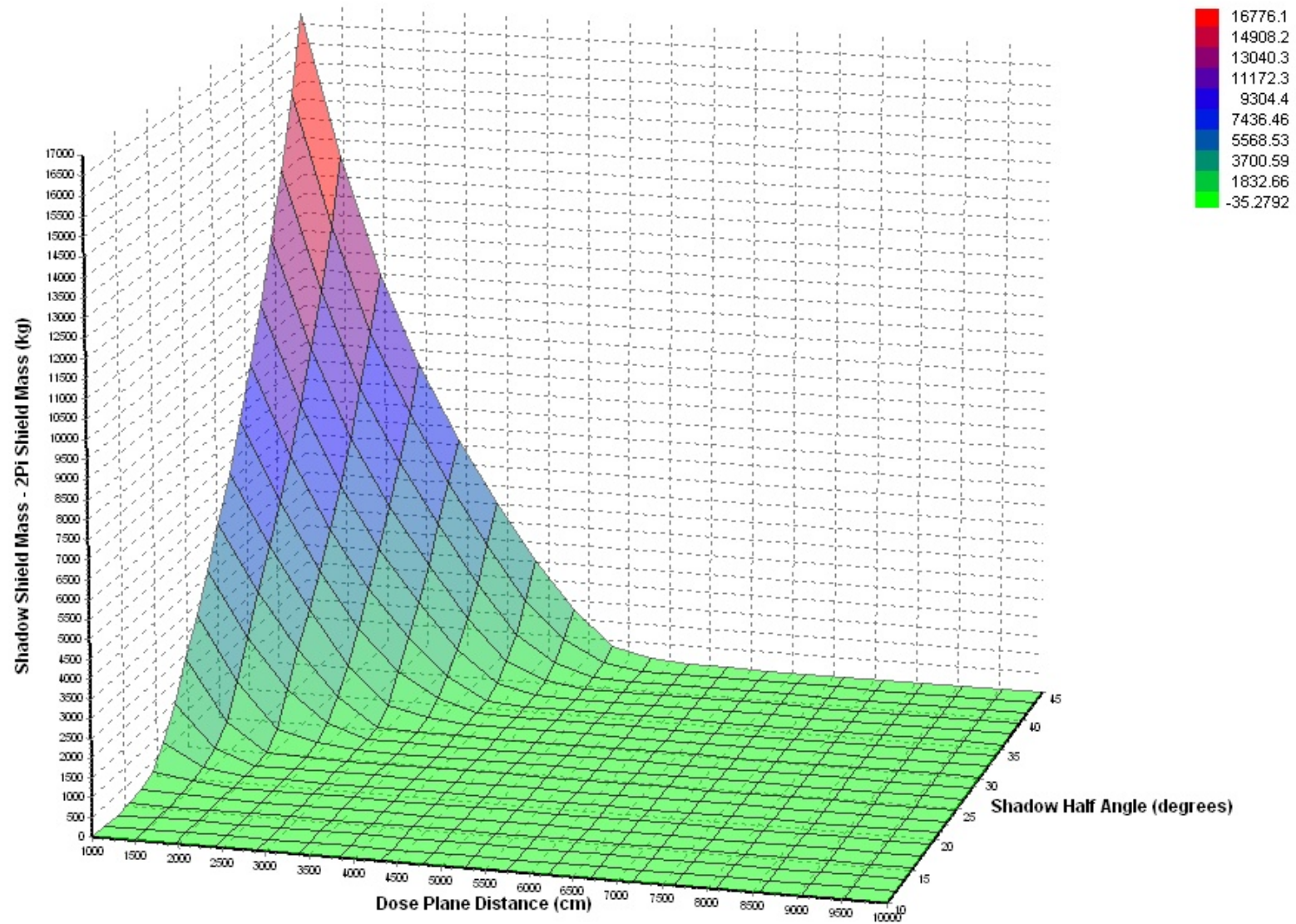
APENDIX C

SHADOW SHIELD VS. 2-PI SHIELD MASS CPMPARISON GRAPHS CARPET PLOTS

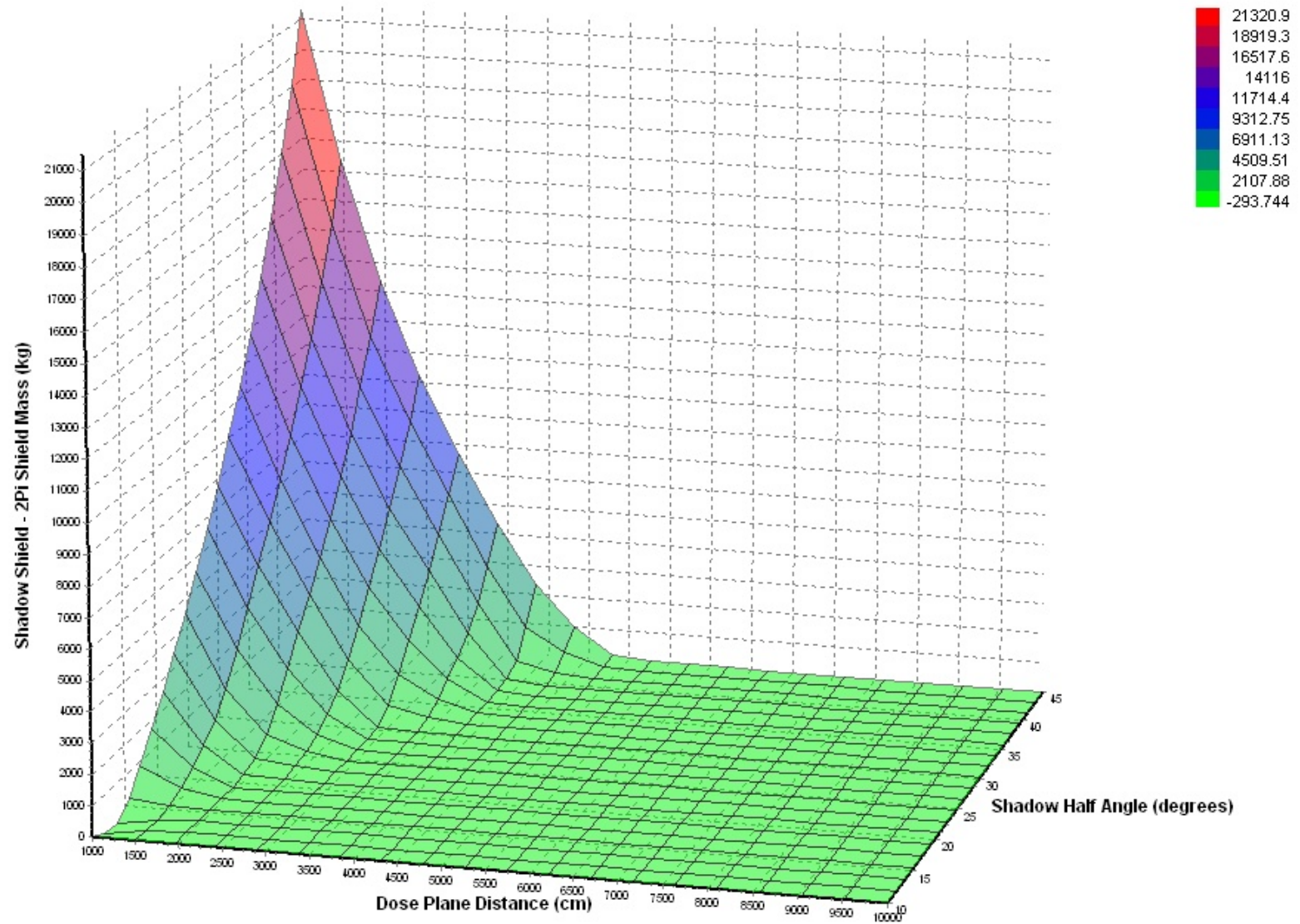
Shadow Shield - 2Pi Shield Mass vs Dose Plane Distance and Shadow Half Angle, 25klbf Thrust, Single Engine



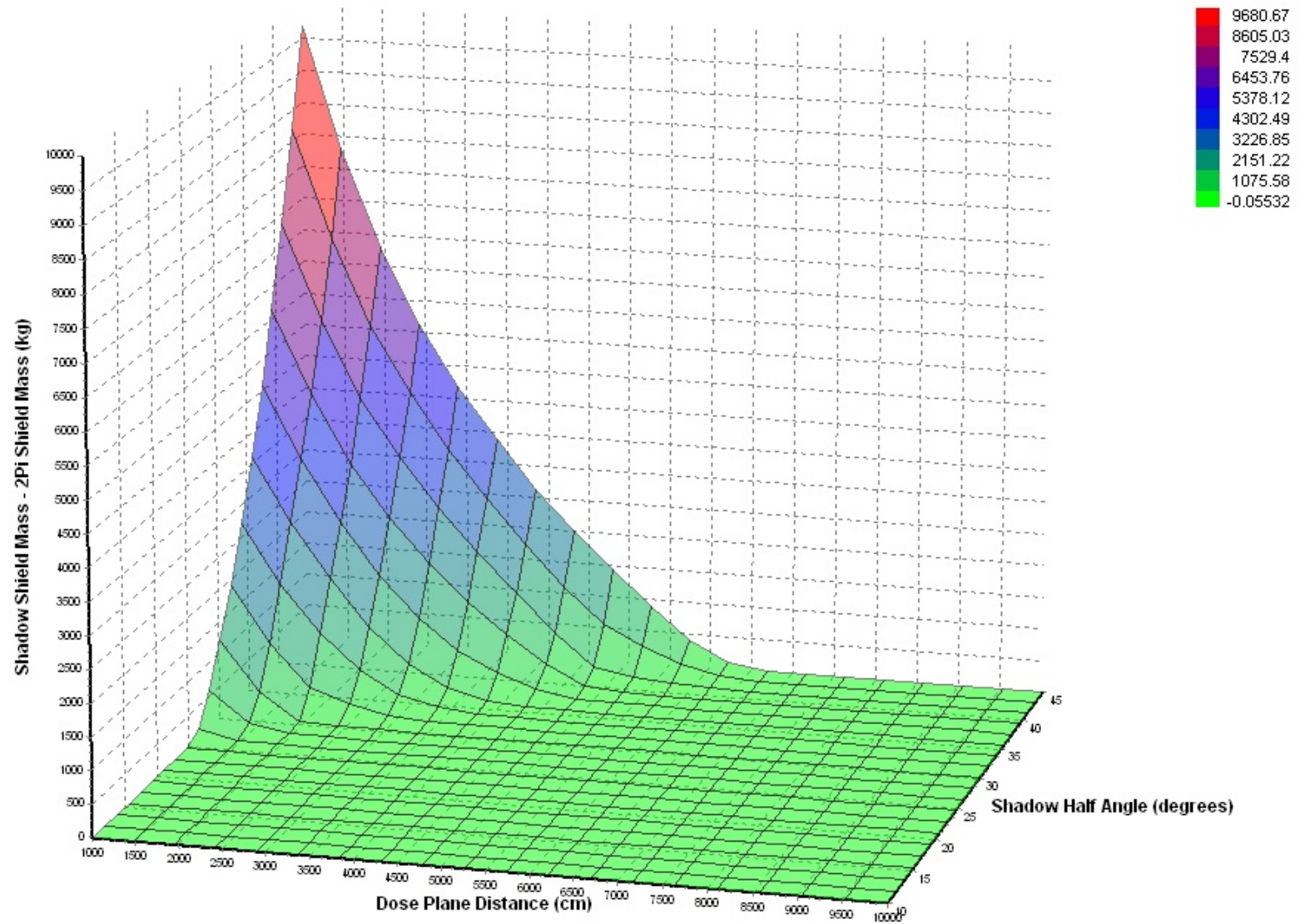
Shadow Shield - 2Pi Shield Mass vs Dose Plane Distance and Shadow Half Angle, 25 klbf Thrust, Two Engine Configuration



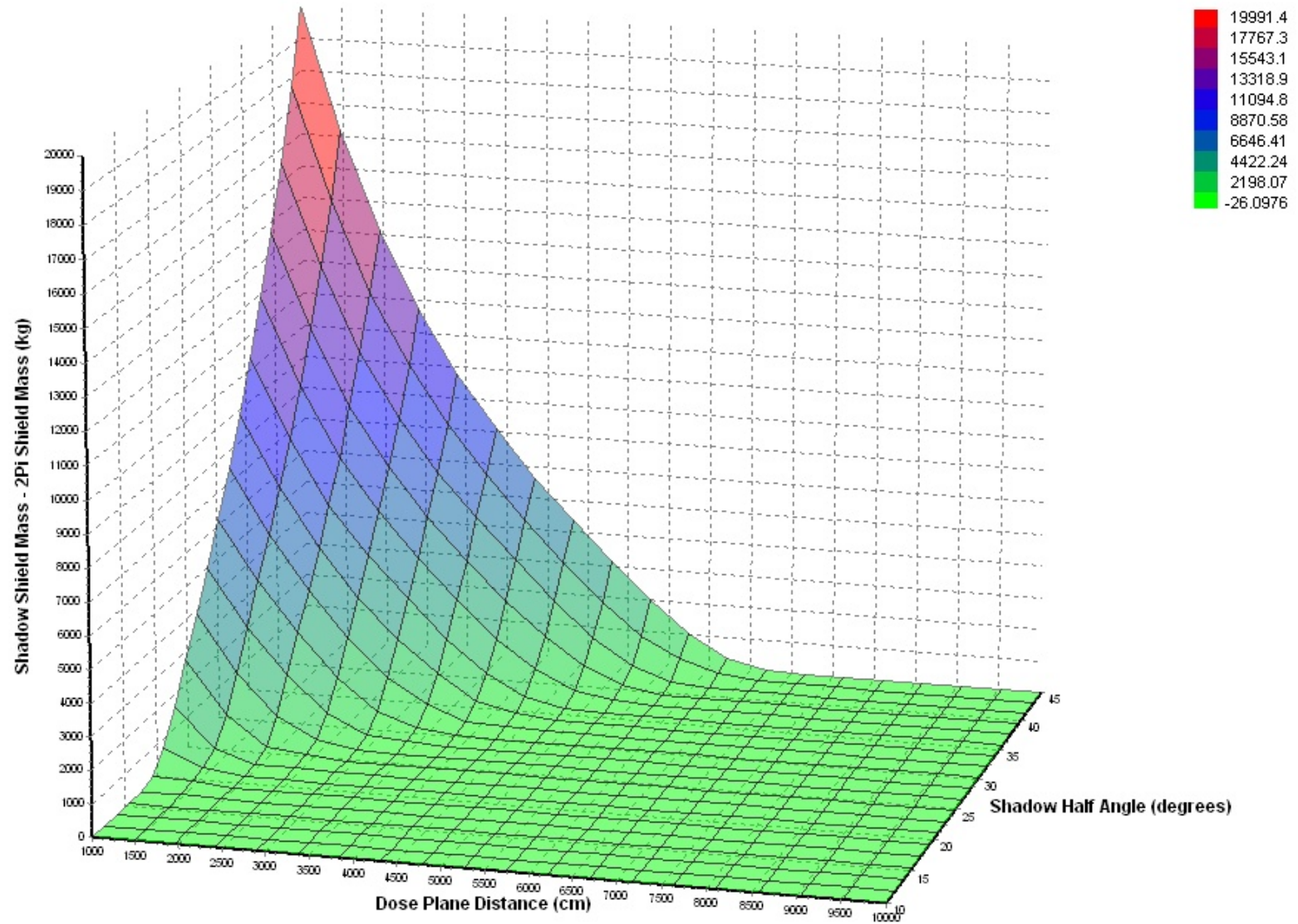
Shadow Shield - 2Pi Shield Mass vs Dose Plane Distance and Shadow Half Angle, 25 klbf Thrust, 3 Engine Configuration



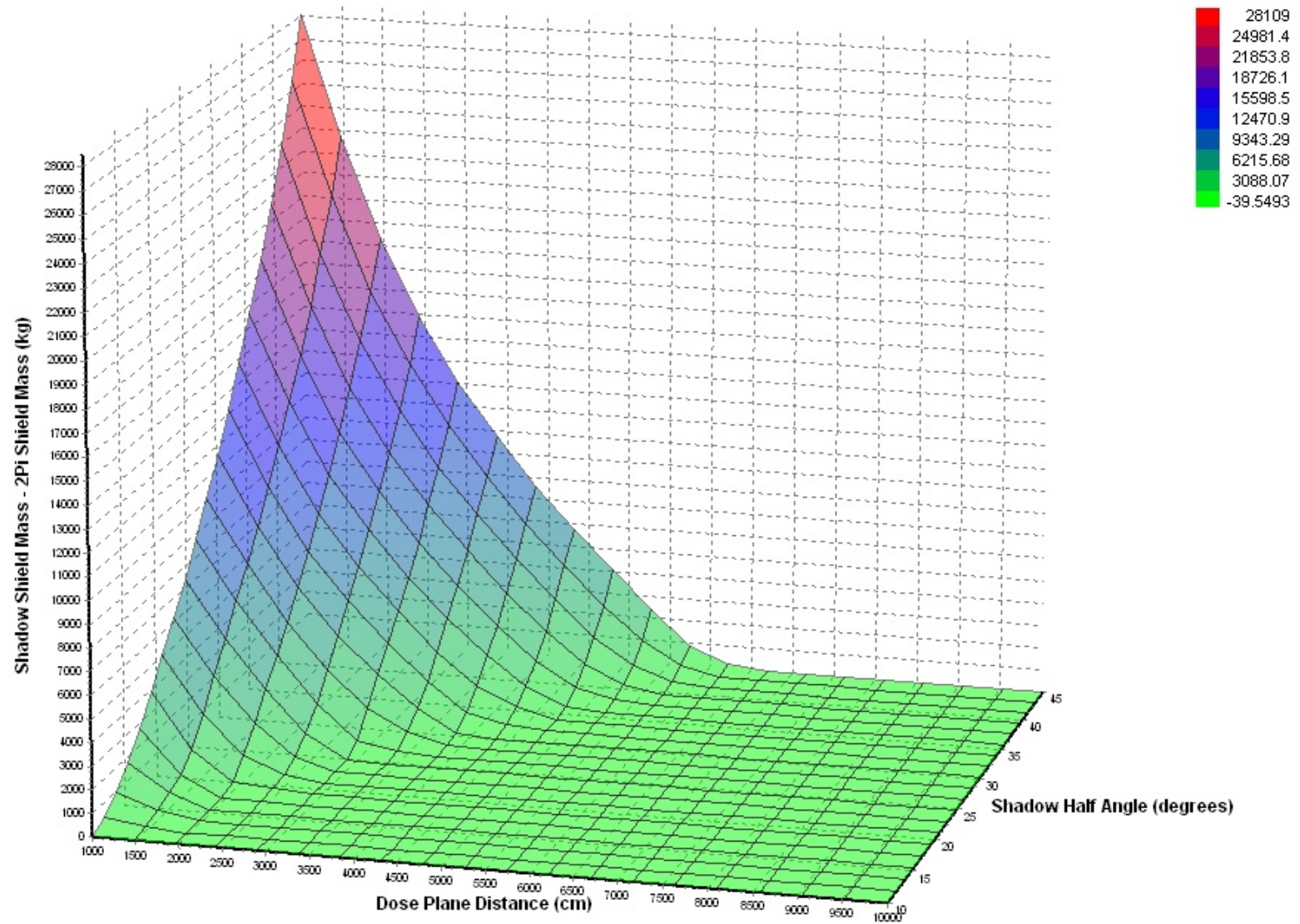
Shadow Shield - 2Pi Shield Mass vs Dose Plane Distance and Shadow Half Angle, 50 klbf Thrust, Single Engine



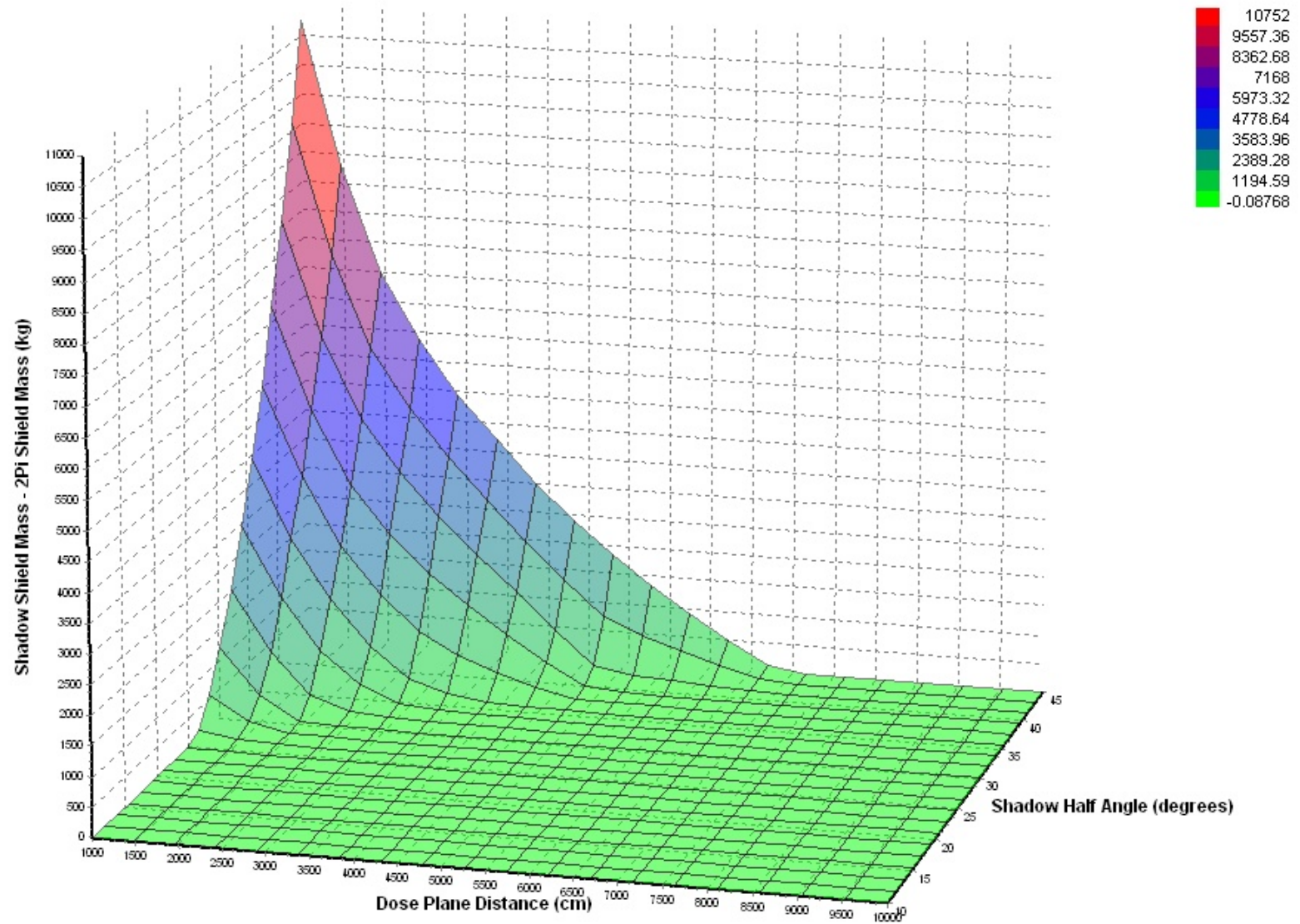
Shadow Shield - 2Pi Shield Mass vs Dose Plane Distance and Shadow Half Angle, 50 klbf Thrust, Two Engine Configuration



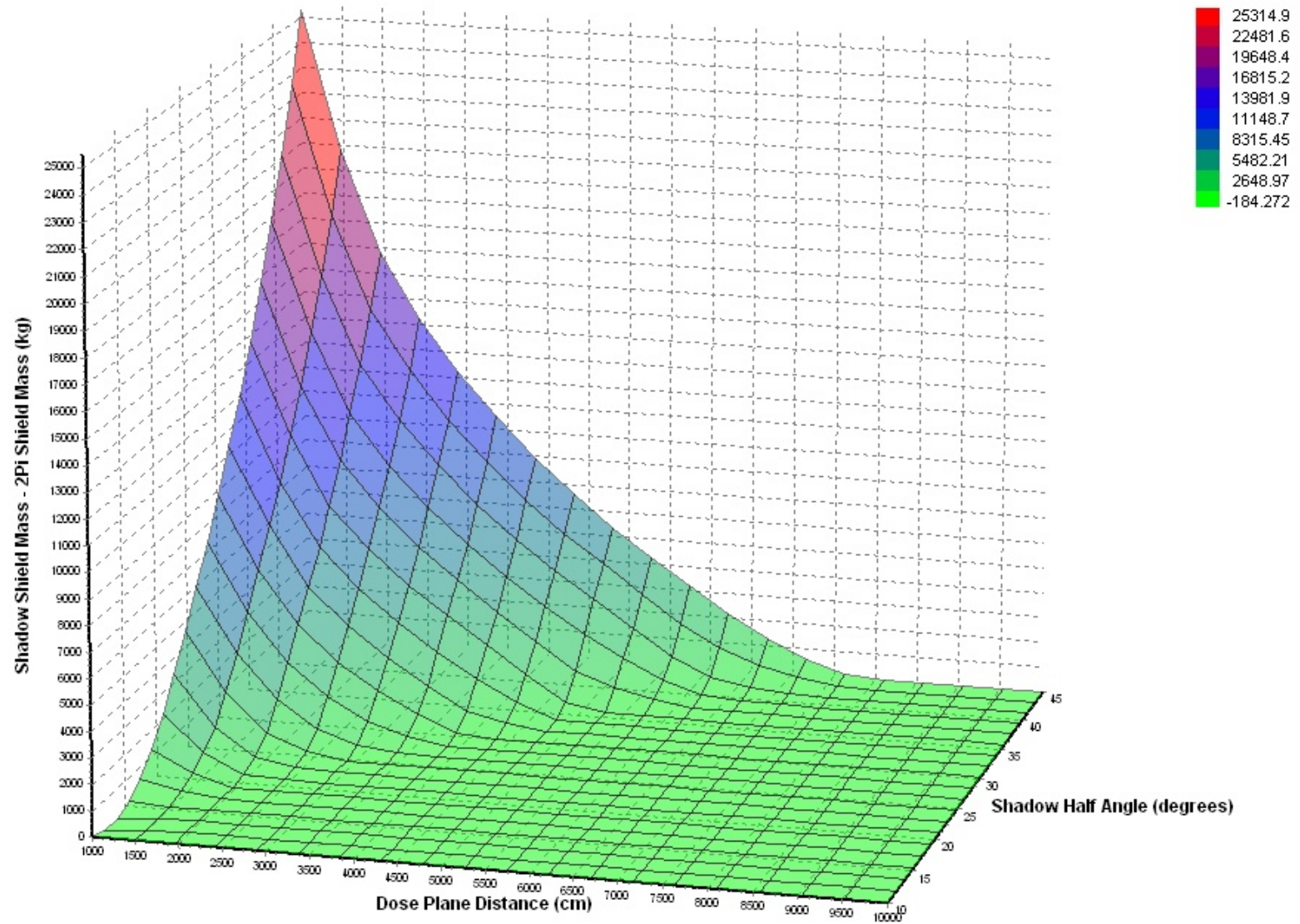
Shadow Shield - 2Pi Shield Mass vs Dose Plane Distance and Shadow Half Angle, 50 klbf Thrust, 3 Engine Configuration



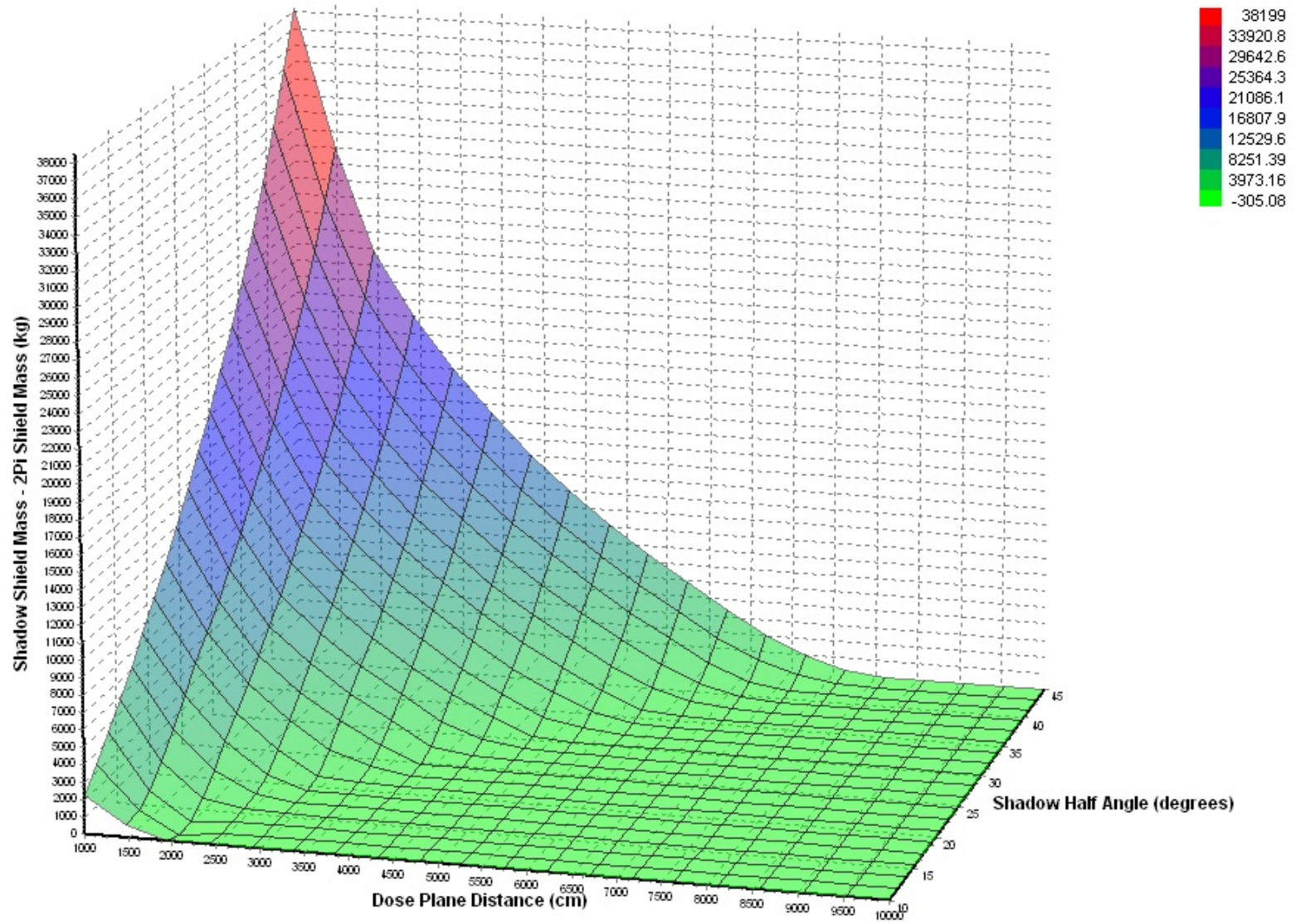
Shadow Shield - 2Pi Shield Mass vs Dose Plane Distance and Shadow Half Angle, 75 klbf Thrust, Single Engine



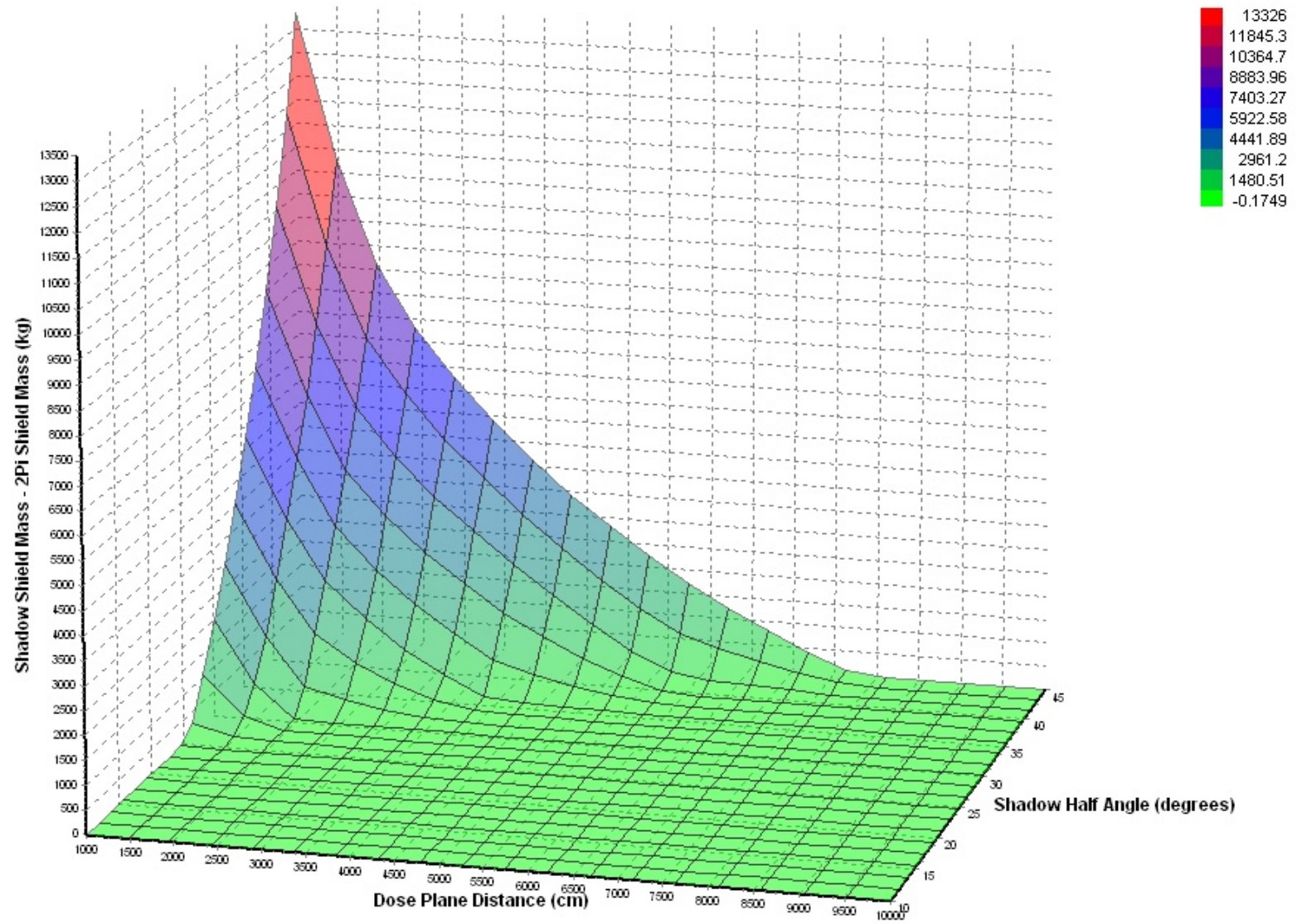
Shadow Shield - 2Pi Shield Mass vs Dose Plane Distance and Shadow Half Angle, 75 klbf Thrust, Two Engine Configuration



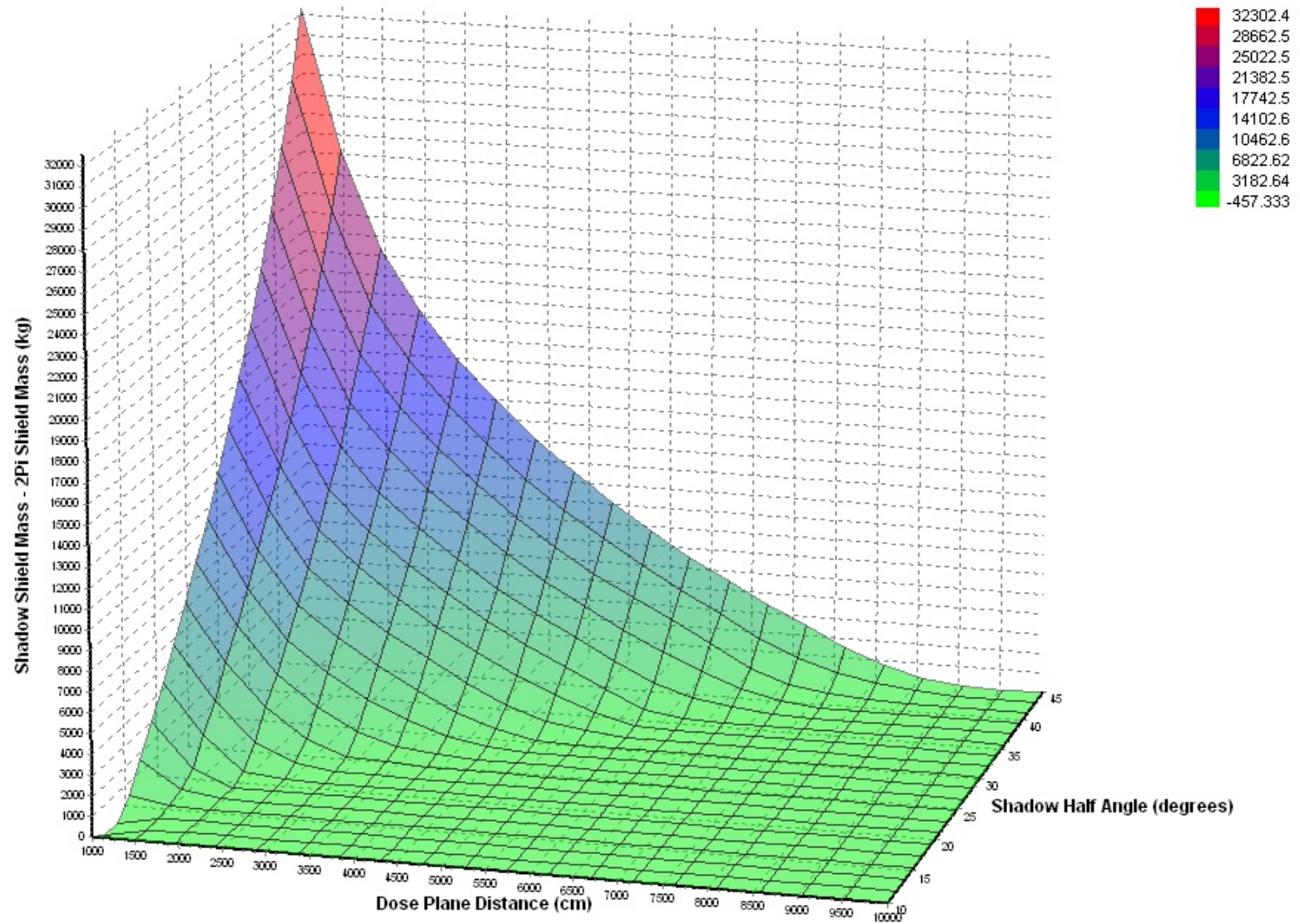
Shadow Shield - 2Pi Shield Mass vs Dose Plane Distance and Shadow Half Angle, 75 klbf Thrust, 3 Engine Configuration



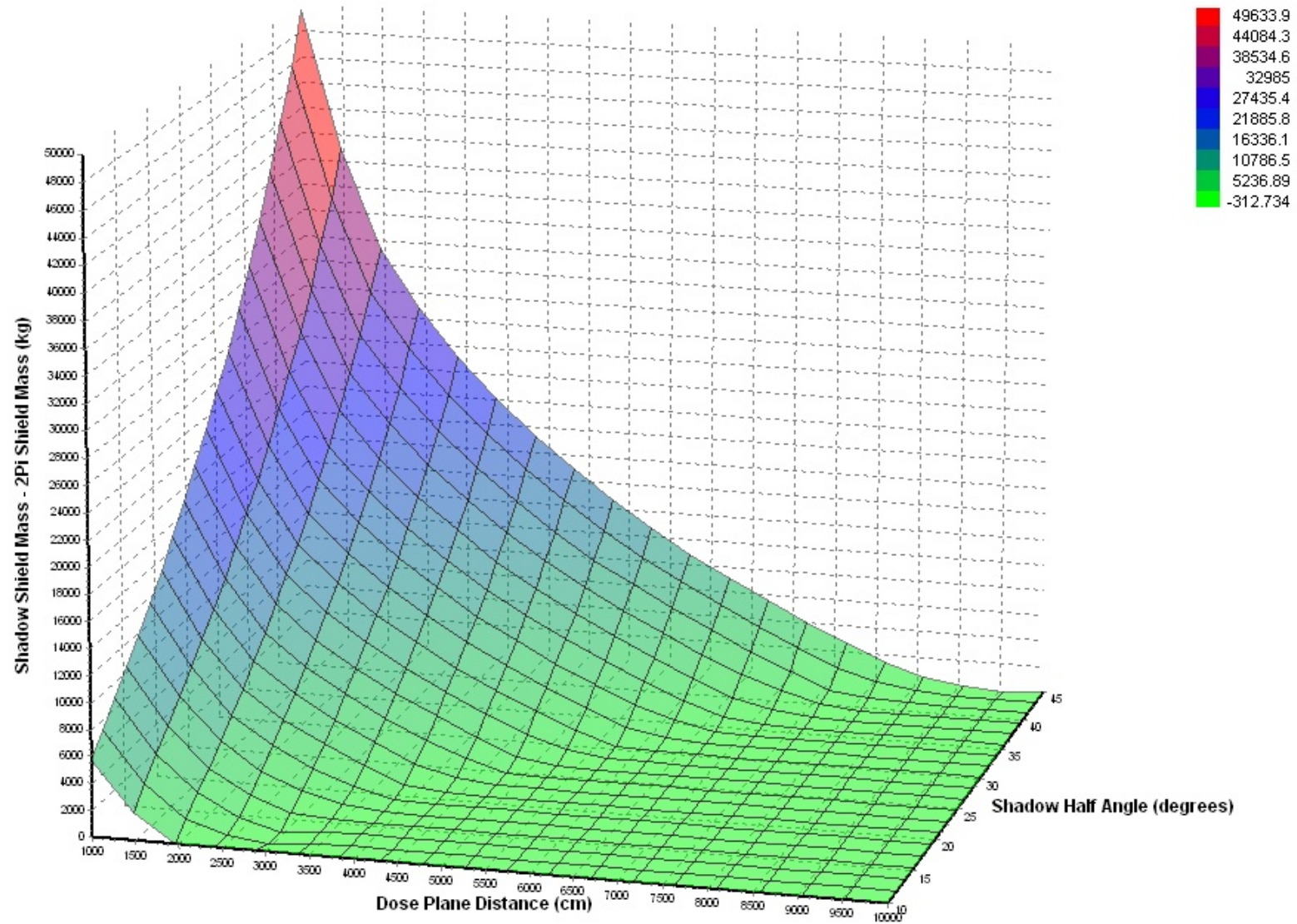
Shadow Shield - 2Pi Shield Mass vs Dose Plane Distance and Shadow Half Angle, 100 klbf Thrust, Single Engine



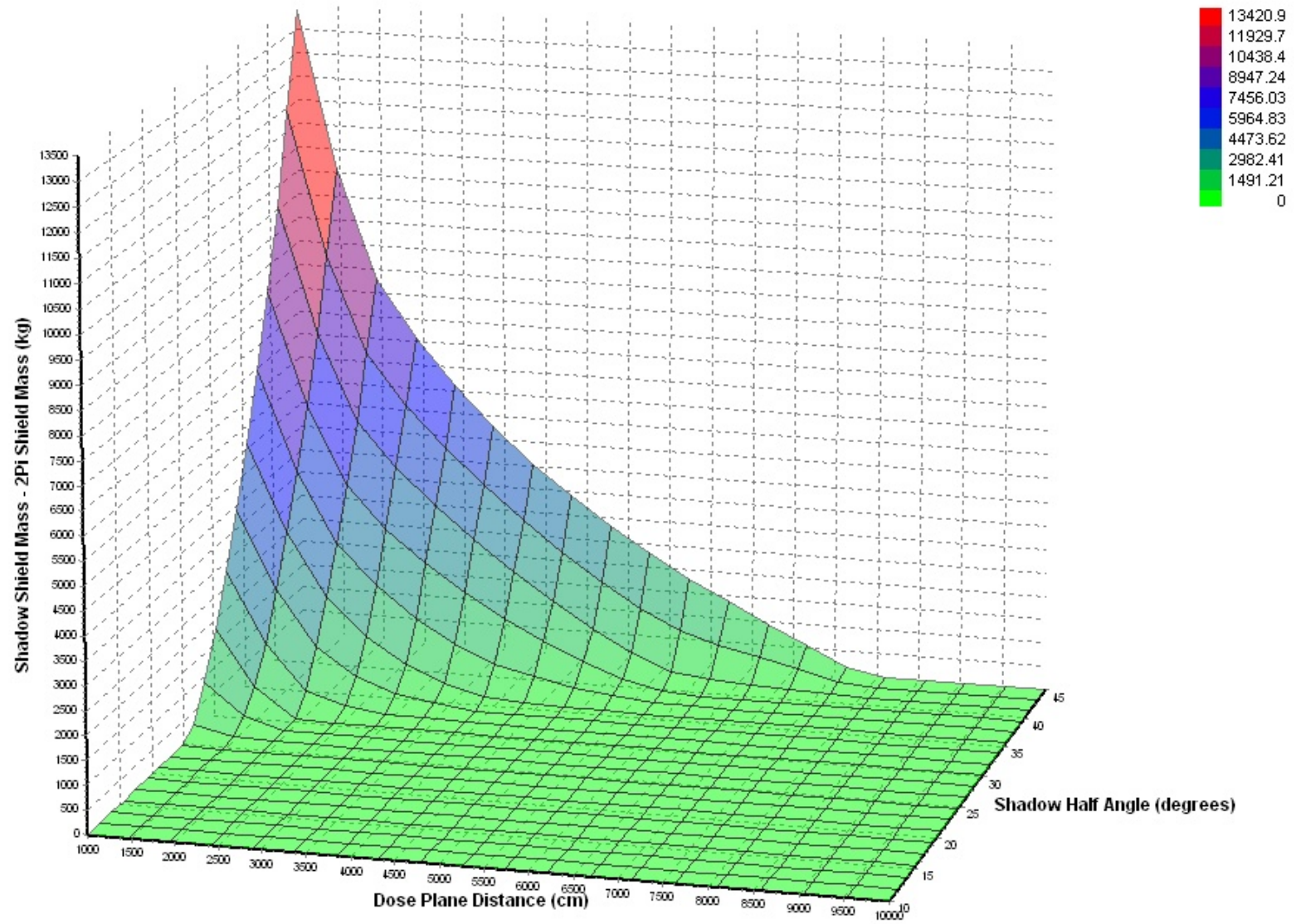
Shadow Shield - 2Pi Shield Mass vs Dose Plane Distance and Shadow Half Angle, 100 klbf Thrust, Two Engine Configuration



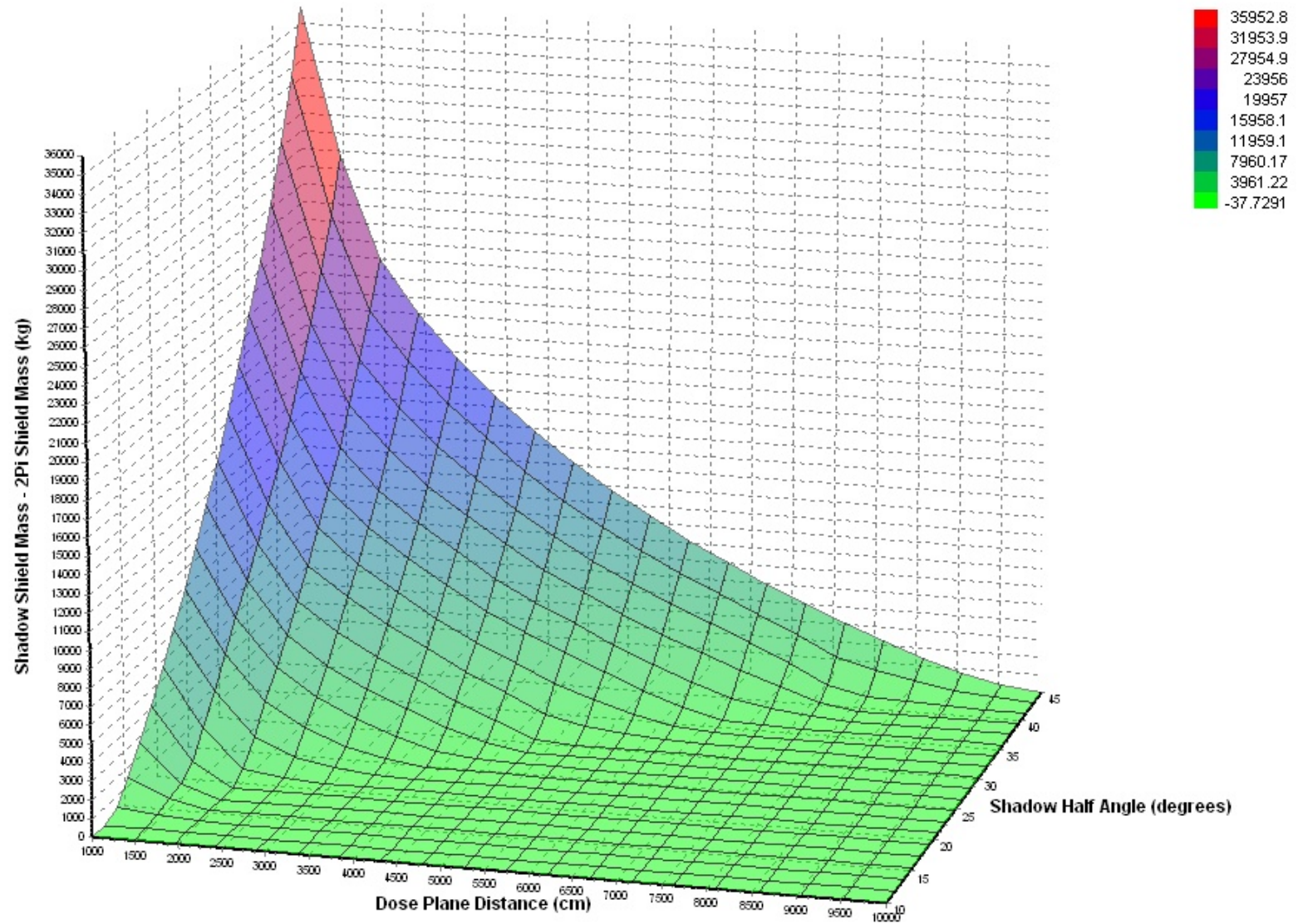
Shadow Shield - 2Pi Shield Mass vs Dose Plane Distance and Shadow Half Angle, 100 klbf Thrust, 3 Engine Configuration



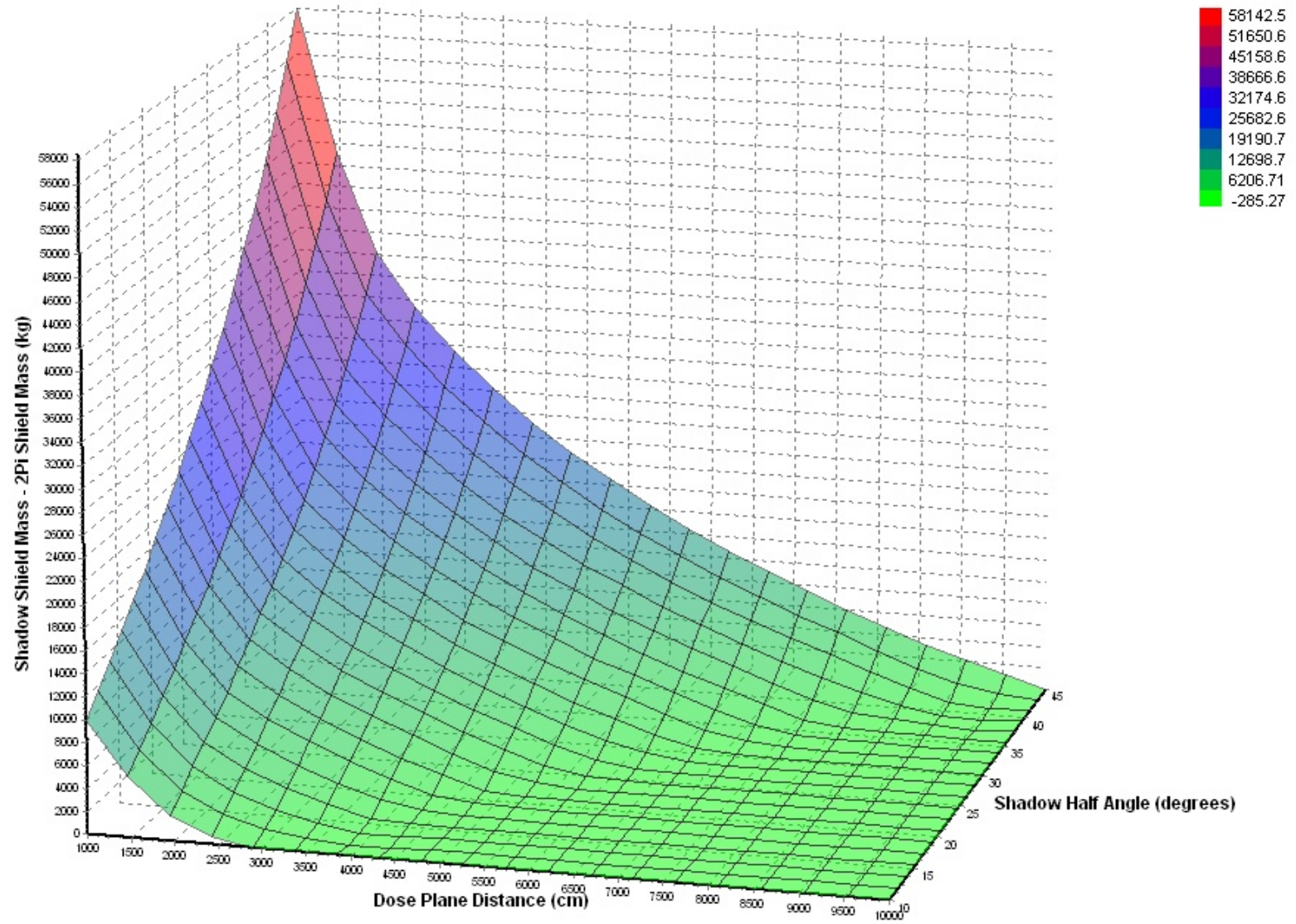
Shadow Shield - 2Pi Shield Mass vs Dose Plane Distance and Shadow Half Angle, 125 klbf Thrust, Single Engine



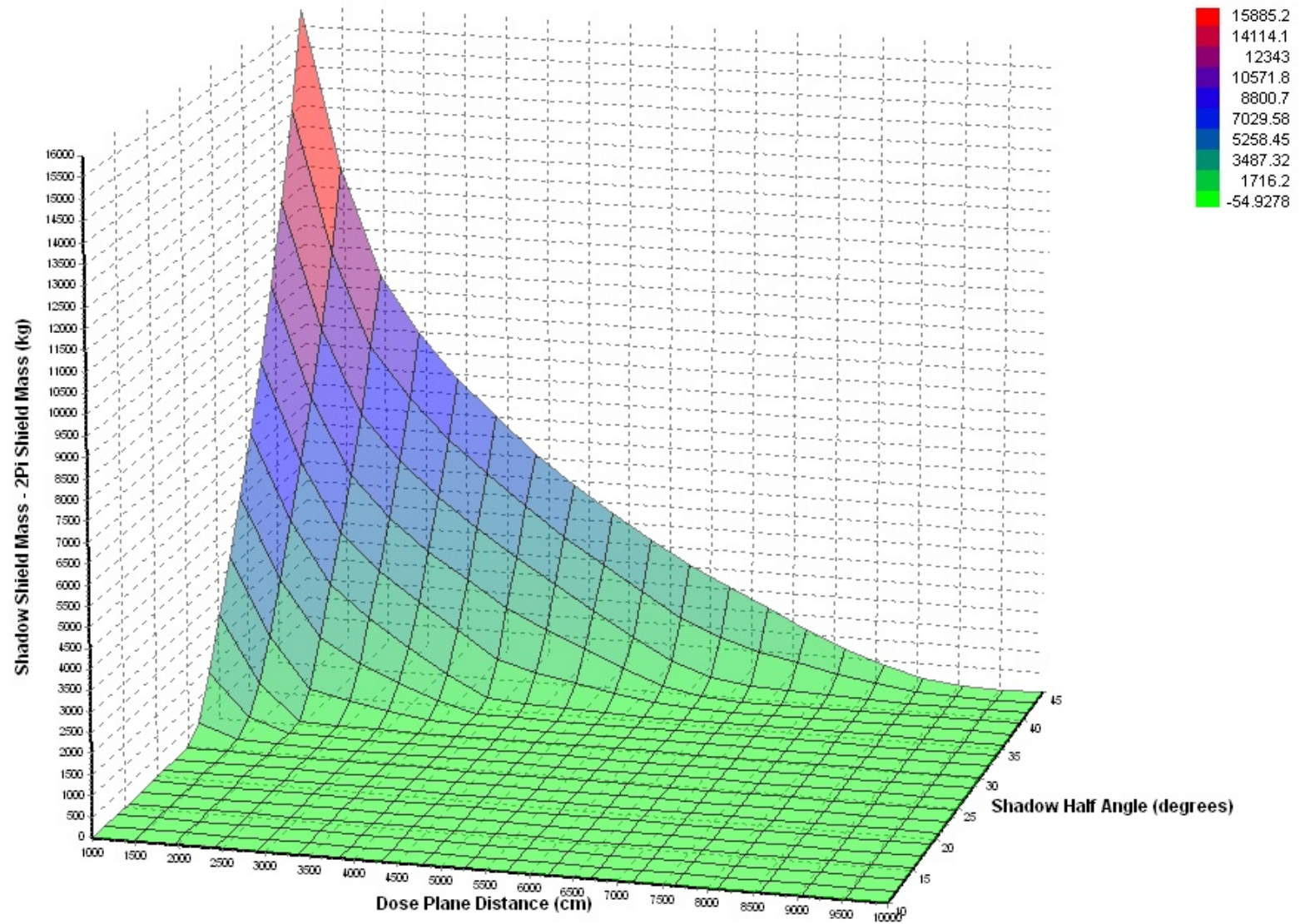
Shadow Shield - 2Pi Shield Mass vs Dose Plane Distance and Shadow Half Angle, 125 klbf Thrust, Two Engine Configuration



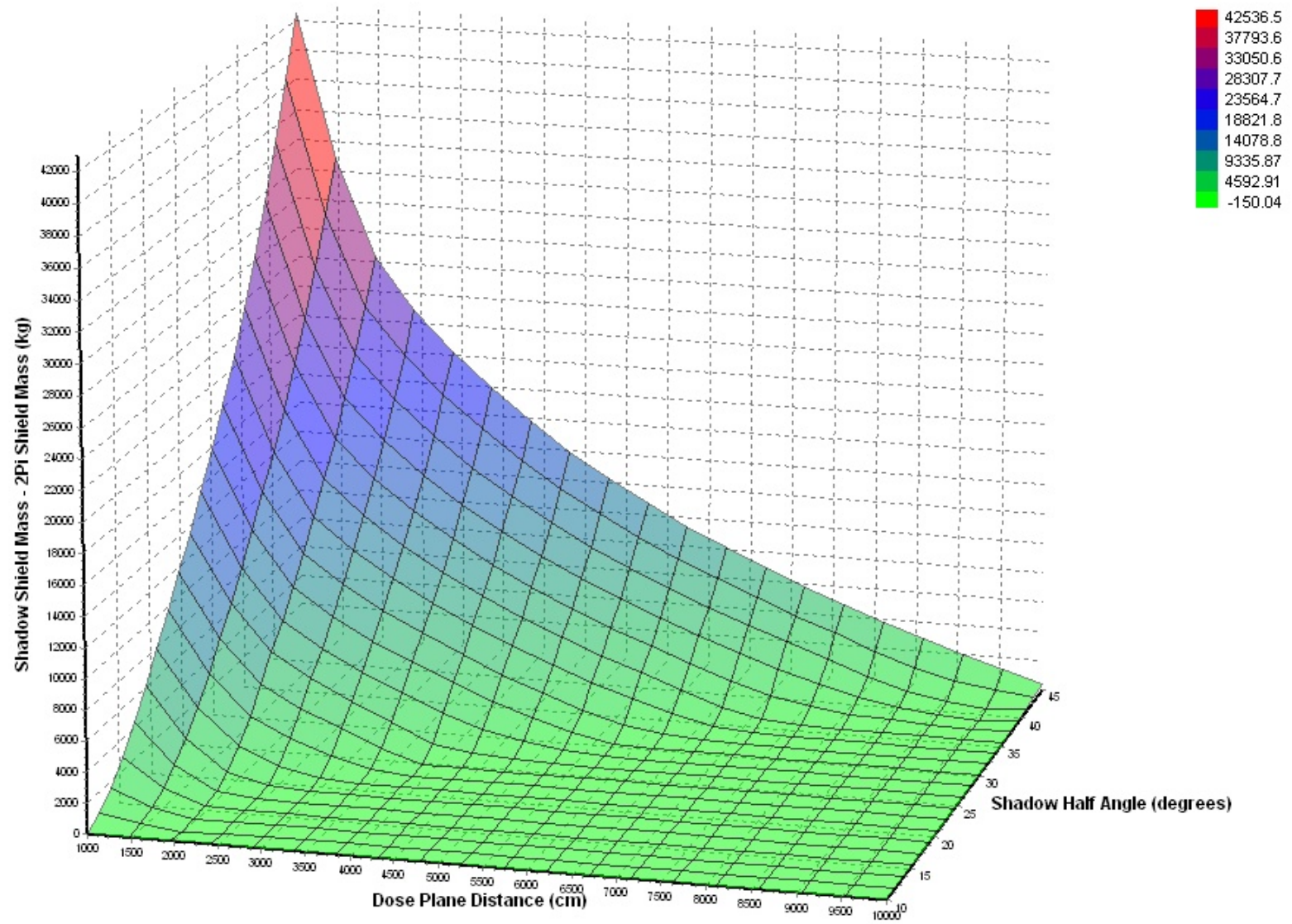
Shadow Shield - 2Pi Shield Mass vs Dose Plane Distance and Shadow Half Angle, 125 klbf Thrust, 3 Engine Configuration



Shadow Shield - 2Pi Shield Mass vs Dose Plane Distance and Shadow Half Angle, 150 Kibf, Single Engine



Shadow Shield - 2Pi Shield Mass vs Dose Plane Distance and Shadow Half Angle, 150 klbf Thrust, Two Engine Configuration



Shadow Shield - 2Pi Shield Mass vs Dose Plane Distance and Shadow Half Angle, 150 klbf Thrust, 3 Engine Configuration

